CHAPTER 4

Results

4.1 Study on the Prevalence of *Echinostoma* sp. in Snails in Chiang Mai Province

4.1.1 Snail samples collected

The snail samples were found on the rock, rough sand, dried leaves and on aquatic plants in all habitat types. A total of 10,692 freshwater snail specimens were collected from different sampling sites in 10 districts of Chiang Mai province. On the basis of shell morphology, the snail samples were classified into 12 species (Figure 4.1). They were 1,006 *Clea helena*, 450 *Lymnaea auricularia rubiginosa*, 190 *Adamietta housei*, 550 *Thiara scabra*, 1,658 *Melanoides tuberculata*, 1,431 *Tarebia granifera*, 110 *Eyriesia eyriesi*, 322 *Bithynia funiculata* and 764 *B. siamensis siamensis*. Of the *Filopaludina* spp., 1,684 belonged to *F. doliaris*, 864 were *F. sumatrensis polygramma* and 1,663 were *F. martensi martensi*.

4.1.2 Morphology of metacercariae and adults

The metacercariae and adult worms in this study were identified as *Echinostoma revolutum* (Fröelich, 1802) Looss, 1899 based on the biological features of adult worms recovered; including the morphology, morphometrics, host-parasite relationships and geographic distribution (Appendix B). The general morphology of the metacercariae and adult worms was as follows:

Metacercaria:

Metacercaria, folded within transparent cyst (Figure 4.2 C), was spherical, 136.0-195.0 μm in diameter, with a bilayered wall (n=30). Cyst wall consisted of outer, transparent layer, about 4.4-12.0 μm thick, and inner, opaque layer, about 2.5-6.0 μm thick. Collar spines, 37 in total, were presented in both fresh and fixed specimens, excretory granules and suckers were visible through the cyst wall and the excretory

organs filled with concretions through the cyst wall. Cysts were found clumped together in the pericardial sac, with each cyst enveloped by thin connective tissues of the snail host origin (Figure 4.2 A-C).

Adult:

Most adult worms were recovered from the duodenum of hamsters, and from the jejunum and ileum of chicks with morphological description as described followings;

Adult worms (n=20) were elongated, 6.4-11.6 (8.9) mm in length, dorso-ventrally flattened, somewhat attenuated at both ends, and ventrally slightly bent (Figure 4.2 E). Tegument of anterior body armed with numerous small spines which extended to the posterior end of ventral sucker. Head crown distinct, well developed, with ventral ridge. There are 37 collar spines arranged in a semicircle around the collar, double row and dorsally uninterrupted; spine arrangement: 5 corner spines on each side, 6 lateral on each side in a single row; 15 dorsal spines in a double row. Oral sucker ventro-subterminal, spherical or subspherical, and prepharynx absent or very shot. Pharynx well developed, muscular, elongate-oval, esophagus long. Intestinal bifurcation anterior to ventral sucker; intestinal caeca blind and extending almost to posterior extremity. Ventral sucker spherical, muscular, very large, middle located and protruded ventrally. Testes 2, tandem, beginning at mid-hind body, elongate-oval, slightly lobed or slightly irregular in outline. Cirrus sac muscular, well developed, elongate-oval, antero-dorsal to ventral sucker, median and immediately preacetabular and ventral sucker. Cirrus unarmed and unclear length. Genital pore median, preacetabular, followed by genital atrium. Ovary spherical or nearly oval, compact, at or anterior to midbody. Mehlis' gland located between the ovary and anterior testis. Uterus moderately developed, with intercaecal loops between ovary and ventral sucker. Eggs numerous, egg size, 72.5-120 × 40-82.5 μm (n=20). Eggs operculated, elliptical, yellowish, and thin-shelled. Vitellarium follicular, forming 2 lateral fields and extending from short distance posterior ventral sucker to the posterior body end. Excretory vesicles not observed, excretory pore terminal.

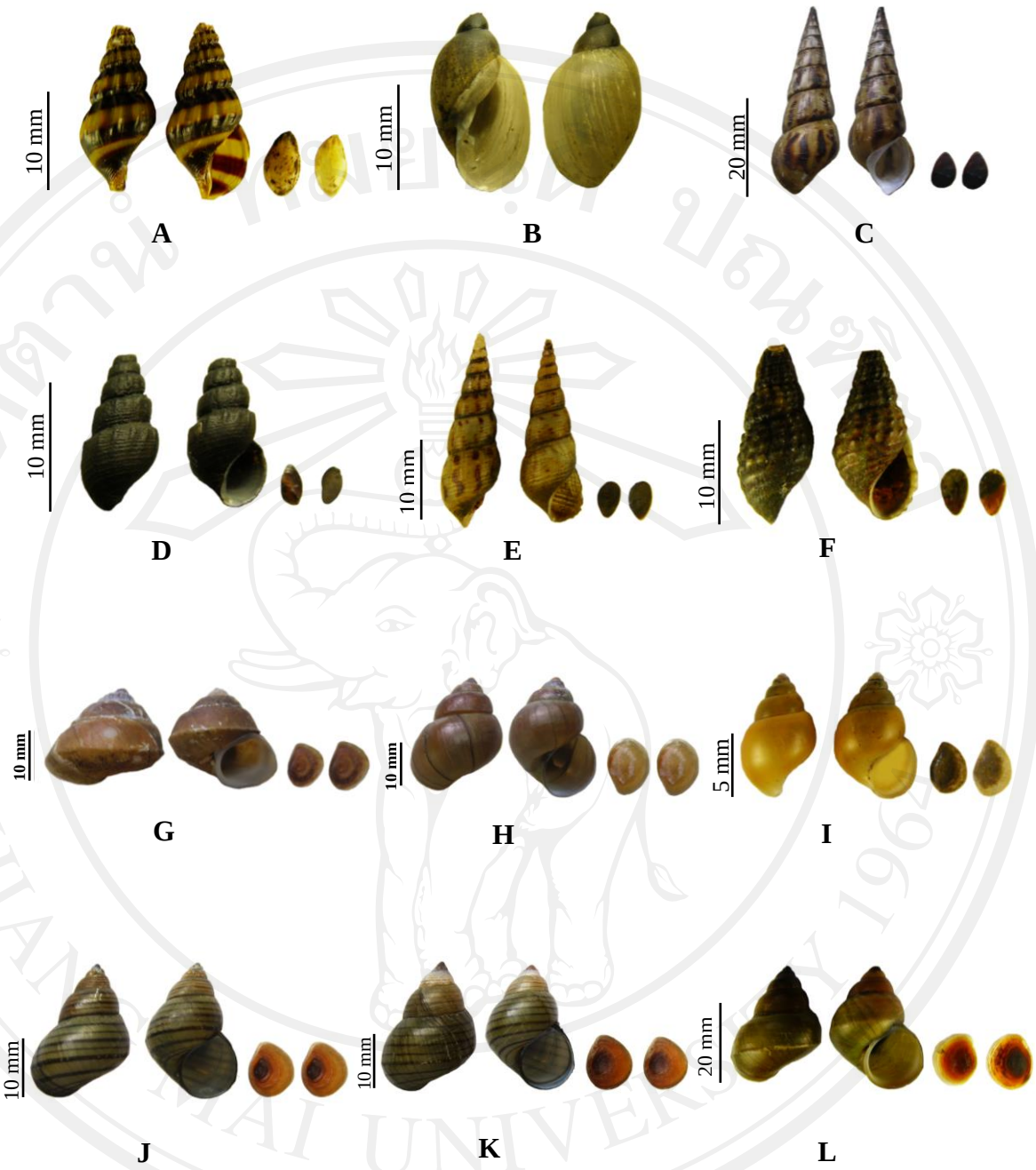

Figure 4.1 Characteristics of shell and operculae of snails collected from 10 districts of Chiang Mai province; **(A)** *C. helena* **(B)** *L. auricularia rubiginosa* **(C)** *A. housei* **(D)** *Th. scabra* **(E)** *M. tuberculata* **(F)** *Ta. granifera* **(G)** *E. eyriesi* **(H)** *B. funiculata* **(I)** *B. siamensis siamensis* **(J)** *F. doliaris* **(K)** *F. sumatrensis polygramma* and **(L)** *F. martensi martensi*.

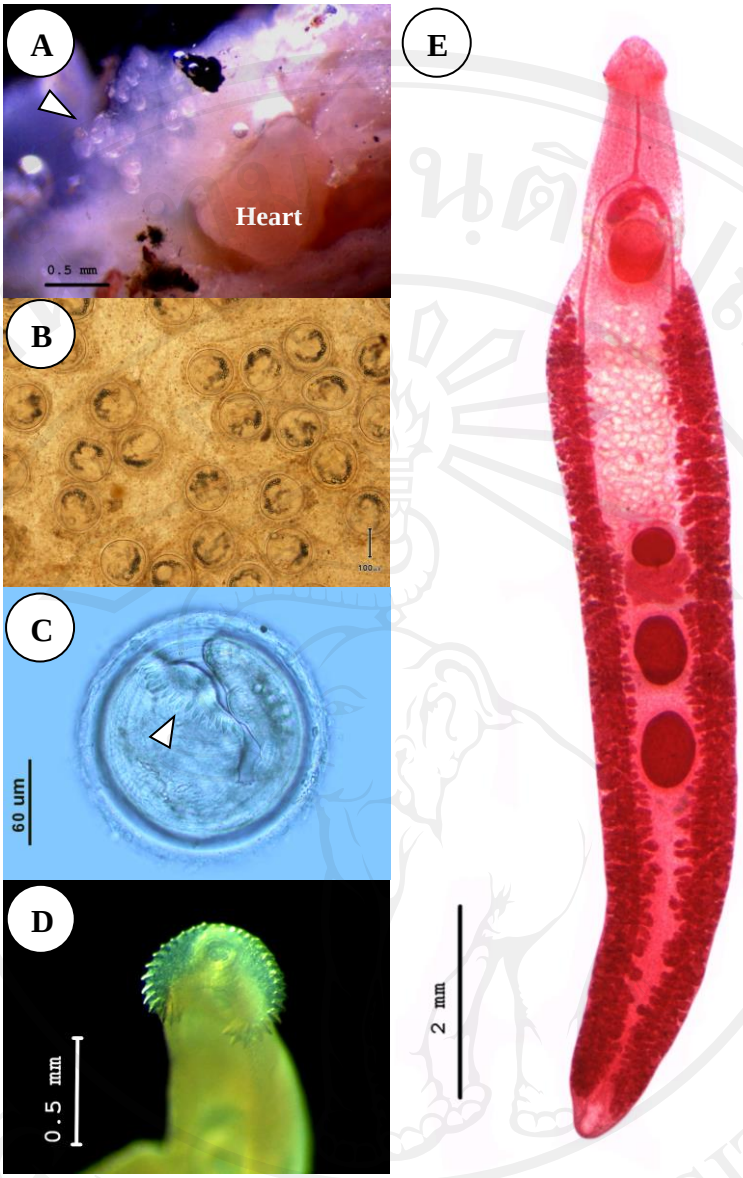

Figure 4.2 *Echinostoma revolutum*: **(A)** Metacercariae (white spots, arrowhead) in the pericardial sac of *Filopaludina* spp. snails; **(B)** Metacercarial cysts were clumped together in the pericardial sac, compressed under a cover slip; **(C)** An isolated metacercaria showing a well-developed oral sucker and head collar with collar spines (arrowhead); **(D)** A live specimen showing a prominent head collar; **(E)** An adult specimen recovered from an experimental host at day 20 post-infection.

4.1.3 Infection status of snails with *E. revolutum* metacercariae

Total of 2,586 of 10,692 snails examined were infected with *E. revolutum* metacercariae. The overall infection rates and numbers of these metacercariae recovered from snail species are shown in Table 4.1. Throughout the course of our survey, 41,909 metacercariae were recovered from 7 snail species, including *Clea helena, Eyriesia eyriesi, Bithynia funiculata, B. siamensis siamensis, Filopaludina doliaris, F. sumatrensis polygramma* and *F. martensi martensi*. The remaining five species, i.e., *Lymnaea auricularia rubiginosa, Adamietta housei, Thiara scabra, Melanoides tuberculata* and *Tarebia granifera* were found not to be infected with these metacercariae.

The overall prevalence of infection was 24.2% (2,586/10,692). Most metacercariae were recovered from *Filopaludina* spp., and the least from *C. helena* (1%, 10/1,006). A total of 41,909 *E. revolutum* metacercariae were found in the pericardial sac of infected snails (Figure 4.2 A-B), with a mean intensity of 16.2 metacercaria per snail. The intensity of infection ranged from 1.2 to 131.0 metacercariae per snail. The most heavily infected species of snails were *F. doliaris* (63.1%), *F. sumatrensis polygramma* (61.0%) and *F. martensi martensi* (55.7%).

Table 4.1 Information about freshwater snails examined in Chiang Mai province, prevalence of infection and number of the *Echinostoma revolutum* metacercariae by host species.

Snail species	No. of snail infected /examined										No. of snail infected /examined	No. of metacercariae, total (range)	Prevalence (%)	Intensity
	Locality[a]													
	DS	HD	MO	MR	MT	MCM	SK	ST	SP	SS				
C. helena	0/150	0/80	0/60	0/60	0/132	0/104	0/180	0/60	10/120	0/60	10/1,006	12 (1-2)	1.0	1.2
E. eyriesi	0/17	7/13	0/21	-	11/59	-	-	-	-	-	18/110	166 (1-24)	16.4	9.2
L. auricularia rubiginosa	-	0/30	0/60	0/60	-	0/60	-	0/120	0/120	-	0/450	-	-	-
A. housei	-	-	0/27	0/19	0/66	-	0/12	0/26	0/40	-	0/190	-	-	-
Th. scabra	0/50	0/50	0/46	0/20	0/60	0/102	0/104	0/58	-	0/60	0/550	-	-	-
M. tuberculata	0/160	0/114	0/180	0/156	0/200	0/150	0/180	0/173	0/165	0/180	0/1,658	-	-	-
Ta. granifera	0/170	0/120	0/120	0/150	0/110	0/120	0/170	0/178	0/113	0/180	0/1,431	-	-	-
B. funiculata	-	0/30	-	0/30	-	0/30	0/80	0/30	22/92	0/30	22/322	65 (1-7)	6.8	3.0
B. siamensis siamensis	0/52	20/90	0/30	0/60	0/134	0/38	-	0/120	0/120	0/120	20/764	56 (1-7)	2.6	2.8
F. doliaris	108/146	82/154	74/148	84/170	149/202	38/129	113/187	111/178	80/130	224/240	1,063/1,684	21,449 (1-353)	63.1	20.2
F. sumatrensis polygramma	64/86	37/70	23/54	26/78	78/132	9/29	16/49	43/84	50/93	181/189	527/864	6,089 (1-97)	61.0	11.6
F. martensi martensi	60/190	93/152	65/160	83/146	108/159	38/113	62/151	114/167	75/180	228/245	926/1,663	14,072 (1-164)	55.7	15.2
Total	232/1,021	239/903	162/906	193/949	346/1,254	85/875	191/1,113	268/1,194	237/1,173	633/1,304	2,586/10,692	41,909 (1-353)	24.2	16.2

Note: [a] The localities are designated in Table 3.1

4.1.4 The prevalence and intensity of *E. revolutum* metacercariae in Chiang Mai Province

The prevalence and intensity of *E. revolutum* metacercariae in 10 districts of Chiang Mai province during 3 seasons for one year-round (November 2011 to October 2012) are shown in Table 4.2-Table 4.3 and Figure 4.3-Figure 4.5.

A total number of 10,692 freshwater snails were collected from natural water resources of Chiang Mai province. They consisted of 12 snail species and separately examined for the presense of the *E. revolutum* metacercaria. The overall infection rates and mean numbers of *E. revolutum* metacercariae recovered from 10 districts were shown in Table 4.2 and Figure 4.4. Throughout the course of our survey, 41,909 *E. revolutum* metacercariae were recovered from the 7 snail species. The overall prevalence rates of 10 districts were varied from 9.7% to 48.5%.

Studies at 10 districts showed that 2,586 of the 10,692 freshwater snails were infected with *E. revolutum* metacercariae. The highest mean intensity of *E. revolutum* metacercariae infection was in Doi Saket district which was 28.8 (1.5-44.8) metacercariae per snail. The highest prevalence was found in San Sai district, 48.5% (633/1,304) (Figure 4.4). Overall prevalence in 10 districts show the highest in rainy and hot-dry seasons were 26.9% and 26.54% respectively and lowest in cool season was 19.1% (Table 4.2 and Figure 4.5).

Table 4.2 Number of snail studies, metacercariae found infected snail according to season and location variations and their prevalence and intensity.

Locality[a]	No. infected/examined snail			No. of metacercariae isolated range (total)			Prevalence (%)			Intensity		
	Cool	Hot-dry	Rainy	Cool	Hot-dry	Rainy	Cool	Hot-dry	Rainy	Cool	Hot-dry	Rainy
DS	4/337	108/324	120/360	6 (1-2)	4,019 (1-209)	2,655 (1-212)	8.0	33.3	33.3	1.5	37.2	22.1
HD	86/328	92/351	61/224	422 (1-33)	787 (1-97)	683 (1-67)	26.2	26.2	27.2	4.9	8.6	11.2
MO	49/357	43/280	70/269	521 (1-43)	545 (1-63)	579 (1-61)	13.7	15.4	26.0	10.6	12.7	8.3
MR	46/272	85/346	62/331	628 (1-56)	1,019 (1-96)	638 (1-53)	16.9	24.6	18.7	13.7	12.0	10.3
MT	114/416	134/455	98/383	1,951 (1-129)	1,916 (1-87)	1,158 (1-96)	27.4	29.5	25.6	17.1	14.3	11.8
MCM	14/246	37/351	34/278	287 (1-57)	290 (1-54)	356 (1-32)	5.7	10.5	12.2	20.5	7.8	10.5
SK	50/396	80/377	61/340	132 (1-22)	859 (1-41)	678 (1-57)	12.6	21.2	17.9	2.6	10.7	11.1
ST	88/386	77/379	103/429	622 (1-219)	1,044 (1-107)	1,168 (1-72)	22.8	20.3	24.0	7.1	13.6	11.3
SP	72/401	80/330	85/442	222 (1-15)	989 (1-84)	1,509 (1-102)	18.0	24.2	19.2	3.1	12.4	17.8
SS	154/404	233/458	246/442	9,706 (2-353)	2,934 (1-118)	3,586 (1-114)	38.1	50.9	55.6	63.0	12.6	14.6
Total	677/3,543	969/3,651	940/3,498	14,497 (1-353)	14,402 (1-209)	13,010 (1-212)	19.1[a]	26.54[b]	26.9[b]	21.4	14.9	13.8

Note: - [a] The localities are designated in Table 3.1

- expotential letter (a, b) determined significantly different at 95% confidence.

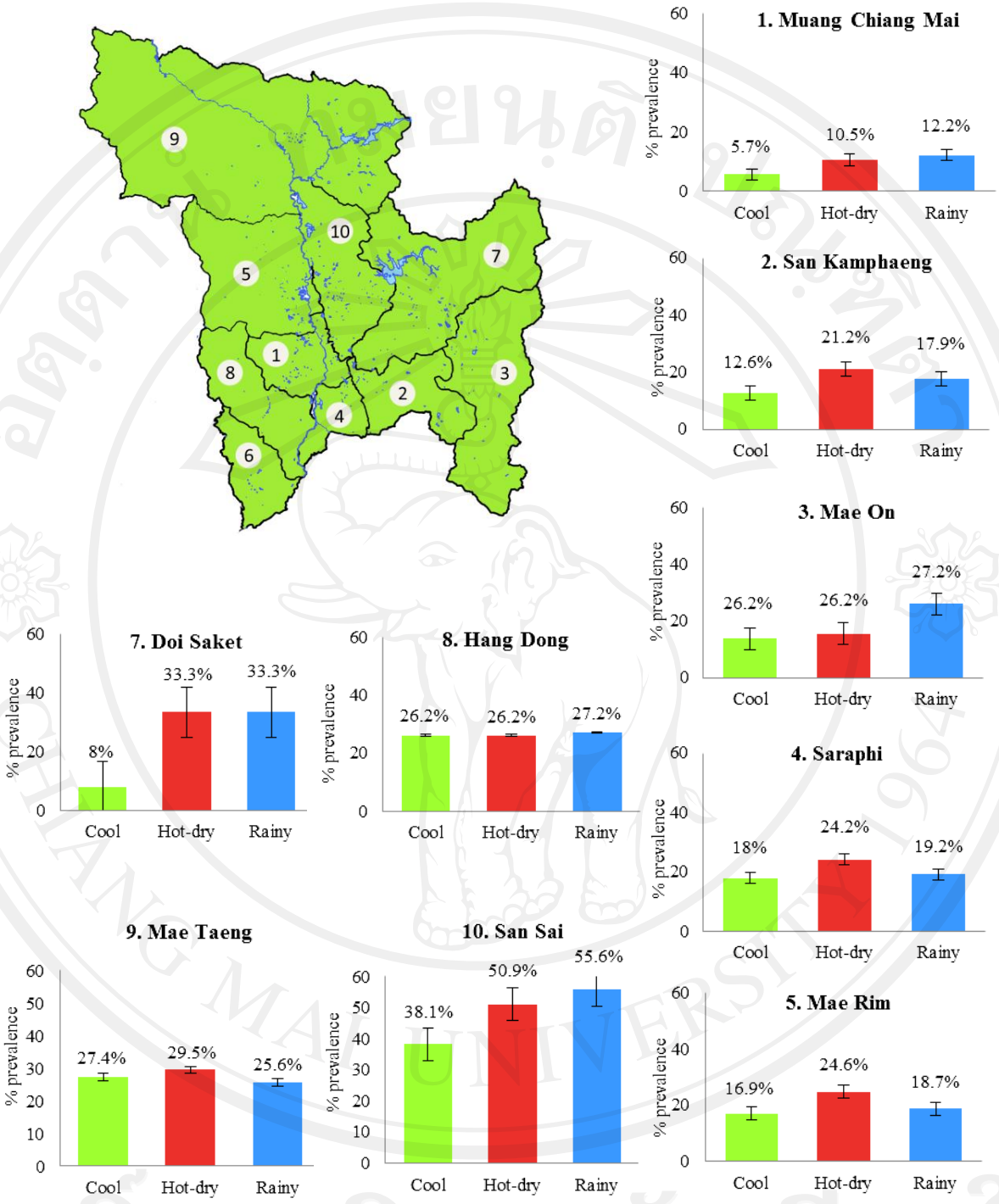

Figure 4.3 Seasonal infection rates of *Echinostoma revolutum* metacercariae (for one year round) in 10 districts of Chiang Mai province.

Table 4.3 Number of *Echinostoma revolutum* metacercariae and prevalence of infections in snails collected from different localities in Chiang Mai province.

Locality	No. of snail infected /examined	No. of metacercariae, total (range)	Prevalence (%)	Mean intensity (range)
Doi Saket	232/1,021	6,680 (1-212)	22.7	28.8 (1.5-44.8)
Hang Dong	239/903	1,892 (1-97)	26.5	7.9 (2.8-23.4)
Mae On	162/906	1,645 (1-63)	17.9	10.2 (7.3-15.1)
Mae Rim	193/949	2,285 (1-96)	20.3	11.8 (9.0-16.6)
Mae Taeng	346/1,254	5,025 (1-129)	27.6	14.5 (10.0-22.9)
Muang Chiang Mai	85/875	933 (1-57)	9.7	11.0 (7.4-24.7)
San Kamphaeng	191/1,113	1,669 (1-57)	17.2	8.7 (1.6-13.1)
San Pa Tong	268/1,194	2,834 (1-219)	22.4	10.6 (4.3-15.9)
Saraphi	237/1,173	2,720 (1-102)	20.2	11.5 (1.2-21.9)
San Sai	633/1,304	16,226 (1-353)	48.5	25.6 (9.0-131.0)
Total	2,586/10,692	41,909 (1-353)	24.2	16.2 (1.2-131.0)

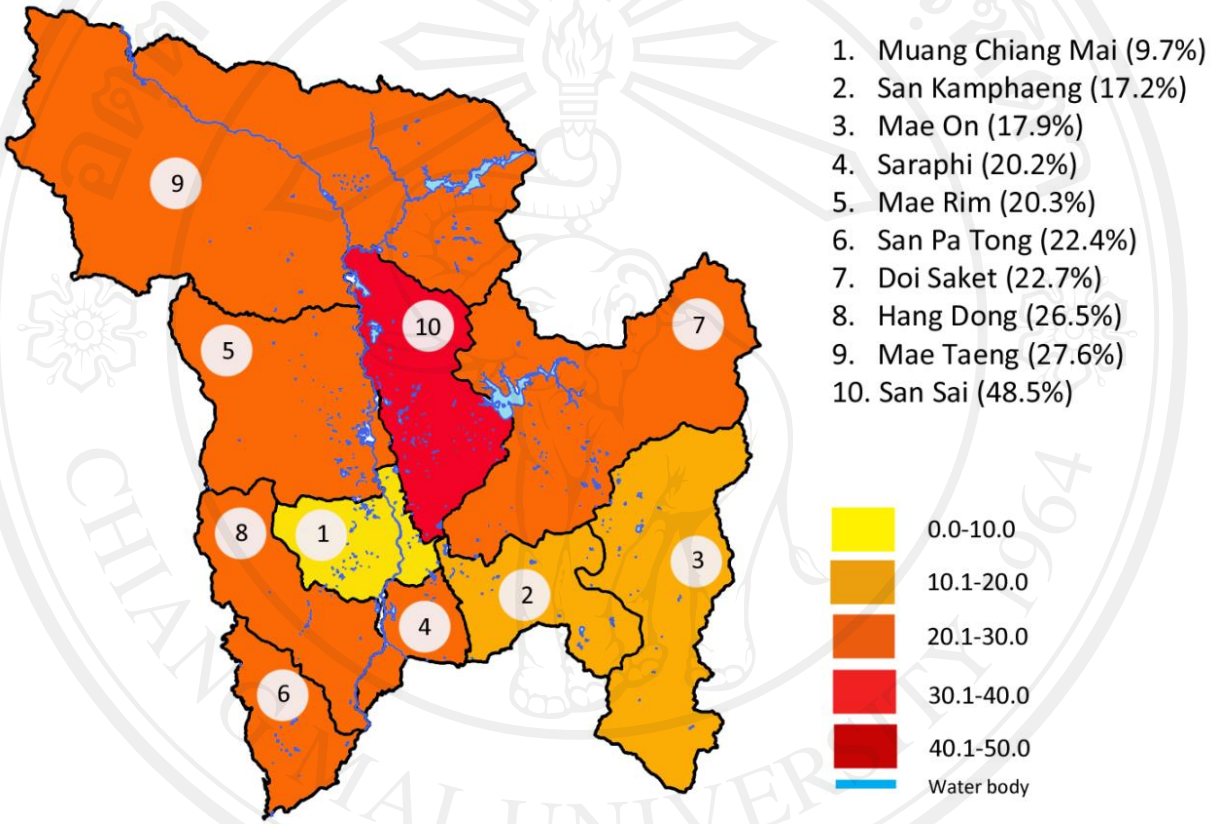

Figure 4.4 Distribution and prevalence of *Echinostoma revolutum* metacercariae in 10 districts of Chiang Mai province (surveyed during November 2011 to October 2012).

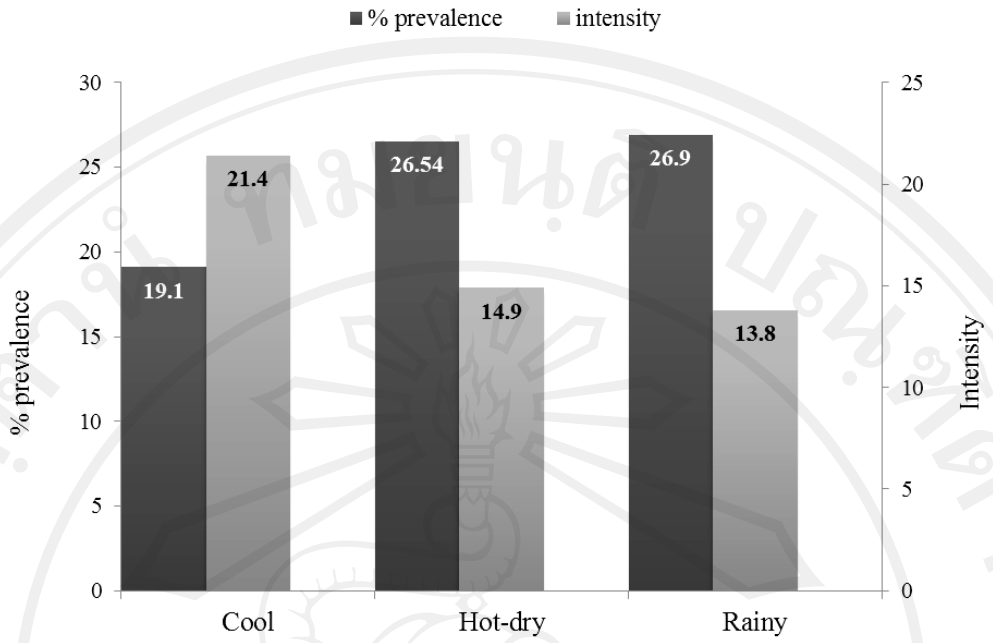

Figure 4.5 The total prevalence and intensity of *Echinostoma revolutum* metacercariae in snails collected from Chiang Mai province during three seasons for one year round.

On the other hand, in some snail species, including *B. funiculata, B. siamensis siamensis, F. doliaris, F. sumatrensis polygramma, F. martensi martensi,* there were mixed infections of several types of cercariae (Figure 4.6 A-E) and unidentified young redia (Figure 4.6 F). They included monostome cercariae, distome cercariae, xiphidiocercariae, gymnocephalus cercariae and furcocercous cercariae. There were found as mixed infections in the gastrointestinal organs of infected snails. Moreover, mixed infections with *Asymphylodora* sp. metacercaria (Figure 4.6 G), and 1 unidentified metacercariae (Figure 4.6 H), were found in *B. siamensis siamensis*.

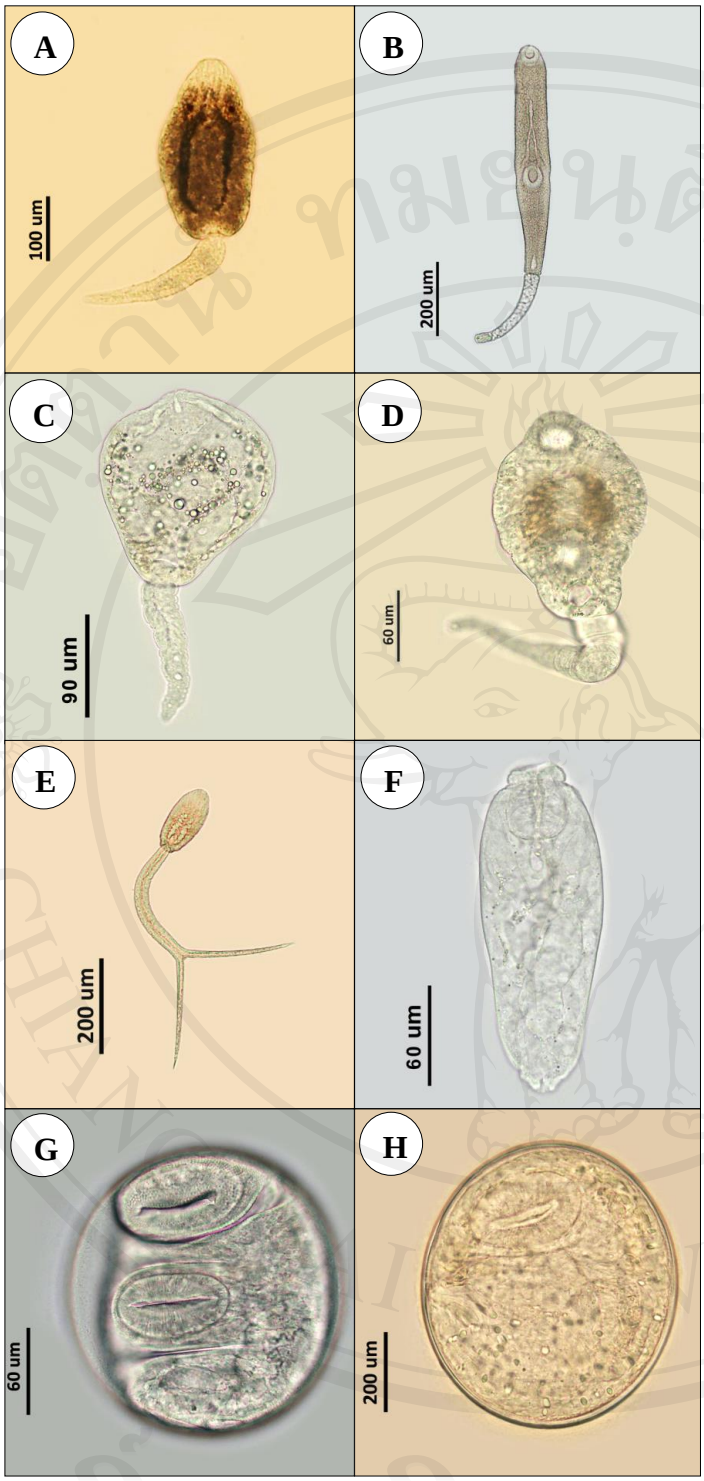

(A) Monostome cercaria

(Host: *B. siamensis siamensis*)

(B) Distome cercaria

(Host: *Filopaludina* spp.)

(C) Xiphidiocercaria

(Host: *Filopaludina* spp. and *B. siamensis siamensis*)

(D) Gymnocephalus cercaria

(Host: *B. siamensis siamensis*)

(E) Furcocercous cercaria

(Host: *Filopaludina* spp. and *Bithynia* spp.)

(F) Unidentified young redia

(Host: *B. siamensis siamensis*)

(G) *Asymphylodora* sp. metacercaria

(Host: *B. siamensis siamensis*)

(H) Unidentified metacercaria

(Host: *B. siamensis siamensis*)

Figure 4.6 Different types of cercariae, young redia and metacercariae found in the freshwater snails.

4.2 Study on the Life History of *Echinostoma revolutum*

4.2.1 Definitive host infections

1) Infectivity of worm

After orally introduced to chicks, the metacercariae were excysted and developed into adults in the small intestine. From day 1 to day 36 PI, a total of 465 worms were recovered from 36 chicks that had been infected with a total of 1,800 metacercariae. Infections were 60.0% (36/60) and the average worm recoveries were 27.1%, which varied from 2.0 to 74.0% (Figure 4.7). Metacercariae of *E. revolutum* developed into mature adults after 8 days PI and ovigerous adults developed after 9 days PI. The worms were recovered from the jejunum (75.2%), ileum (23.4%), and caecum (1.4%). None was found in other parts of the digestive tract. The worms were survived until day 36 PI.

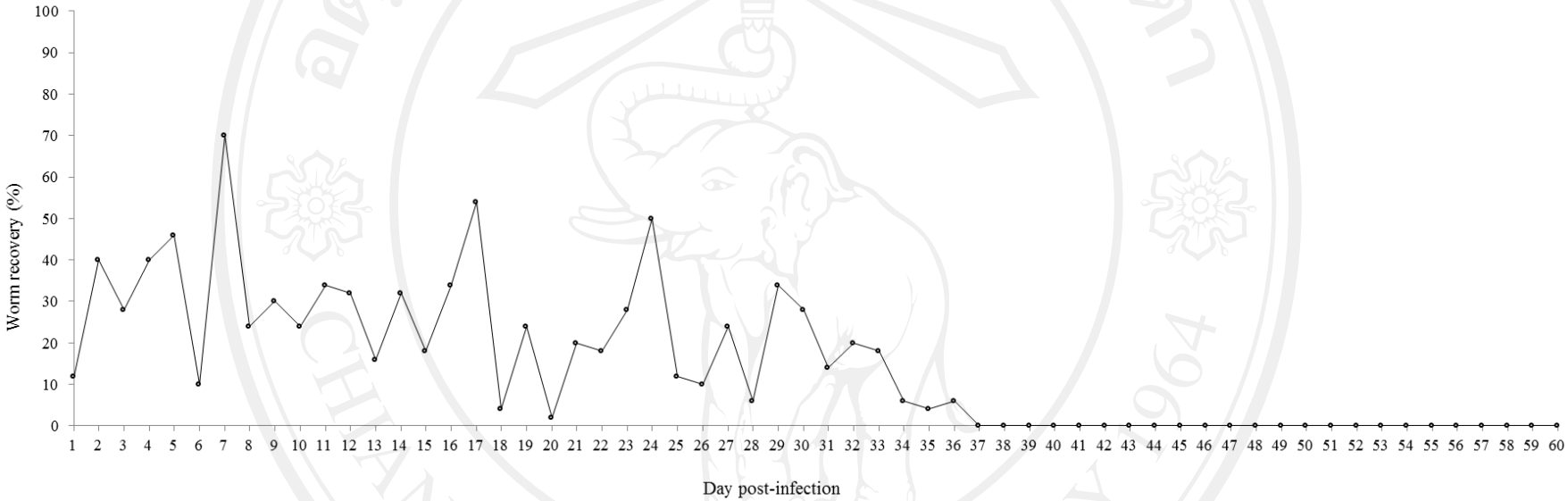

Figure 4.7 The recovery rate of *Echinostoma revolutum* from chicks each experimentally infected with 50 metacercariae 1-60 days post-infection.

2) Growth and development of worm

Several measurements of worms recovered from chick hosts are summarized in Table 4.4. On the basis of the measurements made on specimens of various ages, the growth curves of *E. revolutum* in chicks could be established (Figure 4.8). The body size rapidly increased from day 1-20 PI, but this increase became slower thereafter until day 35 PI (Figure 4.8 A). A difference was noted between the growth patterns of parenchymal and reproductive organs (Figure 4.8 B, C). The parenchymal organs including, oral sucker, head crown, prepharynx, oesophagus and ventral sucker also showed a development pattern similar to the body size from day 1-20 PI, and then remained steady and showed a little fluctuation until day 35 PI (Figure 4.8 B). In reproductive organs including, testes, ovary and cirrus pouch, growth was very rapid during first 20 day PI (Figure 4.8 C). The anterior testis was little larger than the posterior one in width. The sizes of the testes rapidly increased from day 1 to 20 PI, and gradually increased until day 30 PI. The ovary and cirrus pouch developed at a similar speed as the testes. The growth of the ovary rapidly increased up to day 25 PI. The uterine egg was recognized in 60% of specimens on day 10 PI and 100% of specimens on day 11 PI. Eggs in uterine duct were almost constant during days 10-36.

The description presented below is based on several of specimens retrieved from the experimental definitive hosts according to the age of the worms. Morphological traits were studied and measured using the microscope Olympus equipped.

Table 4.4 Measurement (in millimeter) of *Echinostoma revolutum* from experimental chicks during 1-35 days post-infection (PI)

Body organ	Range (mean±SD) at age (day) PI			
	1 (n=6)	5 (n=15)	10 (n=12)	15 (n=9)
BL	0.61-1.40 (0.73±0.28)	3.68-4.50 (4.05±0.304)	5.28-8.95 (6.68±0.771)	10.75-18.00 (11.85±0.636)
BW	0.18-0.28 (0.19±0.06)	0.58-0.80 (0.64±0.047)	0.68-1.00 (0.82±0.114)	1.00-2.59 (1.21±0.267)
CL	0.08-0.09 (0.09±0.03)	0.18-0.27 (0.21±0.025)	0.25-0.30 (0.26±0.017)	0.25-0.70 (0.38±0.150)
CW	0.15-0.18 (0.16±0.05)	0.41-0.48 (0.44±0.021)	0.34-0.70 (0.56±0.096)	0.23-0.80 (0.66±0.194)
OSL	0.06-0.08 (0.07±0.01)	0.13-0.16 (0.15±0.010)	0.15-0.32 (0.19±0.023)	0.20-0.63 (0.23±0.026)
OSW	0.07-0.08 (0.07±0.02)	0.12-0.16 (0.14±0.013)	0.13-0.30 (0.19±0.030)	0.11-0.68 (0.23±0.054)
PL	0.03-0.05 (0.04±0.01)	0.09-0.15 (0.11±0.019)	0.07-0.13 (0.10±0.019)	0.06-0.18 (0.12±0.037)
PHL	0.03-0.05 (0.04±0.01)	0.10-0.13 (0.12±0.012)	0.14-0.20 (0.16±0.019)	0.17-0.36 (0.18±0.011)
PHW	0.03-0.04 (0.04±0.05)	0.11-0.13 (0.12±0.006)	0.13-0.18 (0.16±0.013)	0.18-0.41 (0.22±0.060)
OL	0.14-0.20 (0.17±0.09)	0.49-0.65 (0.57±0.053)	0.60-0.82 (0.71±0.081)	0.25-1.17 (0.81±0.280)
CSL	-	0.10-0.17 (0.14±0.021)	0.17-0.29 (0.23±0.036)	0.20-0.50 (0.28±0.101)
CSW	-	0.10-0.23 (0.15±0.037)	0.26-0.37 (0.32±0.038)	0.45-0.58 (0.50±0.038)
VSL	0.10-0.12 (0.11±0.01)	0.35-0.41 (0.38±0.021)	0.40-0.60 (0.47±0.040)	0.53-1.00 (0.58±0.043)
VSW	0.09-0.12 (0.11±0.05)	0.27-0.35 (0.32±0.026)	0.40-0.58 (0.46±0.036)	0.28-1.10 (0.53±0.122)
OVL	-	0.10-0.17 (0.13±0.026)	0.07-0.25 (0.16±0.052)	0.23-0.58 (0.30±0.051)
OVW	-	0.13-0.20 (0.18±0.025)	0.08-0.29 (0.17±0.046)	0.25-0.58 (0.32±0.086)
MEL	-	-	0.10-0.30 (0.18±0.053)	0.30-0.50 (0.41±0.067)
MEW	-	-	0.15-0.36 (0.30±0.063)	0.43-0.63 (0.50±0.077)
ATL	-	0.14-0.23 (0.19±0.028)	0.23-0.62 (0.33±0.073)	0.45-1.20 (0.56±0.087)
ATW	-	0.15-0.20 (0.18±0.016)	0.18-0.41 (0.28±0.051)	0.40-0.9 (0.48±0.088)
PTL	-	0.13-0.25 (0.19±0.042)	0.22-0.58 (0.34±0.074)	0.45-1.20 (0.57±0.093)
PTW	-	0.14-0.19 (0.17±0.019)	0.17-0.40 (0.28±0.054)	0.40-1.0 (0.45±0.048)
EL	-	-	0.11-0.14 (0.12±0.065)	0.11-0.13 (0.13±0.007)
EW	-	-	0.06-0.06 (0.06±0.031)	0.07-0.09 (0.08±0.007)
FOL	0.34-0.48 (0.41±0.20)	1.13-1.40 (1.30±0.099)	1.25-1.93 (1.65±0.223)	1.78-2.33 (2.08±0.222)
PTL	-	0.80-1.23 (1.04±0.141)	0.75-2.05 (1.63±0.394)	3.03-3.78 (3.43±0.247)
VODL	-	0.68-0.90 (0.80±0.071)	0.75-2.10 (1.52±0.508)	3.15-3.88 (3.49±0.252)
BW%	23.1-32.3 (27.2±8.319)	14.1-17.3 (15.7±1.103)	9.8-17.0 (12.4±2.426)	8.4-14.6 (10.3±2.234)
FO%	42.1-46.2 (43.9±21.450)	21.8-33.7 (24.7±3.423)	15.6-36.5 (19.5±6.192)	10.7-14.2 (12.1±1.564)
T%	-	19.7-28.9 (25.5±2.605)	14.2-29.8 (24.2±4.976)	27.6-31.5 (28.9±1.307)
U%	-	15.4-22.3 (19.8±2.008)	13.72-3.5 (22.5±6.332)	26.3-32.3 (29.5±2.071)

Abbreviations: BL, body length; BW, maximum body width; CL, collar length; CW, collar width; OSL, oral sucker length; OSW, oral sucker width; PL, prepharynx length; PHL, pharynx length; PHW, pharynx width; OL, oesophagus length; CSL, cirrus-sac length; CSW, cirrus-sac width; VSL, ventral sucker length; VSW, ventral sucker width; OVL, ovary length; OVW, ovary width; MEL, Mehlis'gland length; MEW, Mehlis' gland width; ATL, anterior testis length; ATW, anterior testis width; PTL, posterior testis length; PTW, posterior testis width; EL, egg length; EW, egg width; FOL, fore body length; PTL, post-testicular region length; VODL, ventral sucker to ovary distance; BW%, body width as a percentage of body length; FO%, fore body as a percentage of body length; T%, post-testicular field as a percentage of body length; U%,ventral sucker to ovary distance as a percentage of body length

Table 4.4 (continued)

Body organ	Range (mean±SD) at age (day) PI			
	20 (n=2)	**25 (n=6)**	**30 (n=14)**	**35 (n=2)**
BL	15.20-18.63 (15.41±0.301)	13.60-18.93 (16.50±1.606)	15.80-19.70 (17.73±1.15)	14.25-18.33 (15.29±1.467)
BW	1.68-2.70 (1.78±0.141)	1.58-2.30 (1.84±0.151)	1.25-2.10 (1.83±0.28)	1.93-2.00 (1.96±0.053)
CL	0.35-0.97 (0.66±0.438)	0.35-0.85 (0.44±0.201)	0.35-1.00 (0.52±0.24)	0.45-0.81 (0.63±0.255)
CW	0.27-0.81 (0.54±0.382)	0.30-0.86 (0.75±0.220)	0.33-2.20 (0.92±0.48)	0.30-0.90 (0.60±0.424)
OSL	0.28-0.70 (0.30±0.028)	0.25-0.70 (0.27±0.027)	0.25-0.75 (0.34±0.15)	0.28-0.70 (0.30±0.028)
OSW	0.13-0.70 (0.20±0.099)	0.17-0.70 (0.26±0.050)	0.28-1.22 (0.44±0.31)	0.08-0.70 (0.20±0.170)
PL	0.08-0.22 (0.15±0.099)	0.12-0.22 (0.16±0.038)	0.10-0.30 (0.17±0.06)	0.12-0.24 (0.18±0.085)
PHL	0.20-0.38 (0.21±0.014)	0.20-0.40 (0.21±0.010)	0.22-0.55 (0.27±0.10)	0.23-0.40 (0.24±0.014)
PHW	0.20-0.42 (0.31±0.156)	0.17-0.42 (0.23±0.094)	0.20-0.50 (0.28±0.11)	0.25-0.43 (0.34±0.127)
OL	0.20-1.8 (0.54±0.477)	0.25-1.53 (0.97±0.410)	0.30-1.30 (1.10±0.29)	0.28-1.08 (0.68±0.566)
CSL	0.25-0.50 (0.38±0.177)	0.23-0.58 (0.32±0.134)	0.25-0.95 (0.36±0.21)	0.25-0.58 (0.41±0.230)
CSW	0.55-0.75 (0.65±0.141)	0.50-0.78 (0.59±0.110)	0.63-0.88 (0.72±0.09)	0.63-0.75 (0.69±0.088)
VSL	0.70-1.00 (0.76±0.088)	0.73-0.90 (0.76±0.026)	0.80-0.90 (0.84±0.03)	0.80-0.85 (0.83±0.035)
VSW	0.50-1.00 (0.60±0.141)	0.48-0.85 (0.71±0.133)	0.50-0.88 (0.78±0.10)	0.45-0.85 (0.65±0.283)
OVL	0.40-0.53 (0.46±0.088)	0.40-0.55 (0.48±0.055)	0.38-0.55 (0.49±0.05)	0.50-0.50 (0.50±0.000)
OVW	0.35-0.50 (0.43±0.106)	0.38-0.63 (0.49±0.092)	0.35-0.63 (0.46±0.08)	0.48-0.50 (0.49±0.018)
MEL	0.50-0.75 (0.63±0.177)	0.43-0.75 (0.59±0.114)	0.50-0.75 (0.61±0.11)	0.75-0.88 (0.81±0.088)
MEW	0.63-0.75 (0.69±0.088)	0.50-0.75 (0.63±0.079)	0.50-0.88 (0.70±0.11)	0.75-0.93 (0.84±0.124)
ATL	0.75-1.00 (0.75±0.000)	0.50-0.90 (0.76±0.151)	0.50-0.95 (0.83±0.13)	0.70-0.88 (0.79±0.124)
ATW	0.45-1.10 (0.49±0.053)	0.50-0.68 (0.57±0.068)	0.43-0.83 (0.58±0.12)	0.58-0.83 (0.70±0.177)
PTL	0.75-1.00 (0.75±0.000)	0.50-1.00 (0.77±0.175)	0.45-0.95 (0.82±0.14)	0.58-0.93 (0.75±0.247)
PTW	0.45-0.90 (0.49±0.053)	0.48-0.68 (0.54±0.074)	0.43-3.98 (0.86±1.10)	0.58-0.58 (0.58±0.000)
EL	0.12-0.12 (0.12±0.005)	0.12-0.13 (0.12±0.005)	0.01-0.13 (0.12±0.04)	0.13-0.14 (0.13±0.007)
EW	0.06-0.07 (0.07±0.007)	0.07-0.08 (0.08±0.004)	0.01-0.09 (0.07±0.02)	0.07-0.08 (0.07±0.005)
FOL	2.13-2.55 (2.34±0.301)	2.30-2.58 (2.47±0.102)	0.10-2.93 (2.48±0.84)	2.55-2.65 (2.60±0.071)
PTL	5.15-5.38 (5.26±0.159)	3.88- 5.75 (5.15±0.664)	0.21-6.18 (4.95±1.73)	3.75-4.85 (4.30±0.778)
VODL	3.95-3.98 (3.96±0.018)	3.48-5.65 (4.62±0.832)	0.17-5.93 (4.58±1.61)	4.10-4.28 (4.19±0.124)
BW%	11.0-12.0 (11.5±0.693)	8.9-13.1 (11.2±1.459)	6.85-12.66 (10.37±1.948)	11.8-14.0 (12.9±1.586)
FO%	9.2-11.5 (10.4±1.633)	8.8-12.5 (10.1±1.348)	0.40-12.02 (9.55±3.316)	11.2-11.8 (11.5±0.407)
T%	33.0-35.4 (34.2±1.698)	28.5-34.0 (31.1±1.954)	1.16-36.12 (27.98±9.642)	26.3-29.7 (28.0±2.399)
U%	25.3-26.2 (25.7±0.616)	24.0-31.2 (27.9±2.940)	0.92-30.71 (25.86±8.904)	26.2-28.7 (27.5±1.828)

Abbreviations: BL, body length; BW, maximum body width; CL, collar length; CW, collar width; OSL, oral sucker length; OSW, oral sucker width; PL, prepharynx length; PHL, pharynx length; PHW, pharynx width; OL, oesophagus length; CSL, cirrus-sac length; CSW, cirrus-sac width; VSL, ventral sucker length; VSW, ventral sucker width; OVL, ovary length; OVW, ovary width; MEL, Mehlis'gland length; MEW, Mehlis' gland width; ATL, anterior testis length; ATW, anterior testis width; PTL, posterior testis length; PTW, posterior testis width; EL, egg length; EW, egg width; FOL, fore body length; PTL, post-testicular region length; VODL, ventral sucker to ovary distance; BW%, body width as a percentage of body length; FO%, fore body as a percentage of body length; T%, post-testicular field as a percentage of body length; U%,ventral sucker to ovary distance as a percentage of body length

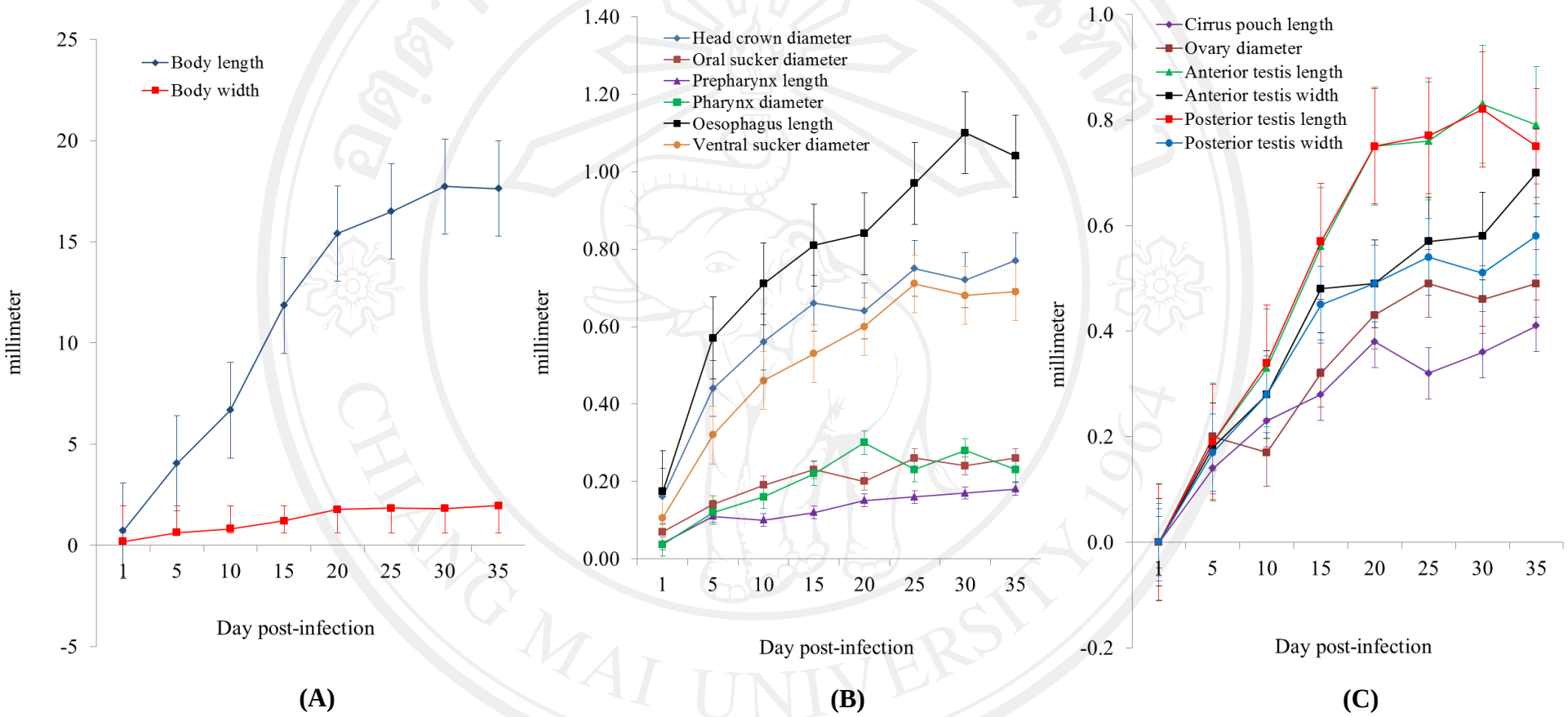

Figure 4.8 Changes of the morphological of *Echinostoma revolutum* recovered form experimental chicks; **(A)** Growth curves of the whole body, **(B)** parenchymal organs, **(C)** and reproductive organs. Vertical bars indicate standard deviations.

1. Newly excysted metacercaria:

Newly excysted metacercariae (O day old worms) was elongated and oval in shape, 610-1,150 μm long and 180-260 μm wide (Figure 4.9). The excysted metacercaria presence of the oral sucker, with a prominent head crown and collar spines, the ventral sucker, located near the equatorial line of the body, and 2 genital primordia was recognisable. The primordium of the cirrus pouch was seen near the anterior margin of the ventral sucker, and 1 primordium was visible in the posterior part of the body.

For the scanning electron microscopy (SEM) observations showed the topography surface of newly excysted metacecaria (Figure 4.11). The body of excysted metacercaria was elongated, ventrally concave and pointed posteriorly. The anterior half body surface was covered with numerous peg-like tegumental spines and became slightly finer posteriorly. Peg-like tegumental spines were densely distributed on the anterior surface to the posterior margin of ventral sucker level except the adjacent areas of the head crown devoid of spines, and became sparsely distributed and disappeared posteriorly. The anterior peg-like tegumental spines were larger than posterior tegumental spines. The oral sucker, circular and was situated subterminally at the antero ventral side of the body. The lip of the oral sucker was devoid of spines. The lip of oral sucker appeared wrinkled cytoplasmic processes and has ciliated knob-like structure papillae (Figure 4.10 F). Ciliated knob-like structure papillae appeared around the oral sucker, the areas of the head crown and sparsely over the body surface between the tegumental spines (Figure 4.10 F-H). The head crown was surrounded by 37 retractable, horseshoe-shaped collar spines, which were embedded in cytoplasmic pockets. The collar spines were arranged in a double row (oral and aboral), and had end grouped spines (corner spines) (Figure 4.10 A). Ventral sucker was median at one third of the body (Figure 4.10 E). Surface of the ventral sucker was covered with cytoplasmic processes arranged radially. On the lip of the ventral sucker was encircled with button shaped papillae (Figure 4.10 E). Of the circle of button shaped papillae located along outer margin of the ventral sucker. The excretory pore was terminal, and shown a smooth tegument (Figure 4.10 A).

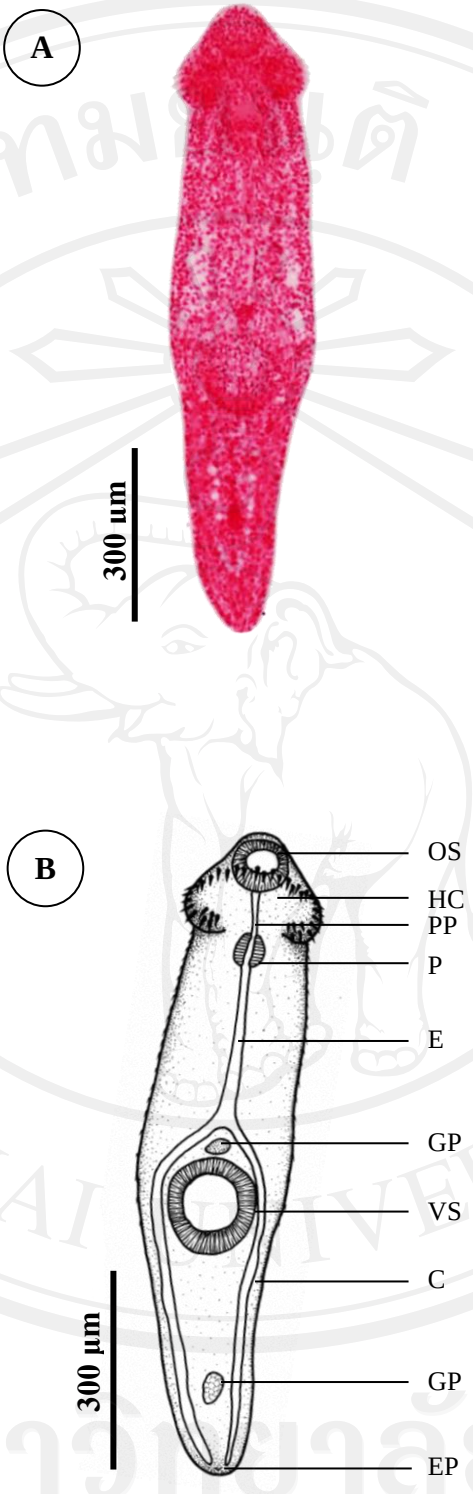

Figure 4.9 Illustration demonstrates morphology of newly excysted metacercaria, *Echinostoma revolutum*; **(A)** Photograph of permanent slide **(B)** Drawing.

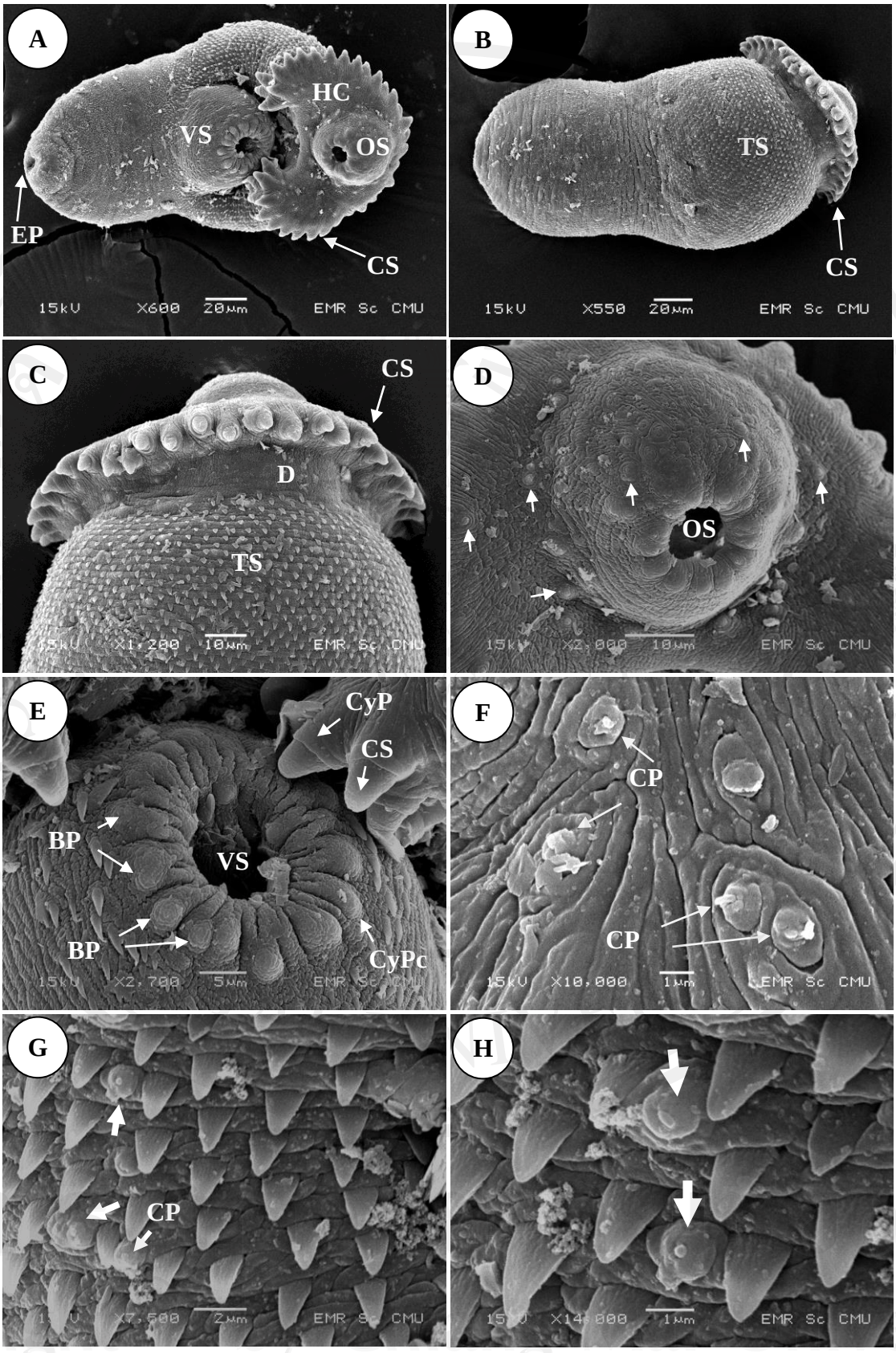

Figure 4.10

Figure 4.10 Scanning electron micrographs of an excysted metacercaria of *Echinostoma revolutum*: **(A)** The whole body (ventral view) showing the oral sucker (OS), head collar (HC), collar spines (CS), ventral sucker (VS) and excretory pore (EP); **(B)** The whole body (dorsal view) showing the tegumentary spines, head collar and collar spines; **(C)** Dorsal view of anterior tip of the body showing the collar spines, head collar and dorsal surface spines tegument separated by a space devoid of spines (D); **(D)** Head collar region showing the oral sucker and distribution of sensory papillae (arrowhead); **(E)** Middle part of body showing the ventral sucker is devoid of spines and has many button shaped papillae (BP) and showing group of corner spines containing collar spines and cytoplasmic pockets (CyP); **(F)** Tegumental surface of head collar region showing ciliated knob-like papillae (CP); **(G)** Anterior tegumental surface showing the peg-like tegumental spines and ciliated knob-like structure papillae between the tegumental spines; **(H)** Enlarge view of tegumental surface showing the ciliated knob-like structure papillae and tegumental spines.

2. Immature adult:

Worms recovered from day 1 to day 7 PI were juvenile stages of development (immature adult). On day 4 PI (Figure 4.11), the worms differed from the excysted metacerariae in the body size. Body was 2.65-3.56 mm long and 0.42-0.70 mm wide. The reproductive organs were developed but were not fully differentiated. Ovary was 87.5-130.0 μm long and 62.5-112.5 μm wide. Anterior testis was 67.5-140.5 μm long and 57.5-120.0 μm wide. Posterior testis was 67.5-160.0 μm long and 65.0-150.5 μm wide. The primordial seminal vesicle appeared but was not fully differentiated. Vitelline follicles were not observed. In parenchymal organs showed a well development than excysted metacercaria.

The surface topography of 4 day old worms were similar to excysted metacercaria in shape, but became much elongated and slightly curved ventrally, which a ventral depression between the oral sucker and ventral sucker (Figure 4.12 A-B). The posterior part of the worms develops more rapidly than the anterior part. The oral sucker, circular and was situated subterminally at the anteroventral side of the body (Figure 4.12 C-D). The lip of the oral sucker was devoid of spines. On lip of oral sucker appeared wrinkled cytoplasmic processes and has ciliated knob-like structure papillae. Ciliated knob-like structure papillae appeared around the oral sucker, the areas of the head crown and sparsely over the body surface between the tegumental spines (Figure 4.12 G). There were collar spines on the head crown, composed of 37 in number. The collar spines were partially covered by the tegument, with the distal end of the spines emerging from the cytoplasmic pocket of the tegument. Numerous ciliated knob-like structure papillae was densely distributed on the lip of the oral sucker, which were dispersed on the head collar tegument. Ventral sucker was median at one third of the body (Figure 4.12 E). Surface of the ventral sucker was covered with cytoplasmic processes arranged radially. On the lip of the ventral sucker, there were numerous button shaped papillae, distributed around the lip of ventral sucker. Peg-like tegumental spines were distributed at the anterior half of the body (Figure 4.12 F-H), over one third of the body, with the posterior half devoid of spines. The tegument, just posterior to the ventral sucker, showed a few sparsely distributed peg-like spines, and the anterior peg-like tegumental spines were larger than posterior tegumental spines.

The tegument in the middle of the body was transversely wrinkled, and covered with button shaped papillae (Figure 4.12 I). The tegument of the posterior extremity was devoid of spines and transversely wrinkled. The extreme posterior comes to a bluntly rounded point, at the end of which is located excretory pore. The excretory pore was terminal and prominent, with a defined rim (Figure 4.12 J).

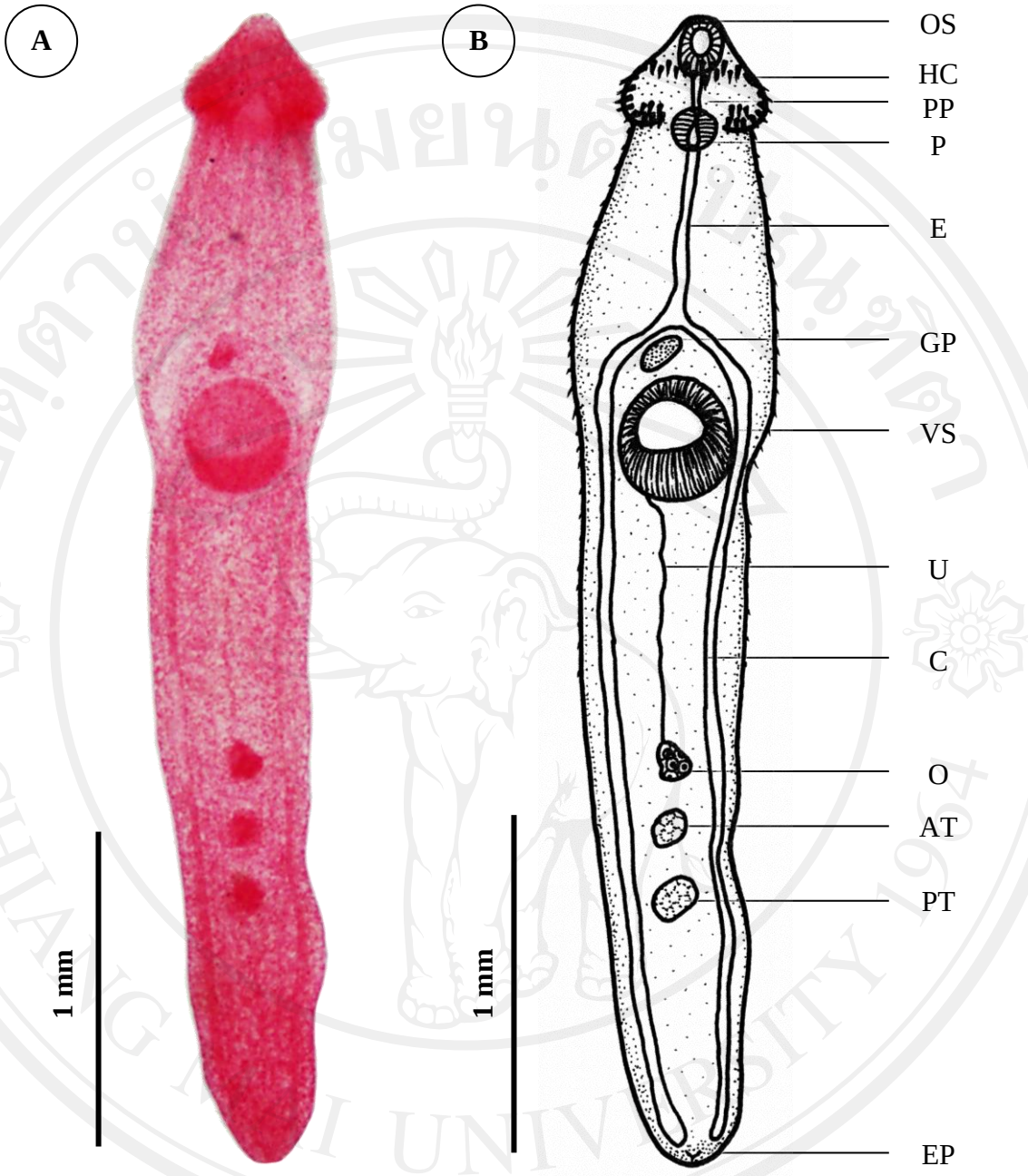

Figure 4.11 Illustration demonstrates morphology of immature adult, *Echinostoma revolutum* 4 day PI; **(A)** Photograph of permanent slide **(B)** Drawing.

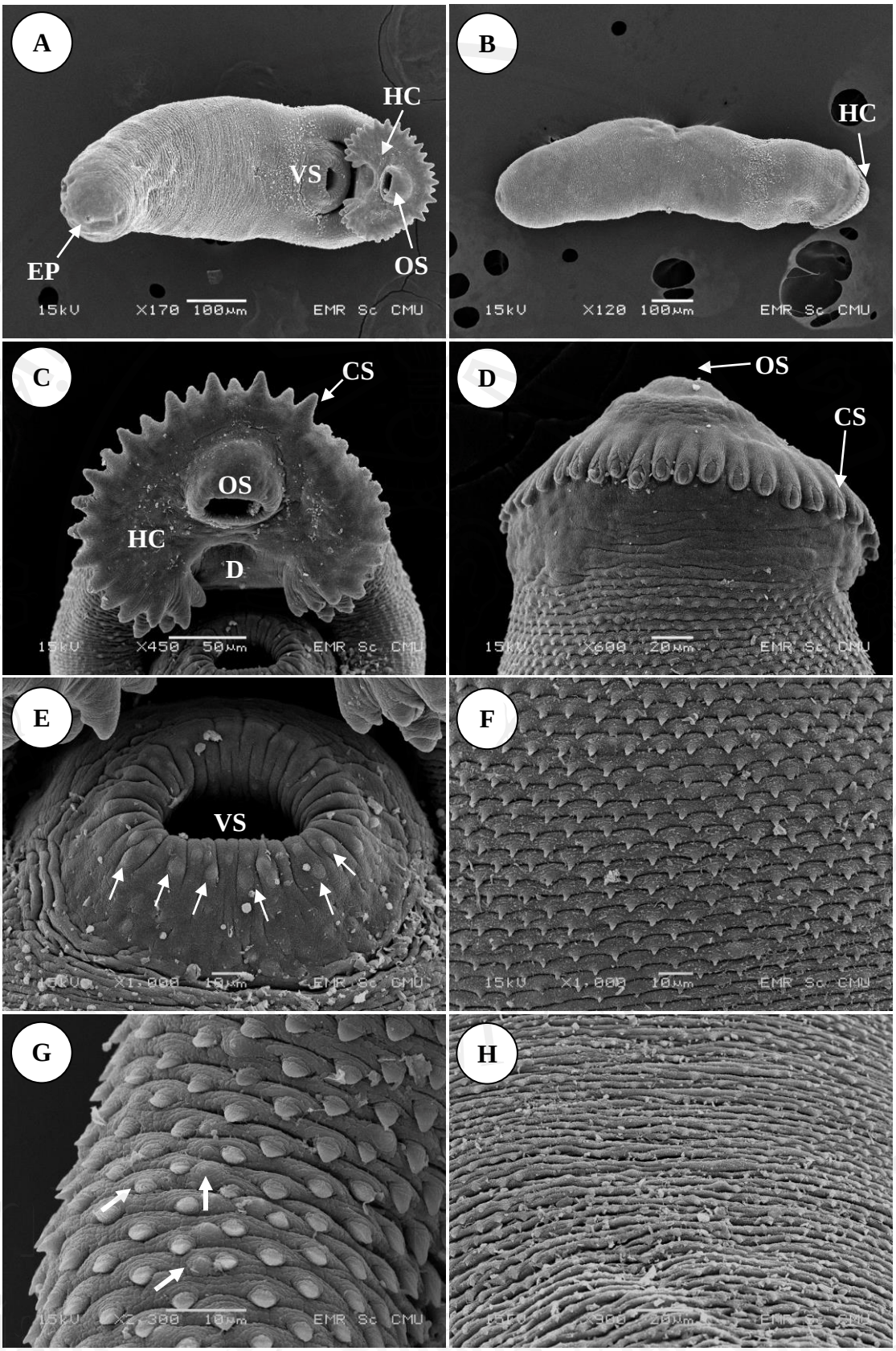

Figure 4.12

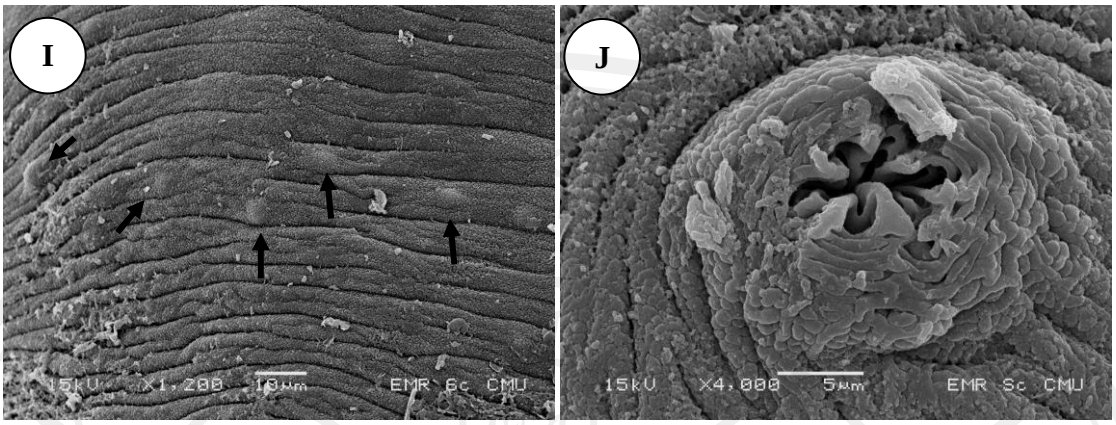

Figure 4.12 Scanning electron micrographs of immature adult (4 day old) of *Echinostoma revolutum*: **(A)** The whole body (ventral view) showing the oral sucker (OS), head collar (HC), ventral sucker (VS) and excretory pore (EP); **(B)** The whole body (dorsal view) showing the tegumentary spines and head collar; **(C)** Ventral view of head collar showing the oral sucker, collar spines (CS) and depression area (D) between the oral sucker and ventral sucker; **(D)** Dorsal view of anterior tip of the body showing the oral sucker, collar spines, head collar and dorsal surface spines tegument separated by a space devoid of spines; **(E)** Middle part of body showing the ventral sucker is devoid of spines and has many button shaped papillae (arrowhead); **(F)** Anterior tegumental surface showing the peg-like tegumental spines; **(G)** Enlarge view of anterior tegumental spines showing the peg-like tegumental spines and ciliated knob-like structure papillae (arrowhead) between the tegumental spines; **(H)** Tegumental spines of posterior showing a smaller than anterior tegumental spines; **(I)** Enlarge view of posterior tegumental surface showing a button shaped papillae (arrowhead); **(J)** The excretory pore.

3. Mature adult:

Mature adults were observed on day 8 PI (Figure 4.13), where the body was enlarged compared to that of 4 day old worm. Body was 6.7-8.3 mm long and 0.90-0.95 mm wide. Oral sucker was spherical or subspherical, located at ventro-subterminal, 205-292 μm long and 240-270 μm wide. The primordial seminal vesicle was fully differentiated into cirrus pouch, with the seminal vesicle, and extended beyond the anterior margin of the ventral sucker. Ventral sucker was 510-591 μm long and 490-565 μm wide. The reproductive organs were fully matured into the testes, ovary, Mehlis' gland and uterine tube, without eggs. Two testes and ovary increased greatly in size. Anterior testis was 480-550 μm long and 310-400 μm wide. Posterior testis was 500-550 μm long and 300-380 μm wide. The ovary, round in shape, was recognized as a separate, round mass. Ovary was 170-240 μm long and 200-290 μm wide. Vitelline follicles were observed became extended from the posterior end of the ventral sucker to the posterior end of the body.

SEM of mature adult worm showed that general topography similar to the juvenile stages (excysted metacercaria and immature adult), but much elongated and leaf-like (Figure 4.14 A-B). The posterior part of the worms develops more rapidly than the anterior part. The head collar which located at anterior end of the body (Figure 4.14 C) and the oral sucker located mainly in the middle of the collar. The collar region was ventral depressed that extended from the ventral sucker to the posterior end of the collar, and covered by tegumentary spines. The collar and the oral sucker are tegumentary spineless. A neck like space surrounding the posterior end of the collar which shaped like a ring is also spineless (Figure 4.14 F). The collar spines topography was similar to those of juvenile stages. The collar spines were partially covered by the cytoplasmic pocket of the tegument, with the distal end of the spines (Figure 4.14 D). On lip of oral sucker and the tegument of head collar has a numerous ciliated knob-like structure papillae (Figure 4.14 E). Ventral sucker located at anterior one-third of body and had winkled tegument and many button shaped papillae (Figure 4.14 G-H). The button shaped papillae are present on the outer lip of the sucker. The anterolateral surface was densely packed with peg-like tegumental spines and disappears at posterior extremity, which wrinkled transversely of tegument (Figure 4.14 J-M). Genital pore ventrally located near

anterior margin of the ventral sucker (Figure 4.14 I). Excretory pore was posterodorsal and prominent, with a defined rim (Figure 4.14 N).

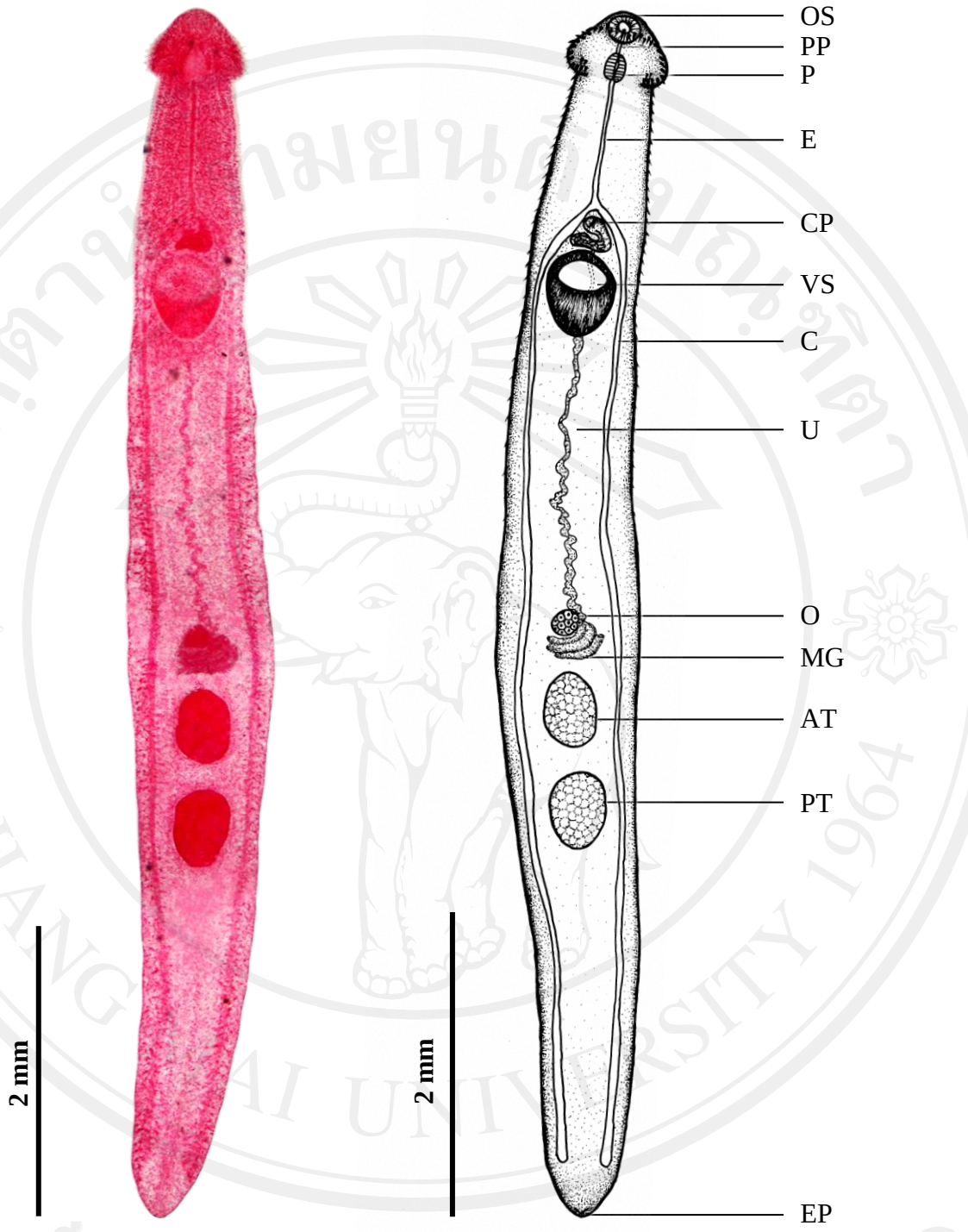

Figure 4.13 Illustration demonstrates morphology of mature adult, *Echinostoma revolutum* 8 day PI; **(A)** Photograph of permanent slide **(B)** Drawing.

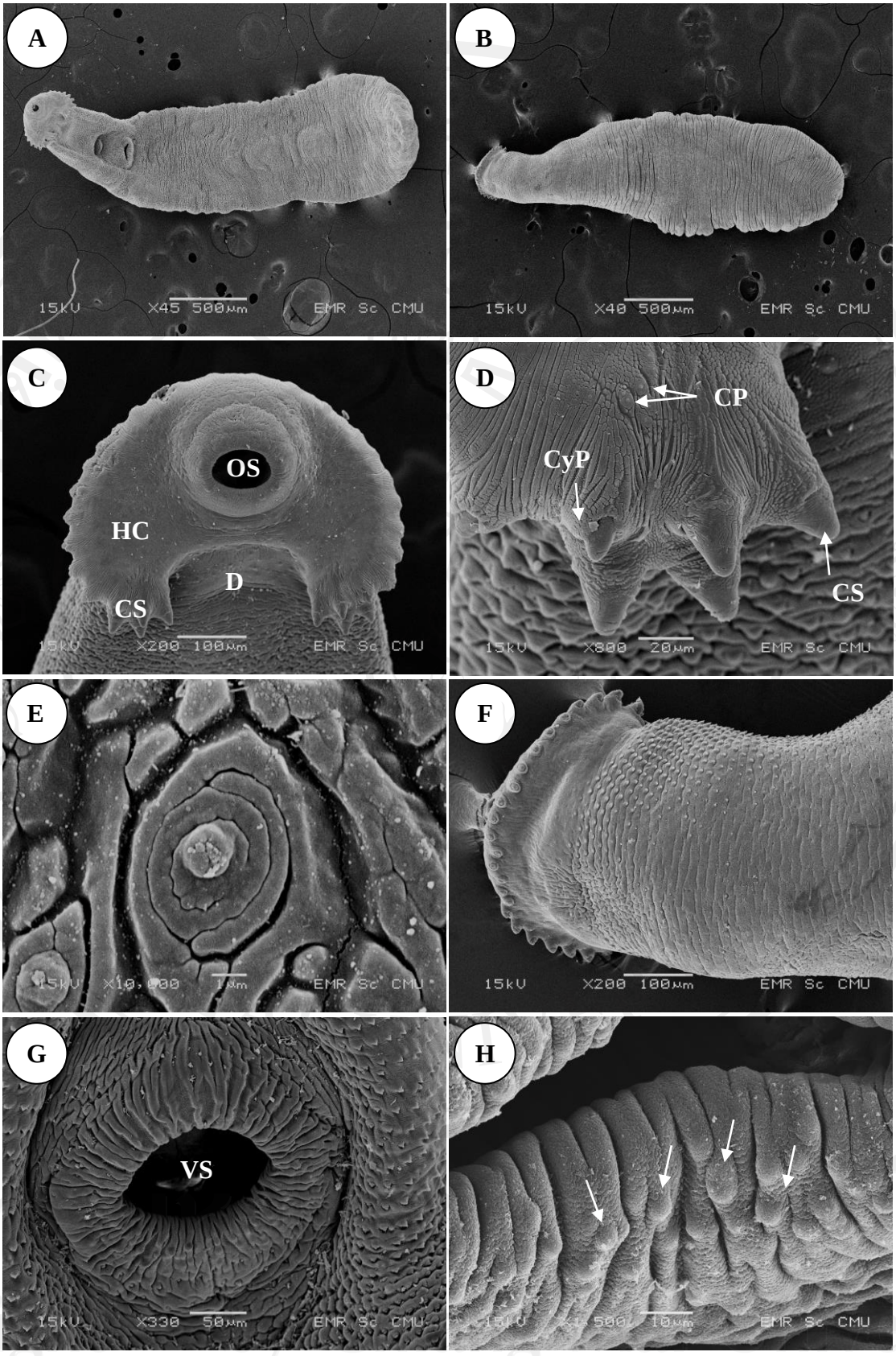

Figure 4.14

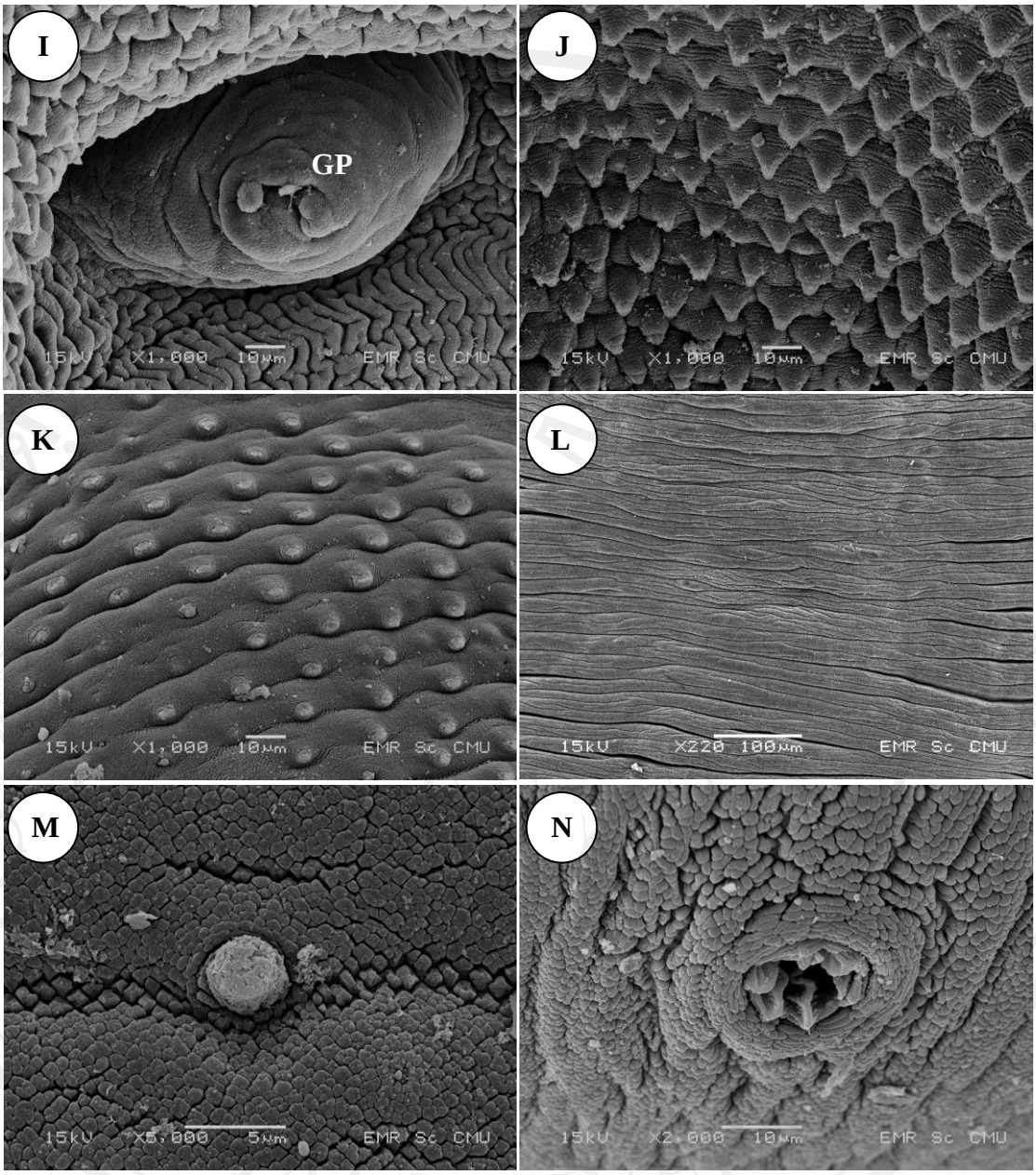

Figure 4.14

Figure 4.14 Scanning electron micrographs of mature adult (8 day old) of *Echinostoma revolutum*: **(A)** The whole body of adult showing the general topography on ventral view; **(B)** The whole body of adult showing the general topography on dorsal view; **(C)** Ventral view of anterior tip of the body showing the oral sucker (OS), head collar (HC), collar spines (CS) and depression area (D); **(D)** Group of corner spines (left side) showing the cytoplasmic pocket (CyP), retraction of collar spines and ciliated knob-like structure papillae (CP); **(E)** Ciliated knob-like structure papillae on the tegumental surface of head collar; **(F)** Dorsal view of anterior showing the collar spines, head collar and dorsal surface spines tegument separated by a space devoid of spines; **(G)** Ventral sucker (VS); **(H)** Enlarge view of the lip of ventral sucker showing the button shaped papillae (arrowhead); **(I)** Genital pore (GP); **(J)** Anterior tegumental surface (ventral) showing the peg-like tegumental spines; **(K)** Anterior tegumental surface (dorsal); **(L)** The tegument of the posterior body showing the transversely wrinkled and was devoid of spines; **(M)** Button shaped papillae on the tegumental surface of the posterior body; **(N)** The excretory pore.

4. Ovigerous adult:

Worms older than 10 days could be regarded as ovigerous adults. An ovigerous adult, the cirrus pouch well developed, with sperm in the seminal vesicle and eggs in the uterus. Ovigerous adult worms at day 14 PI (Figure 4.15) were elongated, 10.8-17.3 mm in length and 1.1-2.5 mm in width, dorso-ventrally flattened, somewhat attenuated at both ends, and ventrally slightly bent. Tegument of anterior body armed with numerous small spines which extended to the posterior end of ventral sucker. Head crown distinct, well developed, 300-700 μm long and 250-690 μm wide, with ventral ridge. On the basis of light microscopy study, general morphology of *E. revolutum* collar spines was described (Figure 4.16). The collar was located terminally around the oral sucker. The collar spines were varied in size (Table 4.5) and position. The arrangement around the collar is according to the formula 5-6-15-6-5 = 37, by forming a typical formula as follow. Two groups of five corner spines (50.0-66.7 μm long and 16.7-20.8 μm wide) are arranged on each left and right ventro-lateral lip of the head collar (Figure 4.16 A-C); one is medio-oral, two latero-oral, one medio-aboral, and one latero-aboral (3 oral and 2 aboral), which were relatively large in size. Two groups of six lateral spines (28.6-53.6 μm long and 10.7-16.7 μm wide) were arranged in single row, located on each left and right lateral surface of the head collar. The last one found closest to the corner spines (Figure 4.16 A, D). One group of fifteen spines was located dorsally in a double row (28.6-47.6 μm long and 9.5-14.3 μm wide). Eight of these were oral and 7 were aboral spines (Figure 4.16 A, E). These fifteen spines were represented three groups: one group of three spines found at mid-dorsal of the double row. One was central-aboral and two are located orally on the left and right sides of central-aboral spines. Two groups of six spines (3 oral and 3 aboral) were located on each left and right side, of the mid-dorsal three spines. Oral sucker ventro-subterminal, spherical or subspherical, 200-625 μm long and 130-675 μm wide and prepharynx absent or very shot. Pharynx well developed, muscular, elongate-oval, 160-400 μm long and 150-325 μm wide, oesophagus about 275-1,160 μm long. Intestinal bifurcation anterior to ventral sucker; intestinal caeca blind and extending almost to posterior extremity. Ventral sucker spherical, muscular, and very large, 525-980 μm long and 605-1,090 μm wide, middle located

and protruded ventrally. Testes 2, tandem, beginning at mid-hind body, elongate-oval, contiguous or nearly contiguous, slightly lobed or slightly irregular in outline; anterior testis, 775-1,154 μm long and 425-865 μm wide, posterior testis of a similar size, 700-1,154 μm long and 417-962 μm wide. Cirrus pouch well developed (Figure 4.17), elongate-oval, 200-550 μm long and 375-750 μm wide, antero-dorsal to ventral sucker, median and immediately preacetabular. Cirrus unarmed and unclear length. Genital pore median, immediately preacetabular, followed by genital atrium. Ovary spherical or nearly oval, compact, at or anterior to midbody, 430-577 μm long and 350-577 μm wide. Mehlis' gland located between the ovary and anterior testis. Vitellarium follicular, forming 2 lateral fields and extending from short distance posterior ventral sucker to the posterior body end. Uterus moderately developed, with intercaecal loops between ovary and ventral sucker. Eggs numerous, the number of uterine eggs was 83-284, egg size, 113.33-133.33 μm long and 60-80 μm wide. Eggs were operculated, elliptical, yellowish and thin-shelled. Excretory vesicle not observed, excretory pore opened at posterior extremity of the body.

Table 4.5 Measurements (in micrometer) of collar spines were based on 15 whole-mounted specimens.

Collar spines		**Range**	**Mean±SD**
Corner spines	length	50.0-66.7	60.84±4.52
	width	16.7-20.8	19.17±1.30
Lateral spines	length	28.6-53.6	45.83±4.43
	width	10.7-16.7.0	15.68±0.93
Dorsal spines	length	28.6-48.6	41.59±4.17
	width	9.5-14.3	13.65±1.10

SEM observations of ovigerous adults (14 day old) of *E. revolutum* showed the general surface ultrastructure. The ovigerous adult worms were elongated and leaf-like, with a distinct head collar, at the center of which is located the sub-terminal oral sucker (Figure 4.18 A-B). Collar well developed, with conspicuous

spines. The collar spines are slightly curved and pointed (Figure 4.18 D). A distinct corner group of five angle spines (Figure 4.18 F-G), slightly larger and more robust in form than those of the rest of the collar, is present at the edge of the collar on each side of the ventral gap. The 5 corner spines on each side were the most prominent ones and characteristic of collar spine cytoplasmic pocket were clearly visible. These spines are cylindrical body which having conical end and covered by the cytoplasmic pocket. Collar spines were retractable, but could be seen partially portion extended in only. Several ciliated knob-like structure papillae (Figure 4.18 E, H), especially on both sides of the oral sucker were observed on the collar tegument. Ventral sucker located at anterior one-third of body and had winkled tegument and many button shaped papillae (Figure 4.18 I-J). Body ventrally curved at ventral sucker level, forming small ventral concavity between ventral sucker and oral sucker. The anterolateral surface between the two suckers was densely packed with tegumental spines (Figure 4.18 L). The tegumental spines began at posterior level of the collar and extended to middle of ventral surface of the body to disappear at posterior extremity. Tegument posterior to ventral sucker and dorsal tegument were wrinkled transversely (Figure 4.18 M). Tegument of the collar and oral sucker were spineless. A neck like space surrounding the posterior end of the collar which shaped like a ring was also spineless and devoid of sensory papillae (Figure 4.18 C). The highly protrusible cirrus is located just anterior to the ventral sucker (Figure 4.18 K). Excretory pore was posterodorsal and prominent, with a defined rim (Figure 4.18 N).

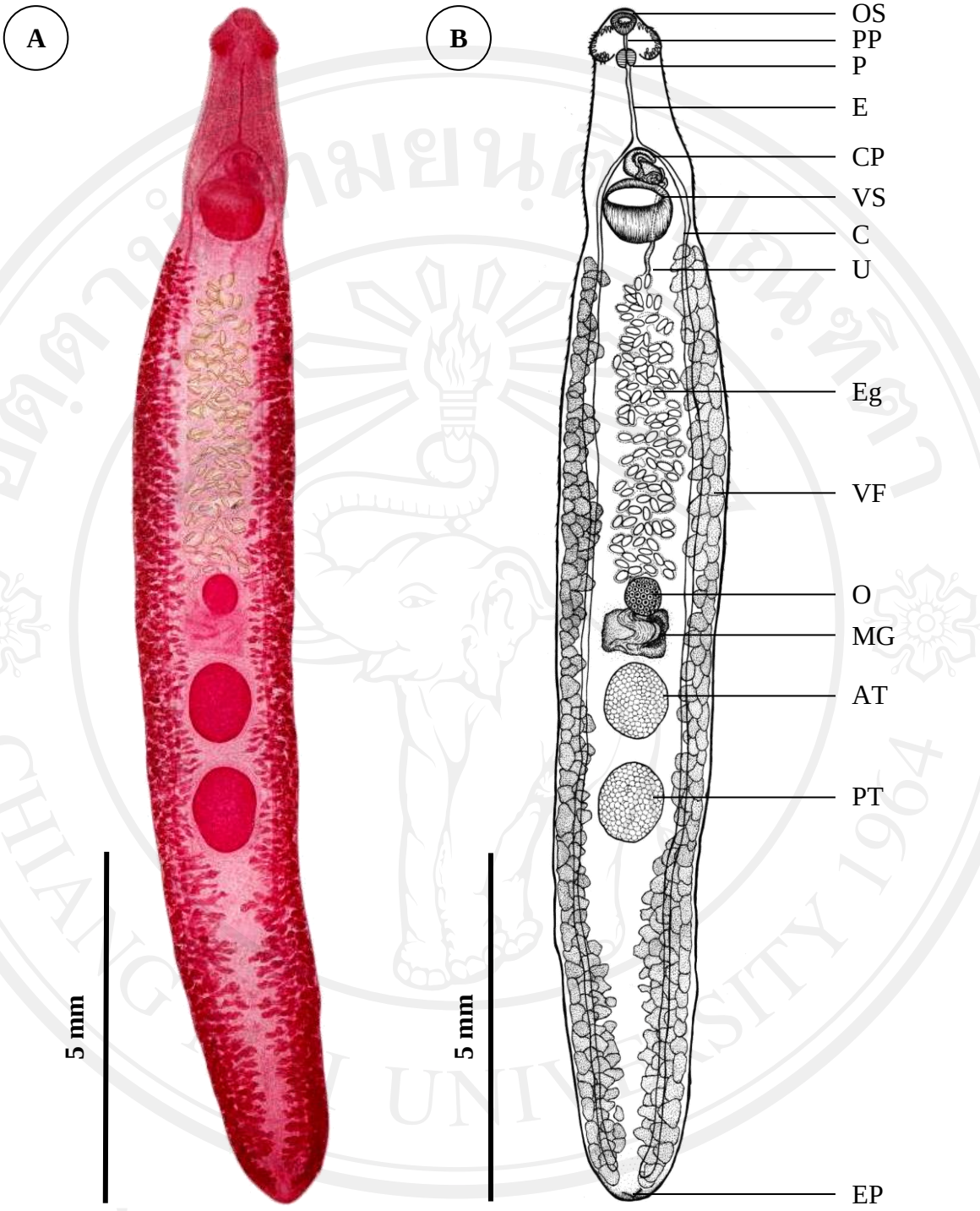

Figure 4.15 Illustration demonstrates morphology of ovigerous adult, *Echinostoma revolutum* 14 day PI. **(A)** Photograph of permanent slide **(B)** Drawing

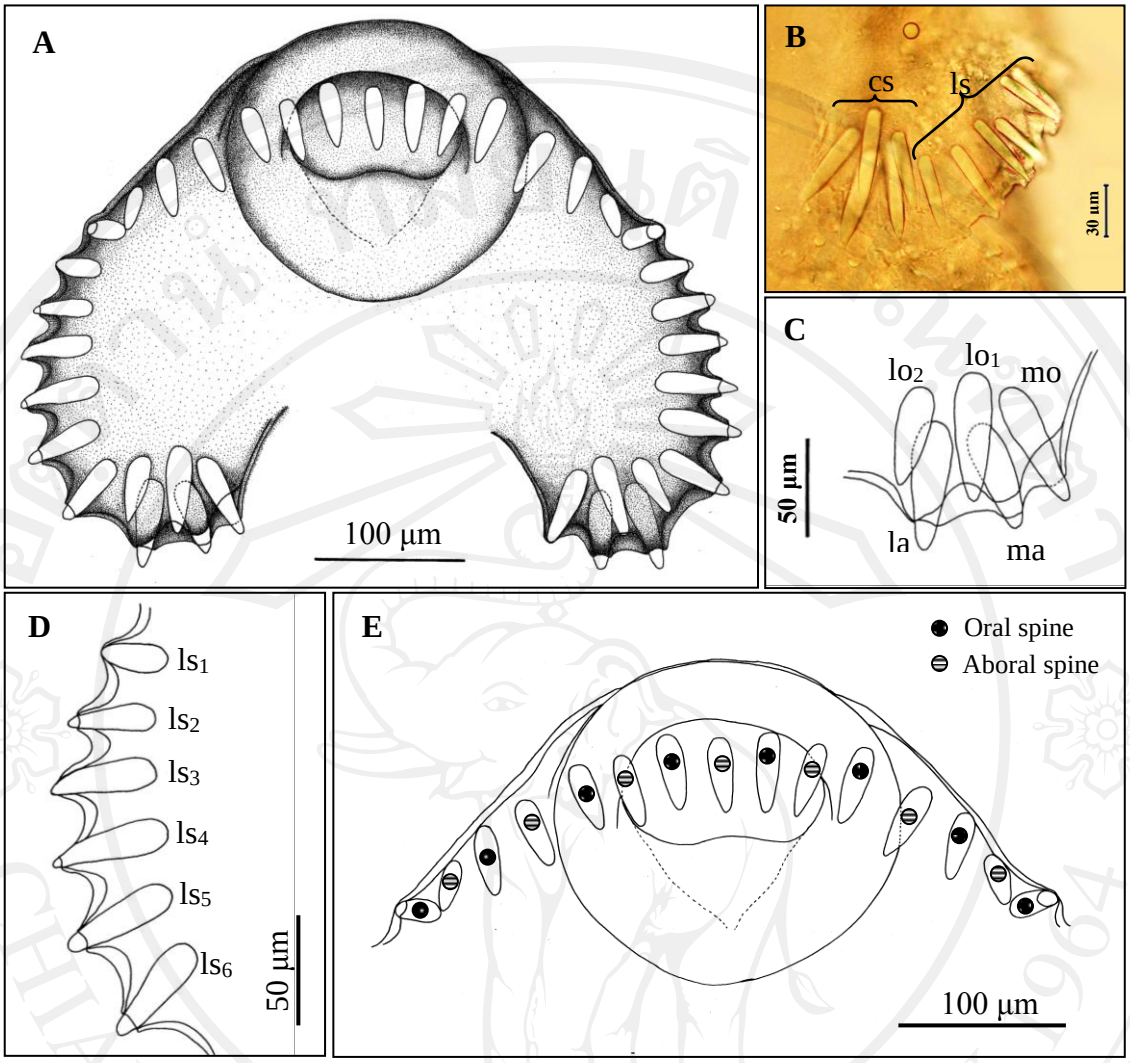

Figure 4.16 Illustration and light microscope views of the head collar of 14 day old worm (ventral view): **(A)** All 37 spines arranged as a complete crown; **(B)** Photograph of live specimen showed corner spines (right side); cs: corner spines, ls: lateral spines; **(C)** Corner spines (left side); la: latero-aboral spine, lo: latero-oral spines, ma: medio-aboral spines, mo: medio-oral spine; **(D)** Lateral spines (left side); ls: lateral spine; **(E)** One group of 15 spines was located dorsally in a double row. Eight of these were oral and 7 were aboral spines.

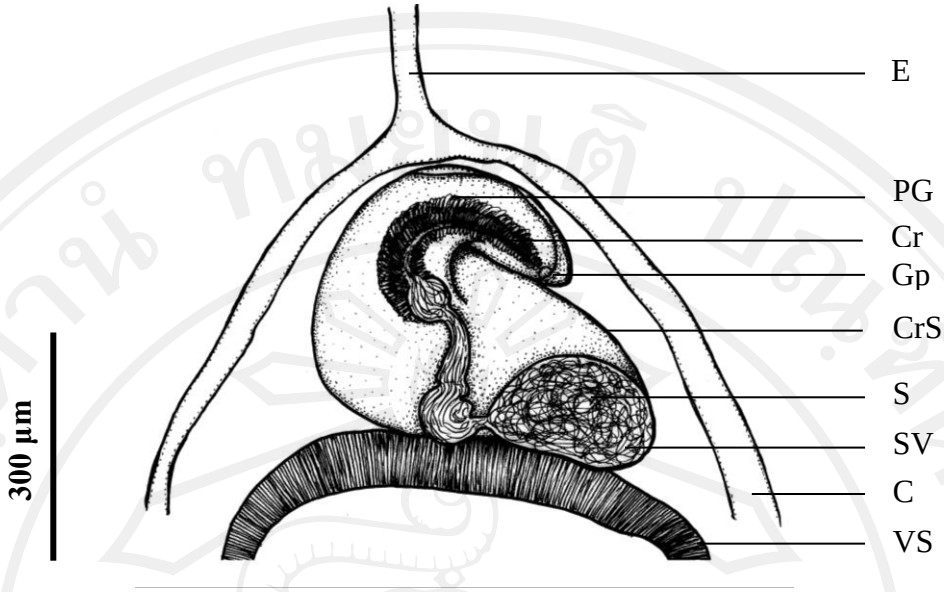

Figure 4.17 Illustration demonstrates morphology of cirrus pouch in 14 day old worm (ventral view).

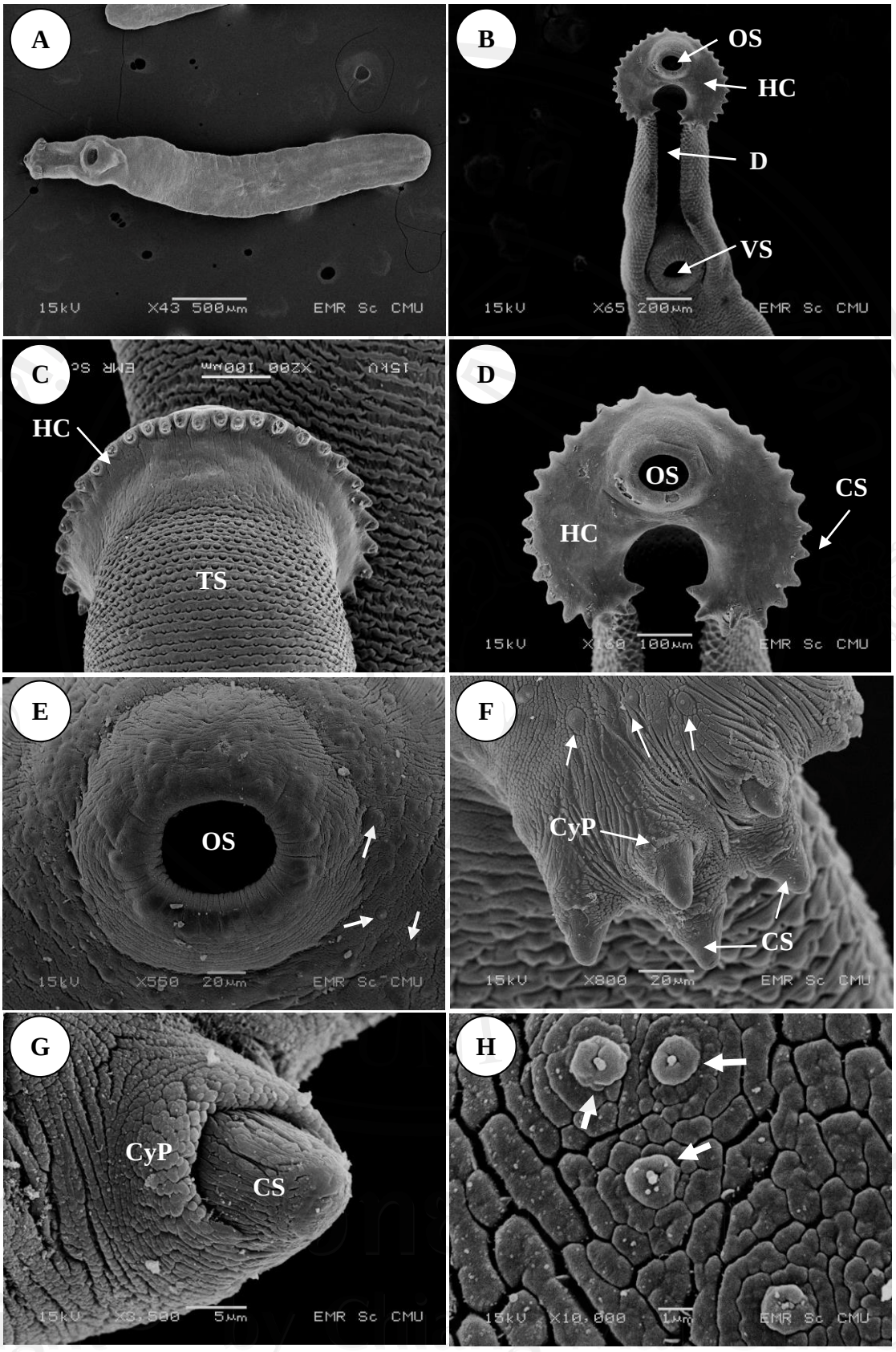

Figure 4.18

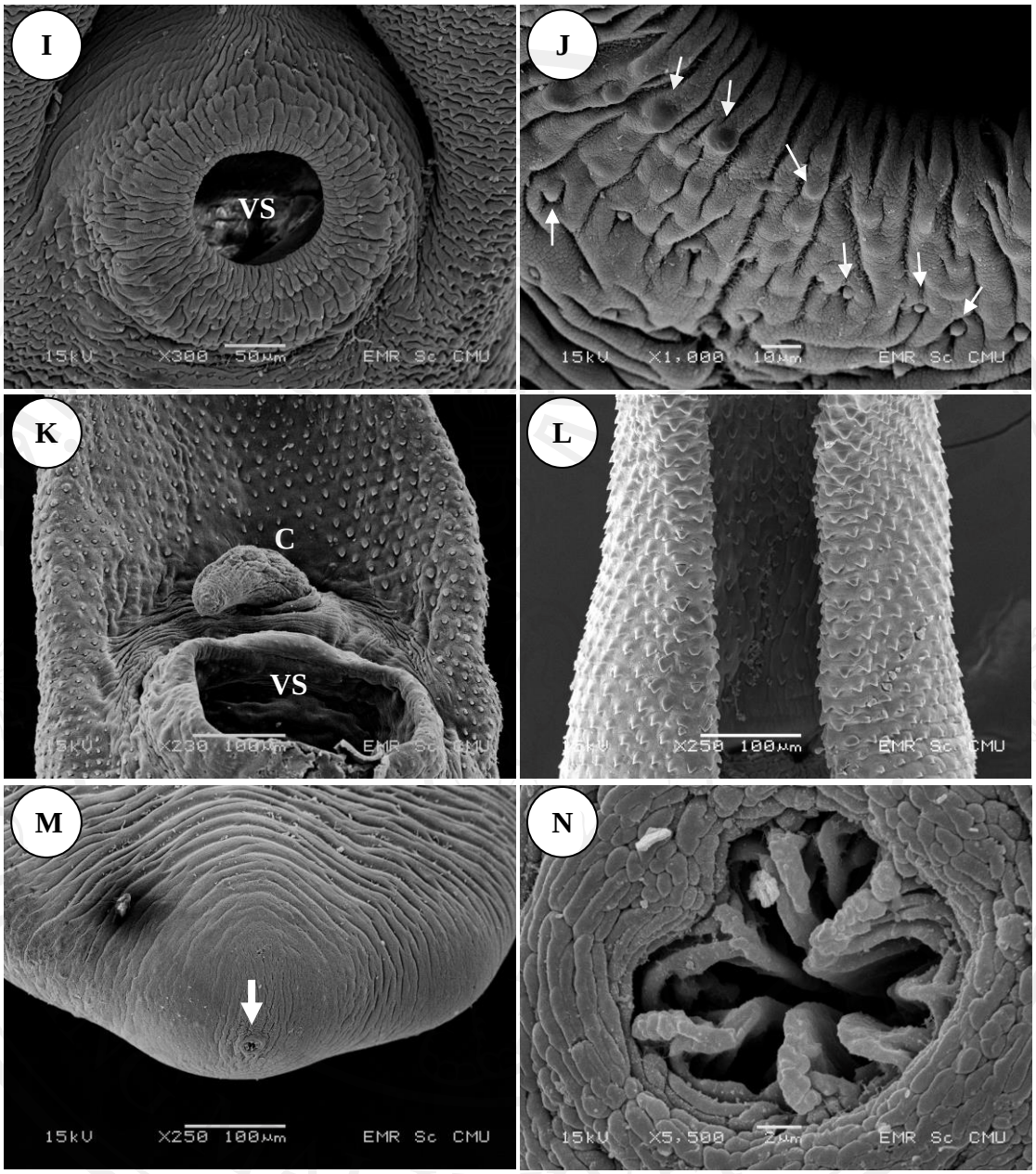

Figure 4.18

Figure 4.18 Scanning electron micrographs of an ovigerous adult (14 day old) of *Echinostoma revolutum*: **(A)** The whole body of adult showing the general topography on ventral view; **(B)** Ventral view of anterior tip of the body showing the oral sucker (OS), head collar (HC), collar spines (CS) and depression area (D); **(C)** Dorsal view of anterior tip of the body showing the head collar and dorsal surface spines tegument (TS) separated by a space devoid of spines; **(D)** Ventral view of head collar showing the oral sucker and collar spines; **(E)** Enlarge view of the oral sucker showing the sucker and the ciliated knob-like structure papillae (arrowhead) distributed around the oral sucker; **(F)** Group of corner spines (right side) showing the cytoplasmic pocket (CyP), retraction of collar spines and ciliated knob-like structure papillae (arrowhead); **(G)** Enlarge view of collar spine showing the cytoplasmic pocket and collar spines; **(H)** Ciliated knob-like structure papillae on the tegumental surface of head collar (arrowhead); **(I)** Ventral sucker (VS); **(J)** Enlarge view of the lip of ventral sucker showing the button shaped papillae (arrowhead); **(K)** Ventral view of middle part of the body showing the ventral sucker and unarmed cirrus (C) was protrude from the genital pore; **(L)** Anterior tegumental surface (ventral) showing the peg-like tegumental spines; **(M)** The tegument of the posterior extremity was devoid of spines and transversely wrinkled and the excretory pore was terminal (arrowhead); **(N)** Enlarge view of the excretory pore.

4.2.2 Fecundity of worm

The worms were ovigerous and began to produce eggs on day 10 PI. Based on the eggs in feces (Figure 4.19), they first appeared 10 day PI (Figure 4.21) and egg release was continuous from the first day until day 36 PI. Egg per gram of feces per worm (EPG/worm) increased slowly and showed a little fluctuation during days 10-22 PI and then slowly decreased until day 36 PI. After that, the worms were expelled from the chicks by day 37 PI. Figure 4.20 also shows that the uterine egg counts per worm (UEC/worm) during early appeared in uterus (10 day PI) to the end of experiment. The UEC/worm rapidly increased during the first two weeks of infection and the mean number of UEC/worm observed daily was 172.8±64.6. When the UEC/worm and EPG/worm were plotted, no correlation was observed between those 2 parameters (*r=0.06*). The worm recovery and number of EPG/worm were highly correlated (*r=0.98*), also the correlation coefficient of worm recovery and UEC/worm were relatively high (*r=0.58*) (Figure 4.20).

Mature worm eggs were collected from chick feces for examination. The morphology of *E. revolutum* eggs were photographed under a light microscope (LM) and SEM (Figure 4.22-Figure 4.23). LM observations revealed the structures of the operculum and abopercular region. The eggs were ovoid, pyriform or elliptical, operculate and yellow-brown. They are unembryonated, with a smooth shell with a definite knob like thickening at the abopercular end of the shell. The eggs of *E. revolutum* were 113-133 μm long and 60-80 μm wide. As determined by SEM, the surface ultrastructure of the eggs showed that the egg shell surface is smooth and has operculum. The operculum was smooth and surrounded by an opercular junction (Figure 4.23 C). The abopercular knob is wrinkled invaginates the egg shell (Figure 4.23 D).

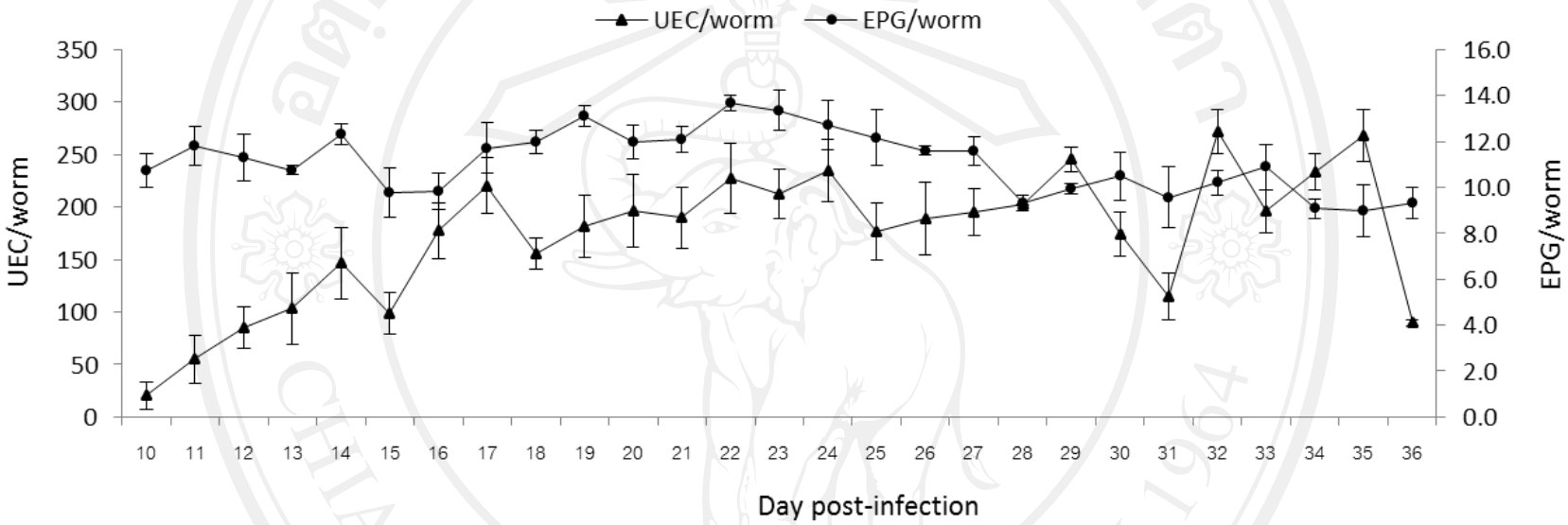

Figure 4.19 Number of uterine egg counts per worm (UEC/worm) and egg per gram of feces per worm (EPG/worm) detected during experimental from day 10-36 post-infection. Vertical bars represent the standard deviation.

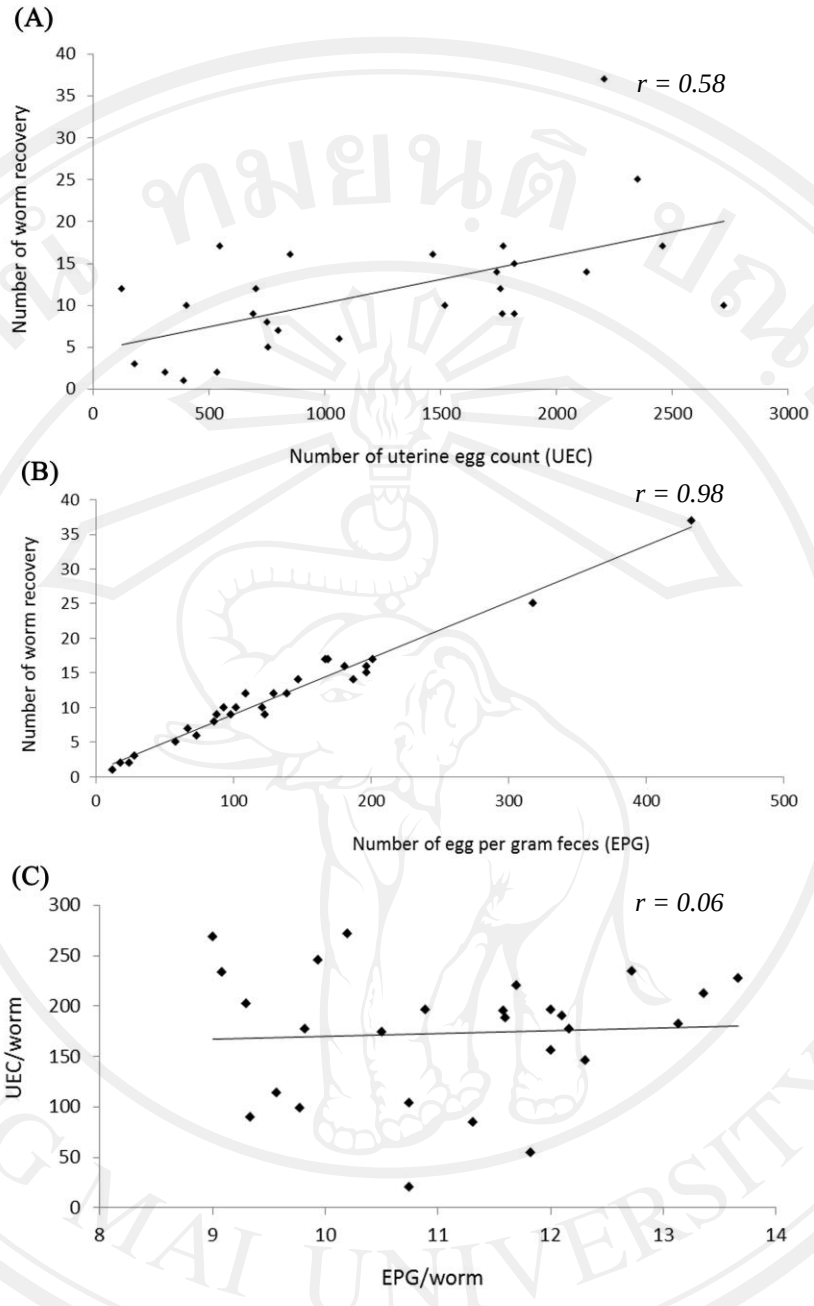

Figure 4.20 Illustrated the correlation among the parameters used in fecundity study: **(A)** Correlation of the worm recovery and uterine egg counts (UEC); **(B)** Correlation of worm recovery and egg per gram of feces (EPG); **(C)** Correlation of UEC per worm (UEC/worm) and EPG per worm (EPG/worm).

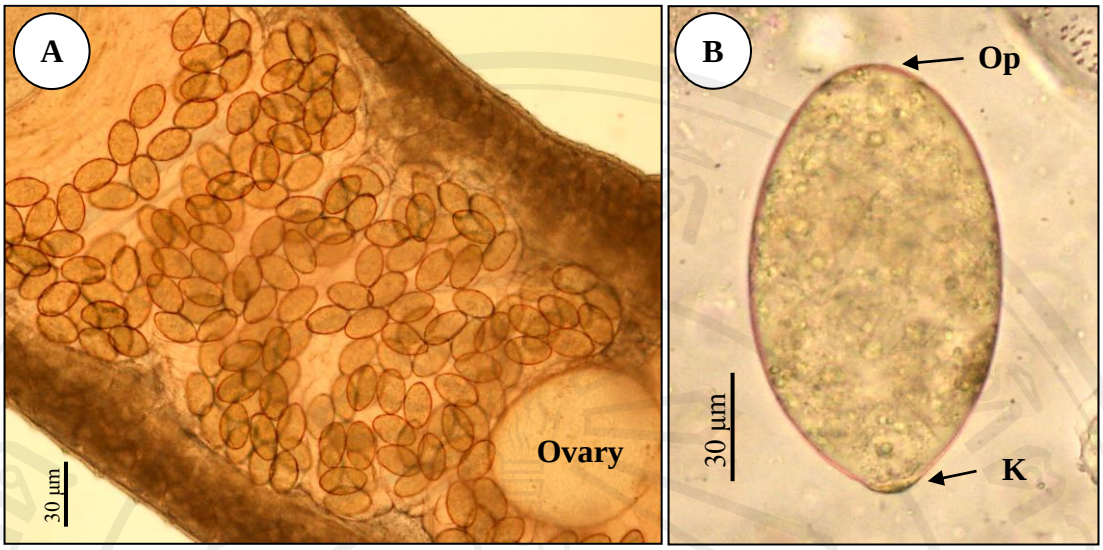

Figure 4.21 Egg of *Echinostoma revolutum*. **(A)** Photograph of eggs in uterus (compressed under cover slip); **(B)** Photograph of a newly laid egg, collected from chick feces showing the operculum (Op) and abopercular knob (K).

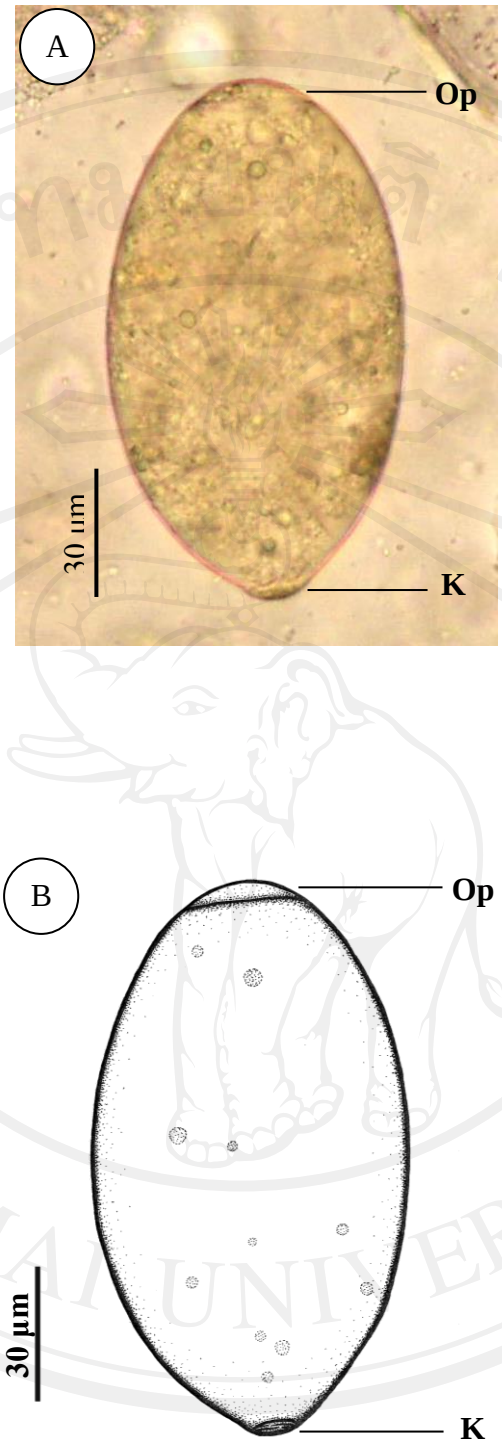

Figure 4.22 Illustration demonstrates morphology of egg of *Echinostoma revolutum* collected from chick feces 14 day PI; **(A)** Photograph **(B)** Drawing.

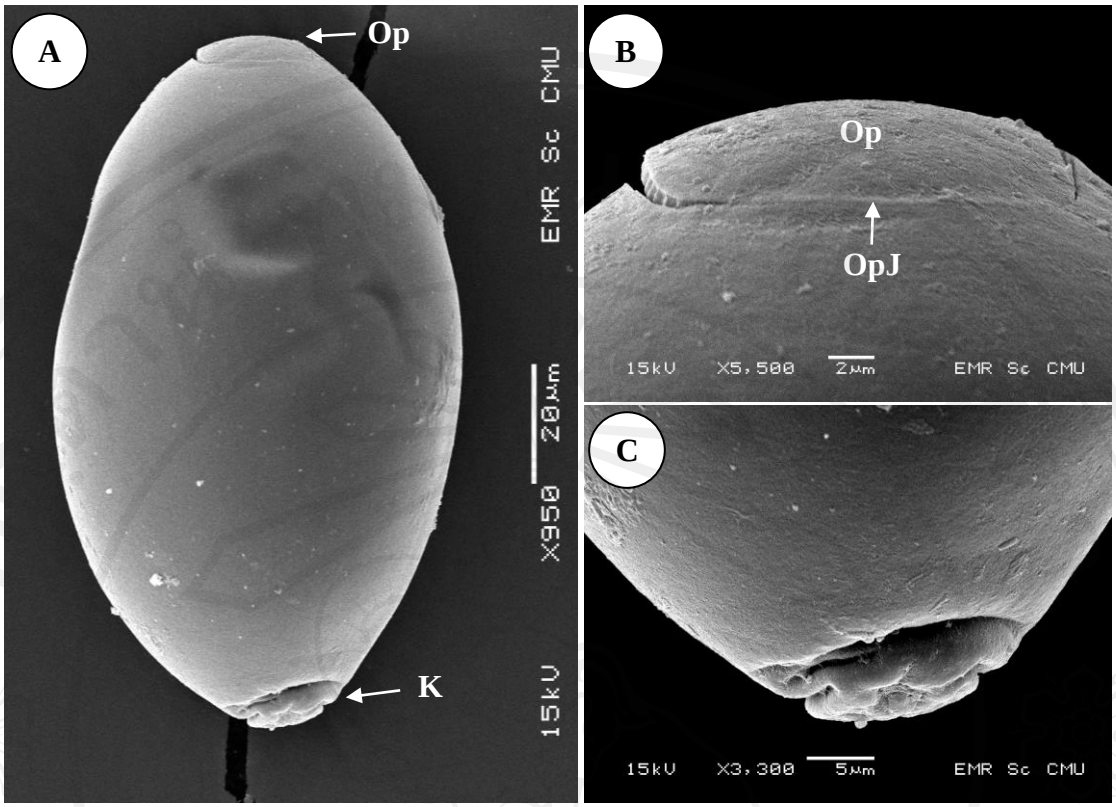

Figure 4.23 Scanning electron micrographs of egg of *Echinostoma revolutum*: **(A)** The surface ultrastructure of the eggs showing the egg shell surface was smooth with the operculum (Op) and abopercular knob (K); **(B)** Enlarge view of operculum showing the operculum and operular junction (OpJ); **(C)** Enlarge view of the abopercular knob.

4.2.3 Collection and incubation of the eggs

1) Observations of egg development and hatching of the miracidium

Egg development is shown in Figure 4.24. The mature eggs were unembryonated when laid (day 0). In 1-3 day old eggs there are clusters of vitellocytes, which are small cells peripheral to the early embryo, like foam bubbles. The vitellocystes became progressively smaller and then not apparent. In 4 day-old eggs the vitellocytes surrounded the embryo. In 5 day-old eggs, there is a spherical core of cells forming the developing embryo with clusters of vitellocytes. In 6 day-old eggs, the growing embryo is surrounded by a layer of vitellocytes. In 7 day-old eggs have larger enlarged embryo, contained in defined clusters of vitellocystes and balloon-like vesicles. At days 8 to 9 the embryo began to resemble a miracidium, contained balloon-like vesicles. The embryo developed a body with cilia and the embryo had attained nearly the same size as the miracidium with apical papillae and the eye spots obvious in 9 day-old eggs. At day 10, the miracidia was oriented along the long axis of the egg and the balloon-like vacuoles filled with a clear refrainment fluid. The vacuoles incompletely encircled the miracidium and they fill a large space between the shell and the miracidium. Most eggs had two vesicles, but some three or only one. Fully developed miracidia were observed by days 10-11 and hatched later.

Miracidia formed within a week and developed slowly. The first miracidia hatched at day 10 and eggs usually hatched in greater numbers by day 11. The miracidia showed slight motility within the eggs, with the larva moving longitudinally from the posterior end to the anterior end of the egg. The miracidial tegument is ciliated and began to beat and showed bending movements. Newly hatched miracidia swim rapidly and change direction frequently. In this study, under laboratory conditions, the longevity of newly hatched miracidia was 4-6 hours at room temperature. Miracidia swam actively during 4 hours, and swimming slowed down for the next 6 hours. The maximal life span was about 8 hours.

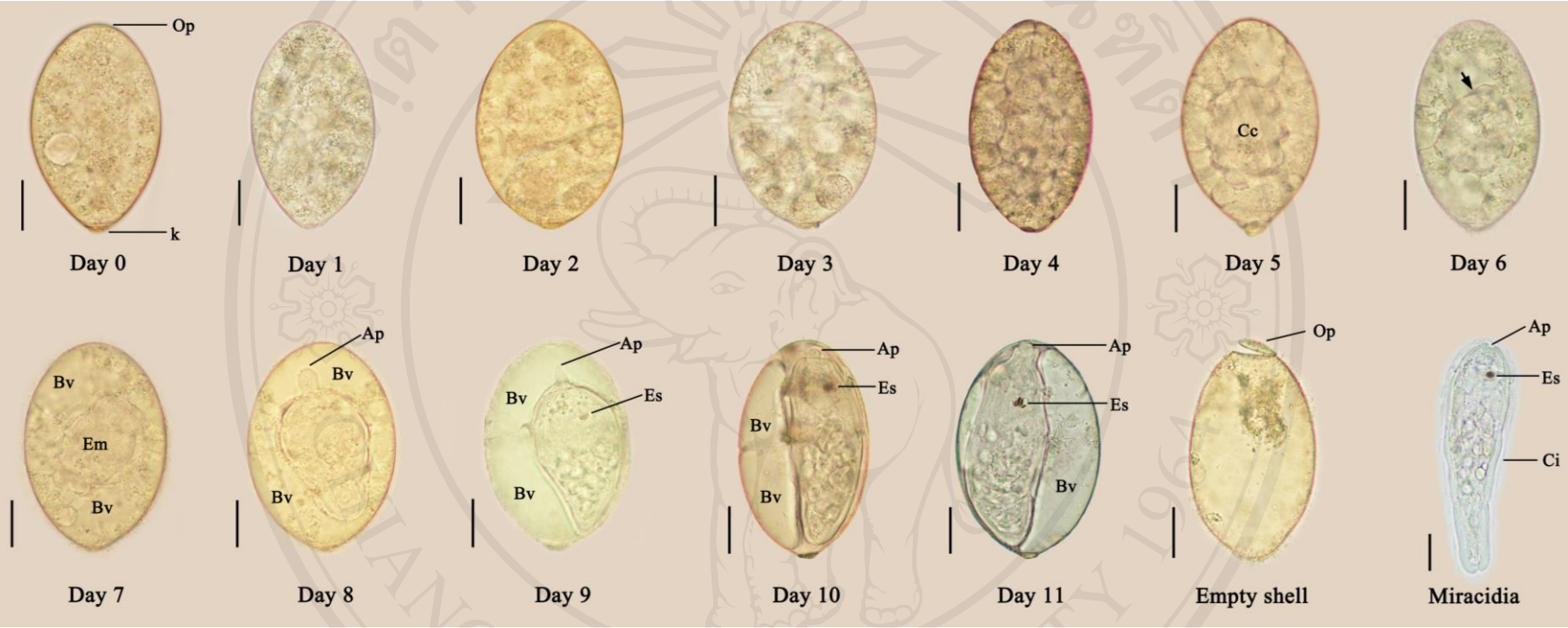

Figure 4.24 Light micrographs of egg development to form mature miracidia of *Echinostoma revolutum*. Note the operculum (Op), abopercular knob (K), the central core cell (CC), the embryo (Em), balloon-like vesicle (Bv), apical papilla (Ap), eye spots (Es), Cilia (Ci) and layer of vitellocytes (arrowhead); Scale bar = 30 μm.

2) Description of miracidium

The miracidium presented a range of variation in size, the length of the body was 99.2-152 μm (Figure 4.25-Figure 4.27), broad anteriorly, and tapering posteriorly to a blunt end and the tegument is ciliated. It has prominent apical papilla, two dark-brown eye-spots, consisting of one paired of pigmented bodies are located side by side. Eye spot are located at the end of the first anterior quarter. Excretory system comprises two flame cells on either side of body, two excretory ducts with two excretory pores. Germinal mass represented by several germ ball cells in middle and posterior parts of body. Neutral red staining showed the appearance of live miracidia, including the apical papilla, germinal mass, eyespots, and two flame cells (Figure 4.25; not all of these structures are seen in this figure). A miracidium fixed and stained in acetocarmine showed the almost location of germinal cells in the middle and posterior of the miracidial body (Figure 4.26-Figure 4.27).

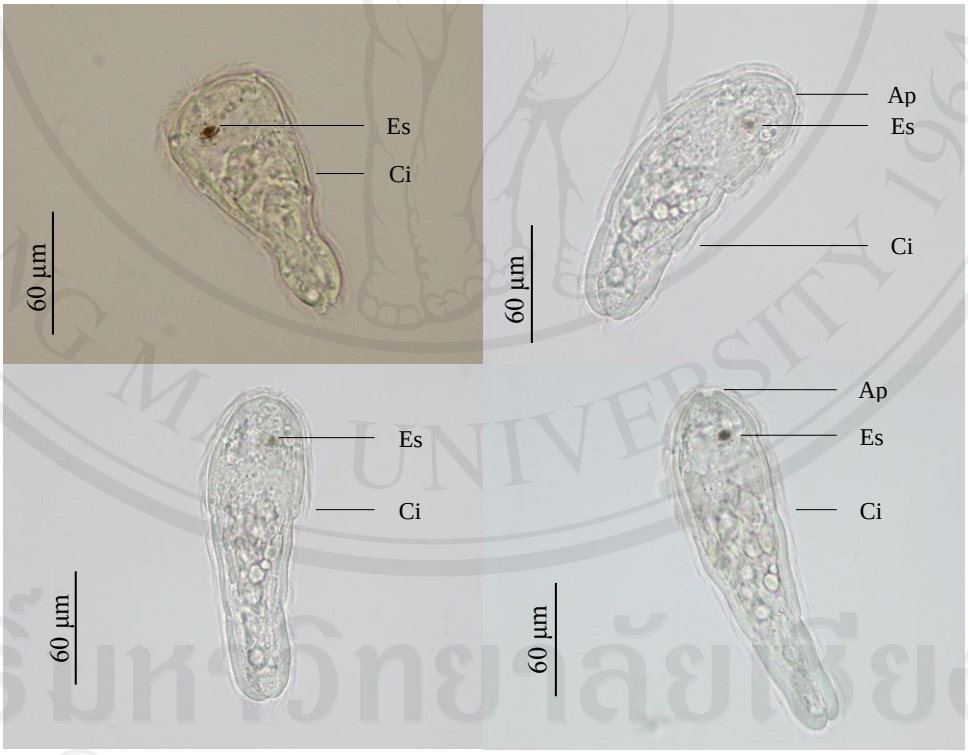

Figure 4.25 Light micrograph of newly hatched miracidia of *Echinostoma revolutum* on day 11 after incubation. Abbreviations: Ap, Apical papillae; Es, Eye spots; Ci, Cilia.

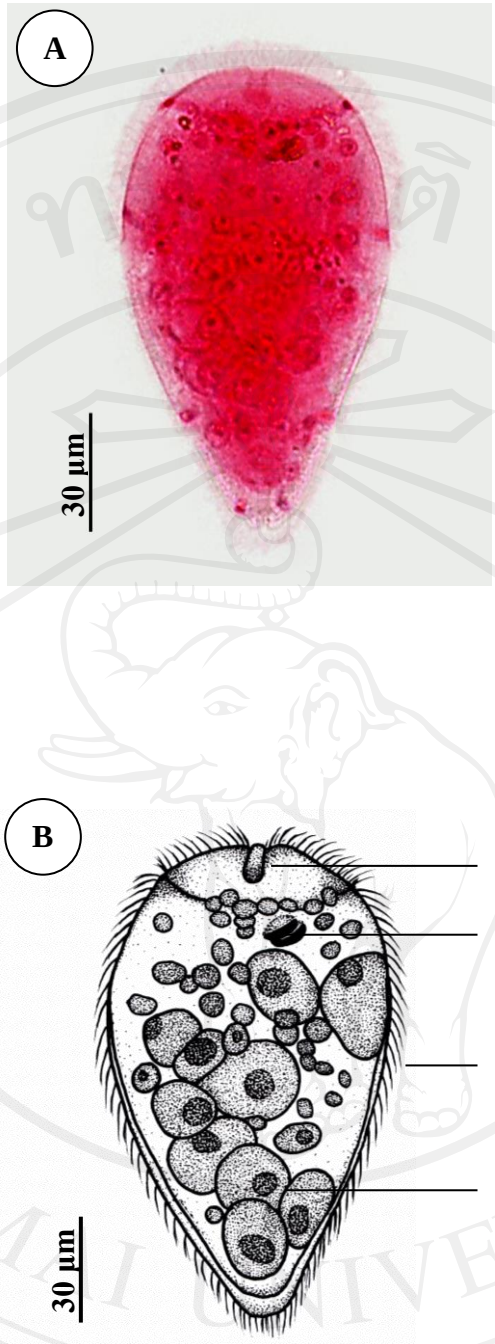

Figure 4.26 Illustration demonstrates morphology of miracidia (contraction form); **(A)** Photograph of permanent slide **(B)** Drawing. Abbreviations: Ap, Apical papillae; Es, Eye spot; Ci, Cilia, Gc, Germ ball cell.

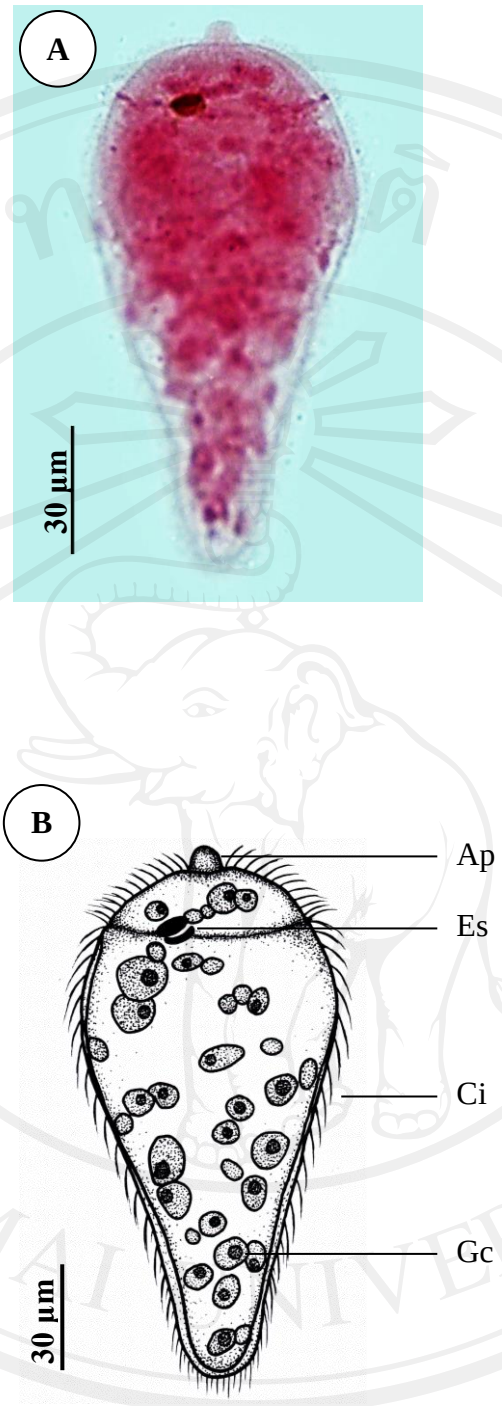

Figure 4.27 Illustration demonstrates morphology of miracidia (relaxing form); **(A)** Photograph of permanent slide **(B)** Drawing**.** Abbreviations: Ap, Apical papillae; Es, Eye spot; Ci, Cilia, Gc, Germ ball cell.

4.2.4 The first intermediate host infections

Experimental infections of the first intermediate host snail with miracidium were taken after complete hatching of the eggs. The expose hosts were investigated for the intramolluscan stages included: sporocysts, rediae (mother redia and daughter redia) and cercariae.

Our results on the infectivity of miracidia to the different snail species under experimental conditions, only viviparid snails: *F. doliaris* and *F. martensi martensi* became infected, but the attempt to infect *L. auricularia rubiginosa* failed. In this study, the sporocysts were observed in snails examined 7 days PI. The mother rediae were recorded in snails examined 16 days PI, and 60 days PI for daughter rediae. The cercarial emergence occurred 60 days PI. The prepatent period in each snail species were observed. The prepatent period in each snail species not differences were detected. The intramolluscan phase of development took at least 2 months.

The description presented below is based on several of specimens retrieved from the infected snails. Morphological traits were studied and measured using the microscope Olympus equipped. All measurements and scales are in micrometers unless otherwise stated.

1) Sporocyst (Figure 4.28-Figure 4.30)

Description: The penetrated miracidia reaches the ventricle of the snail and remains there, where they arrived about 7 days after exposure of snail to miracidia. Sporocysts developed within the cavity of snail heart and attached to ventricle cavity of snail heart, but difficult to separate from the surrounding snail tissues. Sporocysts of days 7 PI were pyriform in shape, 100-156 μm in length and 60-98 μm in width, generally containing germ balls. They developed into contractile, elongate sacs attached by their broader end to heart muscle and with narrow end free in heart cavity. Sporocysts of 10 days old measured 127-180 μm long by 74-12 μm wide; 12 day old sporocysts measured 150-215 μm long by 86-120 μm wide, and 14 day old sporocysts measured 180-236 μm long by 114-160 μm wide. Birth pore of sporocysts were difficult to observed. Sporocysts were almost pyriform in shape and contain several germ balls. They were motionless,

opaque white in colour and with thin and transparent body walls. Body a smooth tube tapering towards each end, capable of pronounced extension and contraction. They presented variable sizes and shapes, from long to small and ovoid sacs. After 14 day old sporocysts, contain several germ balls. They produce first generation rediae which migrate to the heamolymph space surrounding visceral approximately 18 days PI.

Site of infection: ventricle cavity of snail heart

Experimental hosts: Filopaludina doliaris and *F. martensi martensi*

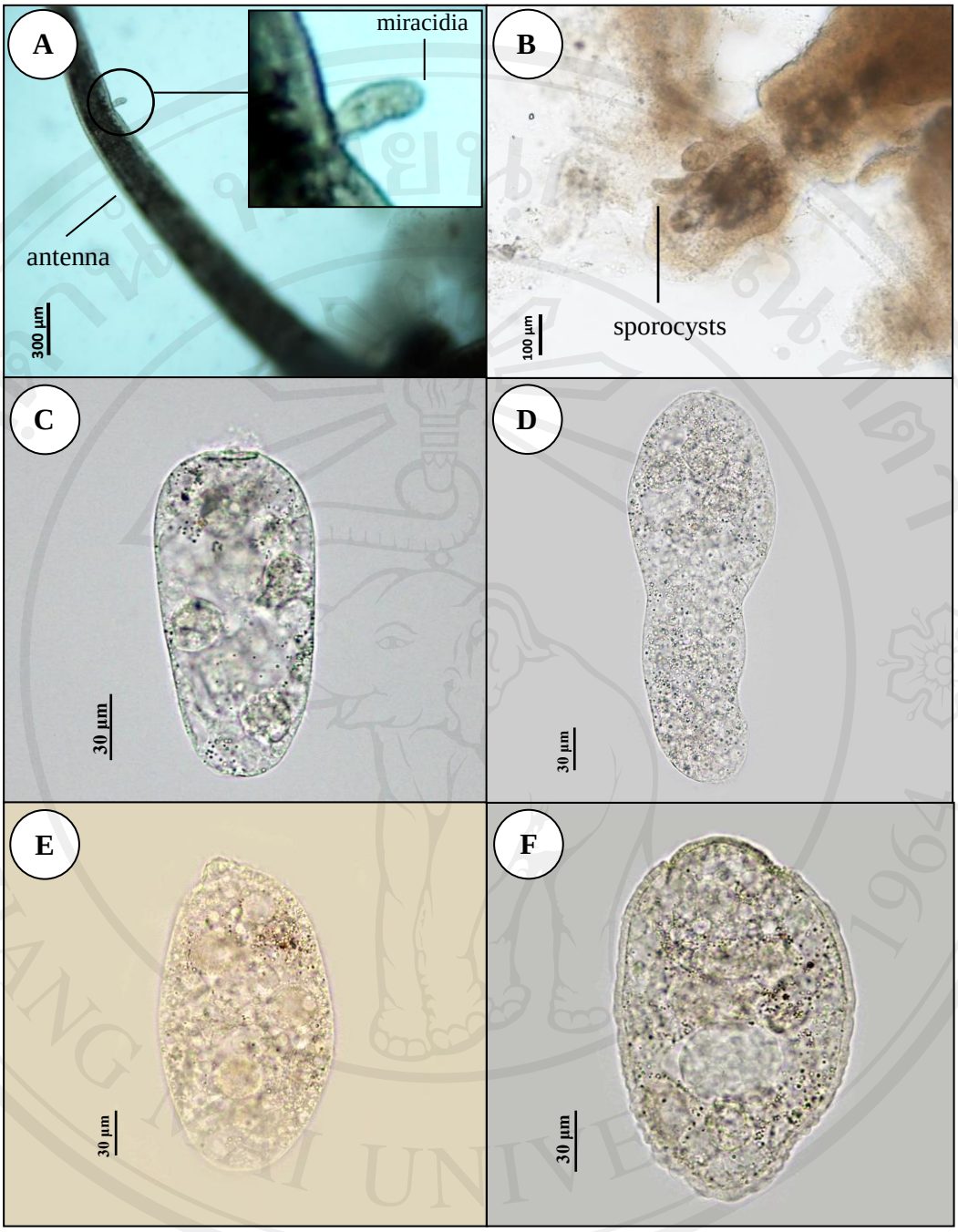

Figure 4.28 Illustration demonstrates miracidium infection and morphology of sporocysts, *E. revolutum*; **(A)** Miracidia penetrate into snail host at antenna; **(B)** Sporocysts were developed within the cavity of snail heart; **(C)** Sporocyst of days 7 PI; **(D)** Sporocyst of days 10 PI; **(E)** Sporocyst of days 12 PI; **(F)** Sporocyst of days 14 PI.

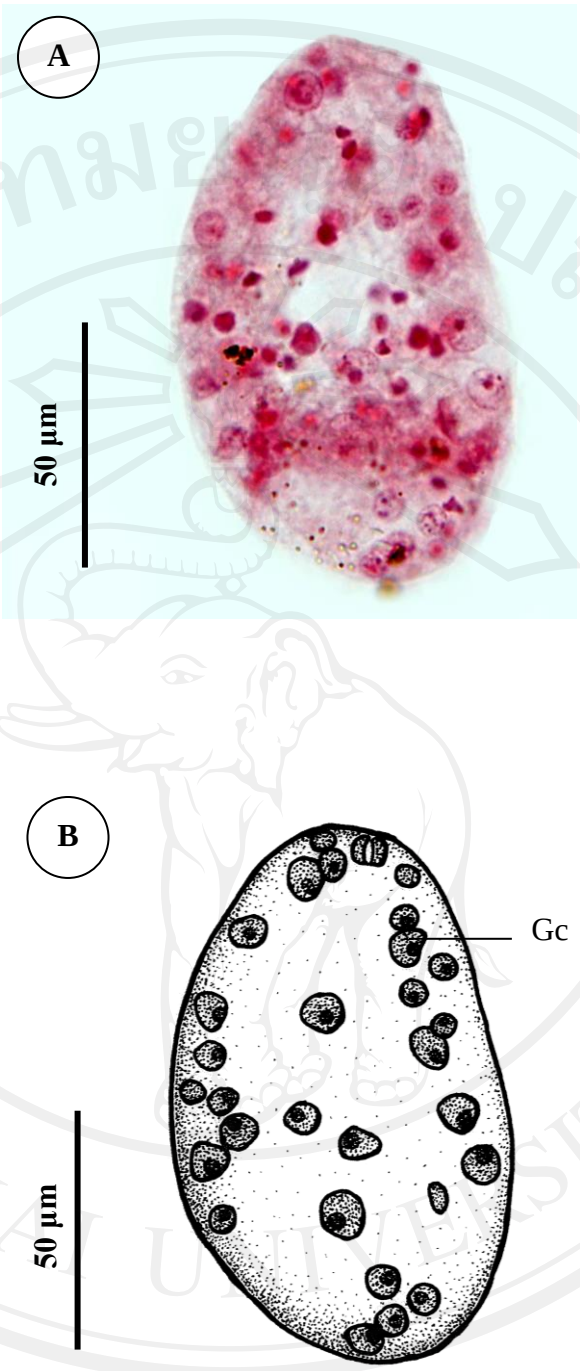

Figure 4.29 Illustration demonstrates morphology of sporocyst, *Echinostoma revolutum* 7 day PI; **(A)** Photograph of permanent slide **(B)** Drawing. Abbreviation: Gc, Germ ball cell**.**

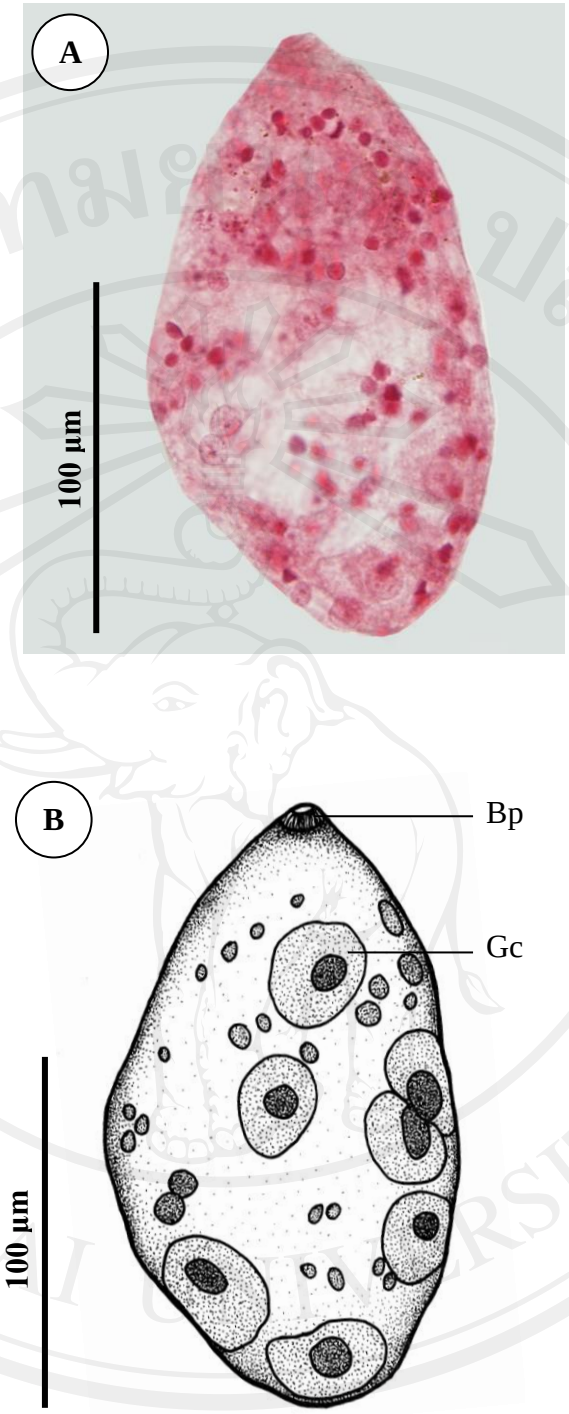

Figure 4.30 Illustration demonstrates morphology of sporocyst, *Echinostoma revolutum* 12 day PI; **(A)** Photograph of permanent slide **(B)** Drawing. Abbreviation: Bp, birth pore; Gc, Germ ball cell**.**

2) Mother redia (Figure 4.31-Figure 4.34)

Description: The snails examined 16 days PI contained young mother rediae (first generation redia) embedded in the same site of sporocyst. The mother rediae are oval, measured, 410-457 μm long by 211-230 μm wide. They are motile, colourless, mouth antero-terminal. Pharynx well developed, muscular, globular, measured 54 -75 μm long by 50-71 μm wide, connected directly to saccular caecum extending in 2/3 of body, the caecum was filled with a yellow-orange material and showed active contraction. They are contained 5-13 germ balls.

Mature mother rediae (32 days PI) usually remain in heart cavity, although some may migrate to haemolymph space surrounding viscera of snail. They are slightly mobile, elongate, measured 639-724 μm long by 192-227 μm wide, pharynx 64-76 μm long and 52-53 μm wide and gut length variable filled with mass of brownish granular material. The birth pore lateral, located at 1/4 from anterior end of the body. They are contained 4-8 germ balls.

At day 45 PI, mother rediae variable in size, measured 1,015-1,176 μm long by 410-456 μm wide, with a pharynx 80.5-90.7 μm long by 81.5-89.0 μm wide. They are slightly mobile and colourless. The length of the caeca varied from about 1/2 to 3/4 the total redial length. They are producing second generation redia (daughter rediae) occur within the first generation rediae, containing many daughter rediae and germ balls.

Site of infection: heart cavity and haemolymph space surrounding visceral organ

Experimental hosts: F. doliaris and *F. martensi martensi*

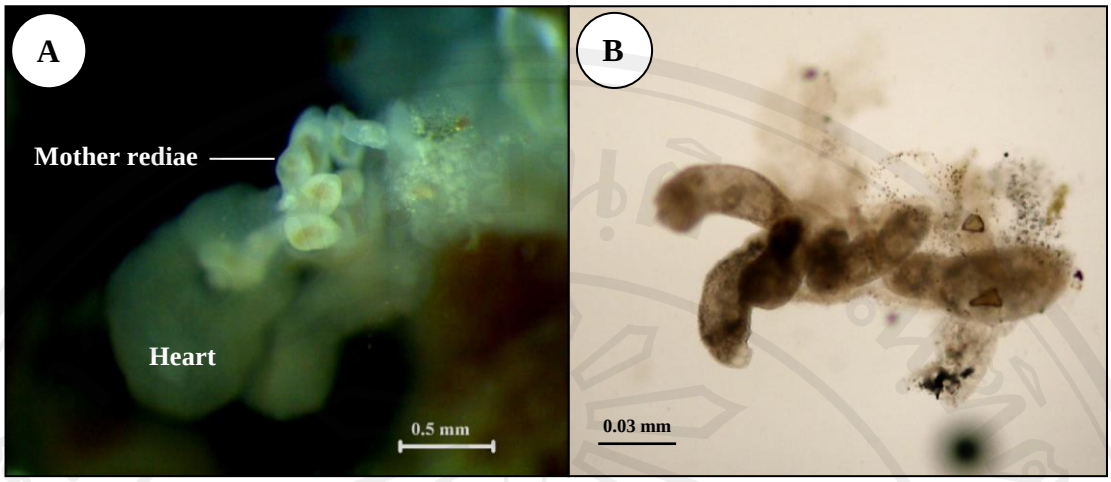

Figure 4.31 Illustration demonstrates mother rediae, *Echinostoma revolutum*; **(A)** the mother rediae of days 16 PI in heart cavity. **(B)** A live mother rediae of days 32 PI, were clumped together in the snail tissue, separated from the heart cavity.

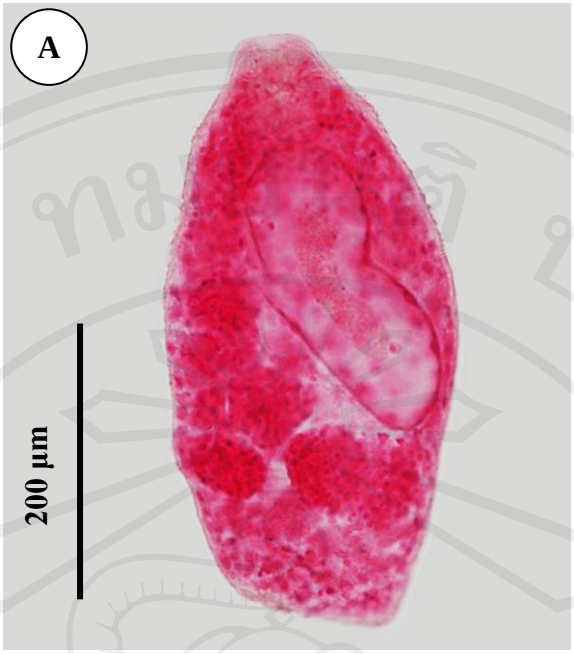

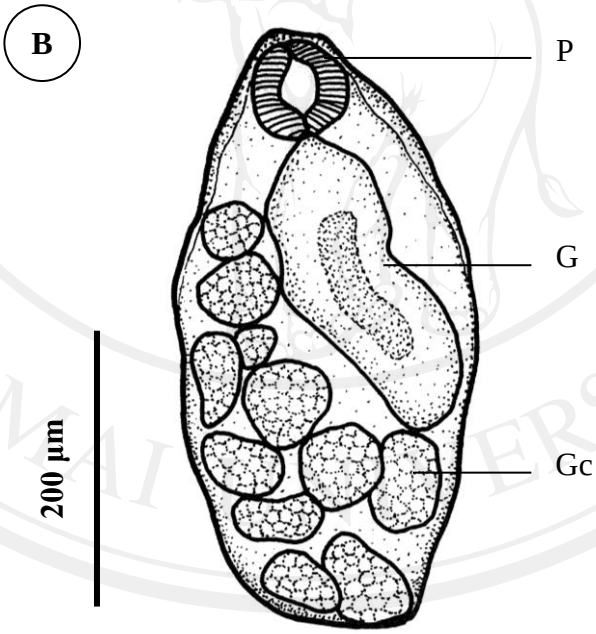

Figure 4.32 Illustration demonstrates mother rediae of days 16 PI, *Echinostoma revolutum*; **(A)** Photograph of permanent slide **(B)** Drawing. Abbreviations: G, Gut; Gc, Germ ball cell; P, Pharynx.

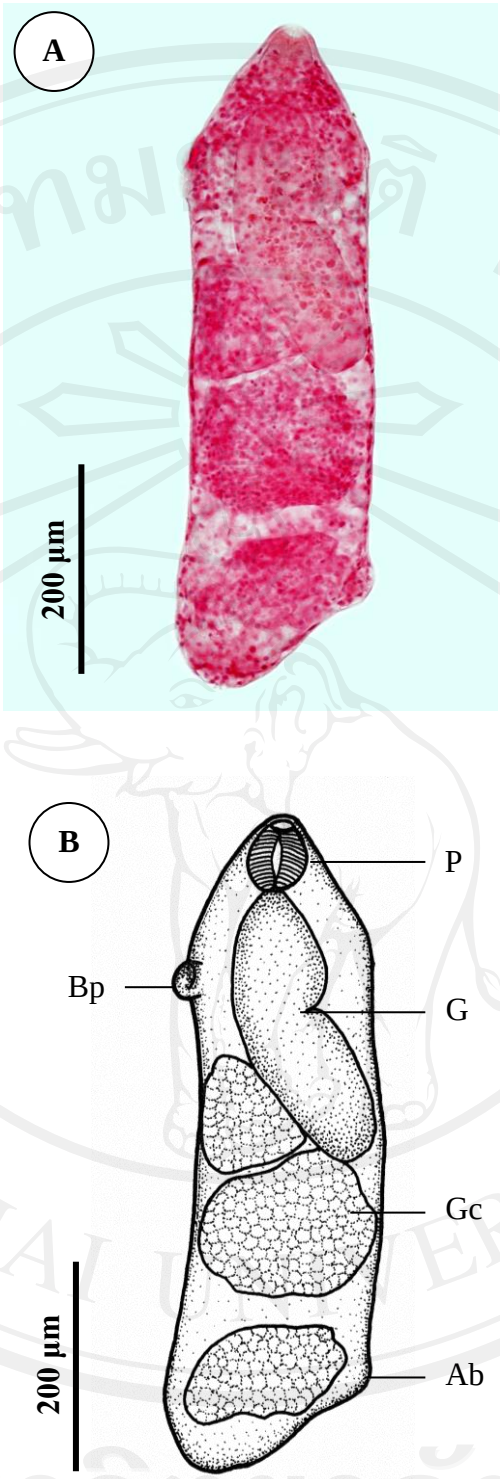

Figure 4.33 Illustration demonstrates mother rediae of days 32 PI, *Echinostoma revolutum*; **(A)** Photograph of permanent slide **(B)** Drawing. Abbreviations: Ab, Ambulatory bud; Bp, Birth pore; G, Gut; Gc, Germ ball cell; P, Pharynx.

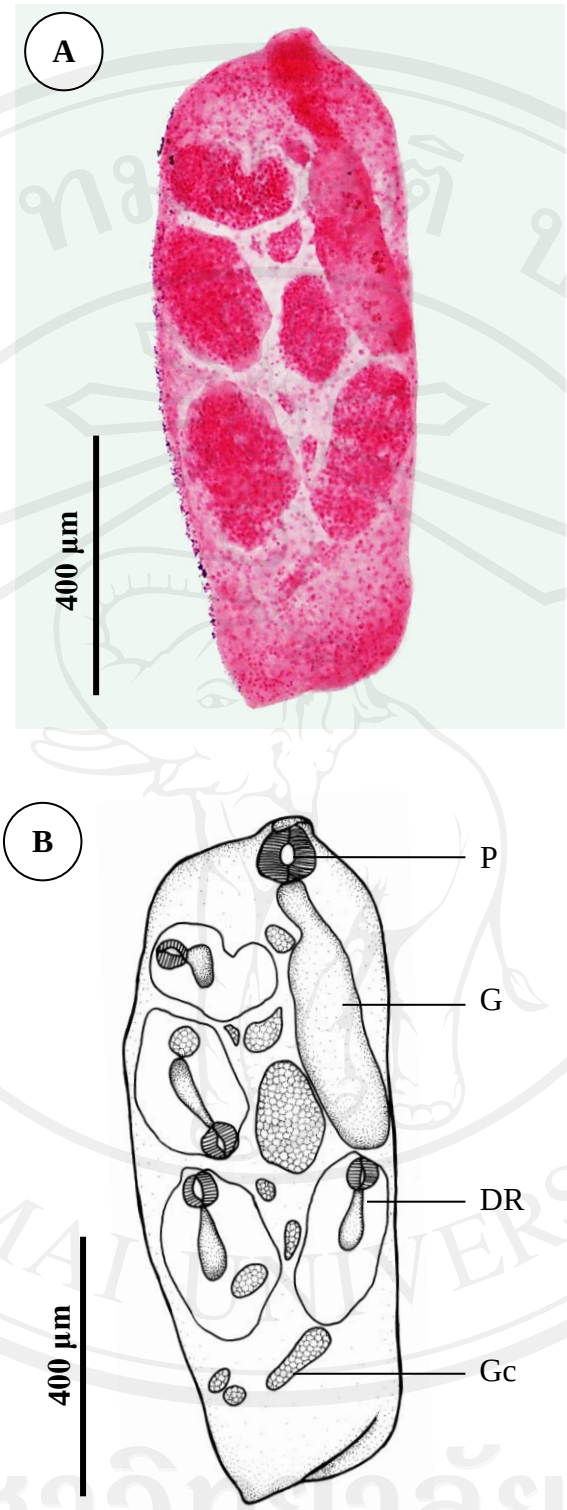

Figure 4.34 Illustration demonstrates mother rediae of days 45 PI, *Echinostoma revolutum*; **(A)** Photograph of permanent slide **(B)** Drawing. Abbreviations: DR, Daughter redia; G, Gut; Gc, Germ ball cell; P, Pharynx.

3) Daughter redia (Figure 4.35-Figure 4.37)

Description: Daughter rediae (second generation) were morphologically similar to mother rediae, but larger. They differ from mother rediae in that they contain cercariae, which clearly distinguished by the presence of oral and ventral suckers, a tail and undeveloped germ balls.

In the snail examined 60 day PI (Figure 4.36), numerous daughter rediae were found in the haemolymph space surrounding viscera and mid-gut of snail. The daughter rediae were elongate, slightly mobile, 1,050-1,564 μm long 240-347 μm wide, with a pharynx 64-75 μm long by 54-63 μm wide and a long gut filled with black-brown granulations. Mouth located at antero-terminal of body. Anterior protrusible birth pore presented just 1/4 from anterior end of the body. Other pronounced structures observed in daughter rediae were the one ambulatory buds at posterior of body. The body cavity was filled with germinal balls and cercarial embryos and some differentiated into fully developed cercariae. Often they were less than 5 cercariae inside. Fully formed cercariae of the echinostome type emerged out of snails.

At 73 days PI, an uncounted number of daughter rediae with developing cercariae had invaded the entire snail usually obtained chief from the surrounding viscera and mid-gut of snail. Body elongated, 1,572-1,611 μm long by 284-297 μm wide, containing many (8 or more) cercariae in various developmental stages as well as a germ balls in body cavity. Pharynx almost spherical, measured 70-81 μm long by 41-53 μm wide. Gut was long and extended.

At day 80 PI (Figure 4.37), the snails that remained alive began producing the cercariae from 60 days PI and the daughter rediae obtained chiefly from mid-gut of snails, contained fully developed cercariae as well as germ balls. Daughter rediae were white and elongate 1,640-1,697 μm long by 253-291 μm wide. Birth pore easily seen during emergence of cercariae (Figure 4.35 C). Muscular pharynx, measured 50-64 μm long by 41-48 μm wide. Gut contained black granulations. Fully developed cercariae were seen within the rediae, the mean number of such cercariae per redia being 8 (including cercarial embryos). They lie freely in the body cavity of the redia and move back and forth with the movement

of the redia. At this stage, daughter rediae contain up to 13 cercariae in body cavity, in addition to number of germ balls. Old rediae were shriveled, with dark-grey bodies and yellow-orange gut.

Site of infection: haemolymph space surrounding viscera and mid-gut of snail

Experimental hosts: F. doliaris and *F. martensi martensi*

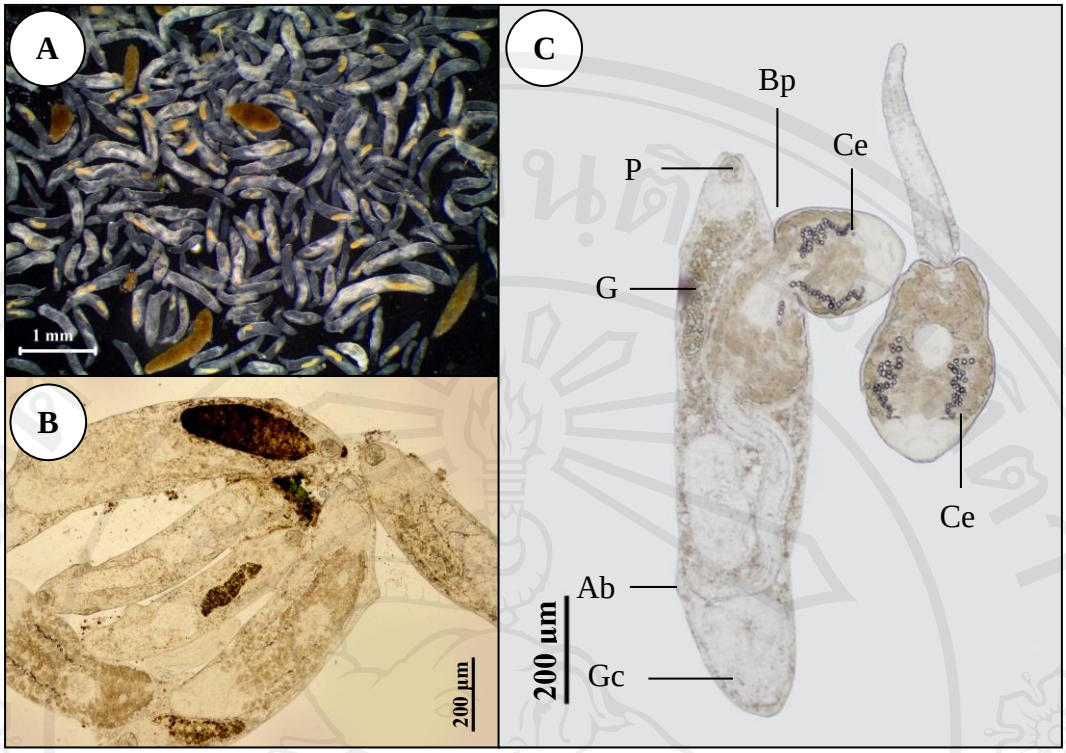

Figure 4.35 Illustration demonstrates daughter rediae, *Echinostoma revolutum*: **(A)** the daughter rediae of days 60 PI in haemolymph space surrounding viscera and mid-gut of snail. **(B)** A live daughter rediae were clumped together in the snail tissue, compressed under a cover slip. **(C)** The general morphology of daughter redia showing the mature cercaria and birth pore easily seen during emergence of cercariae. Abbreviations: Ab, Ambulatory bud; Bp, Birth pore; Ce, Cercaria; G, Gut; P, Pharynx.

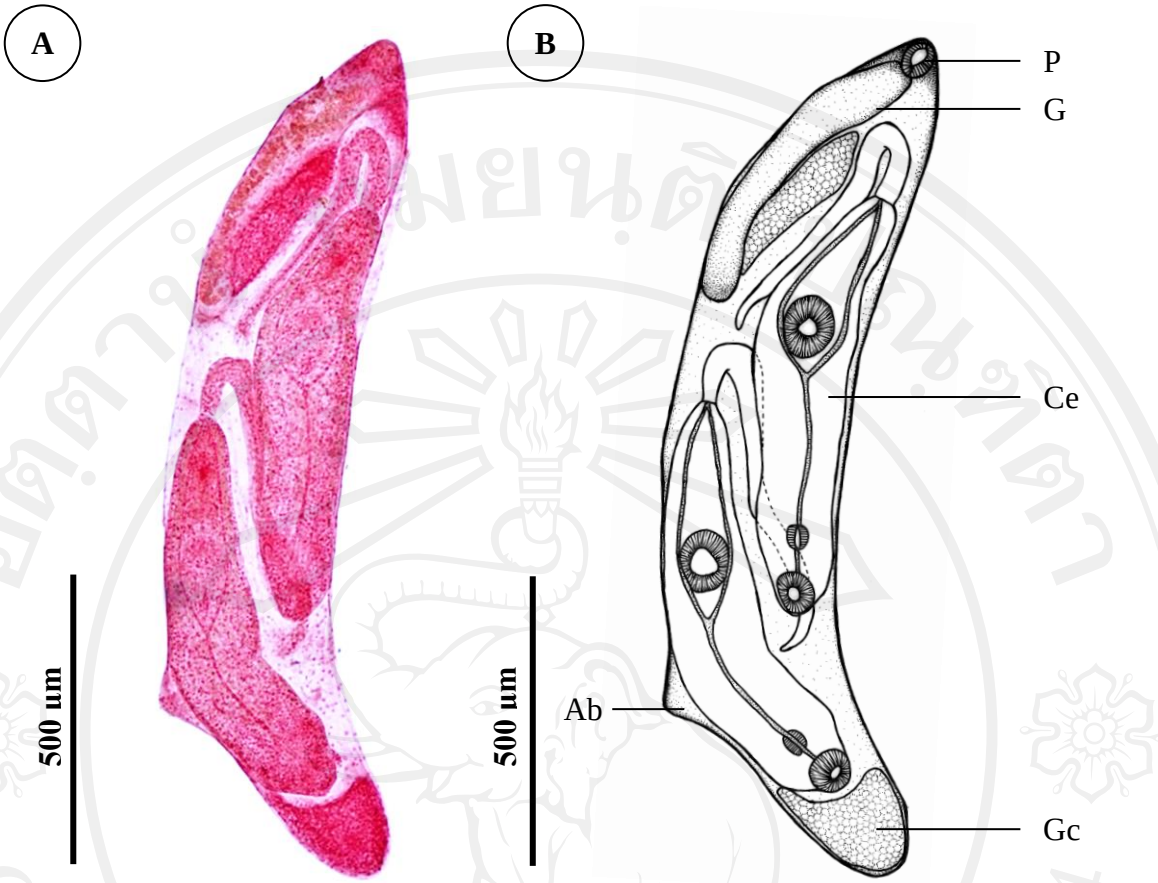

Figure 4.36 Illustration demonstrates daughter redia of days 60 PI, *Echinostoma revolutum*; **(A)** Photograph of permanent slide **(B)** Drawing. Abbreviations: Ab, Ambulatory bud; Ce, Cercaria; G, Gut; Gc, Germ ball cell; P, Pharynx.

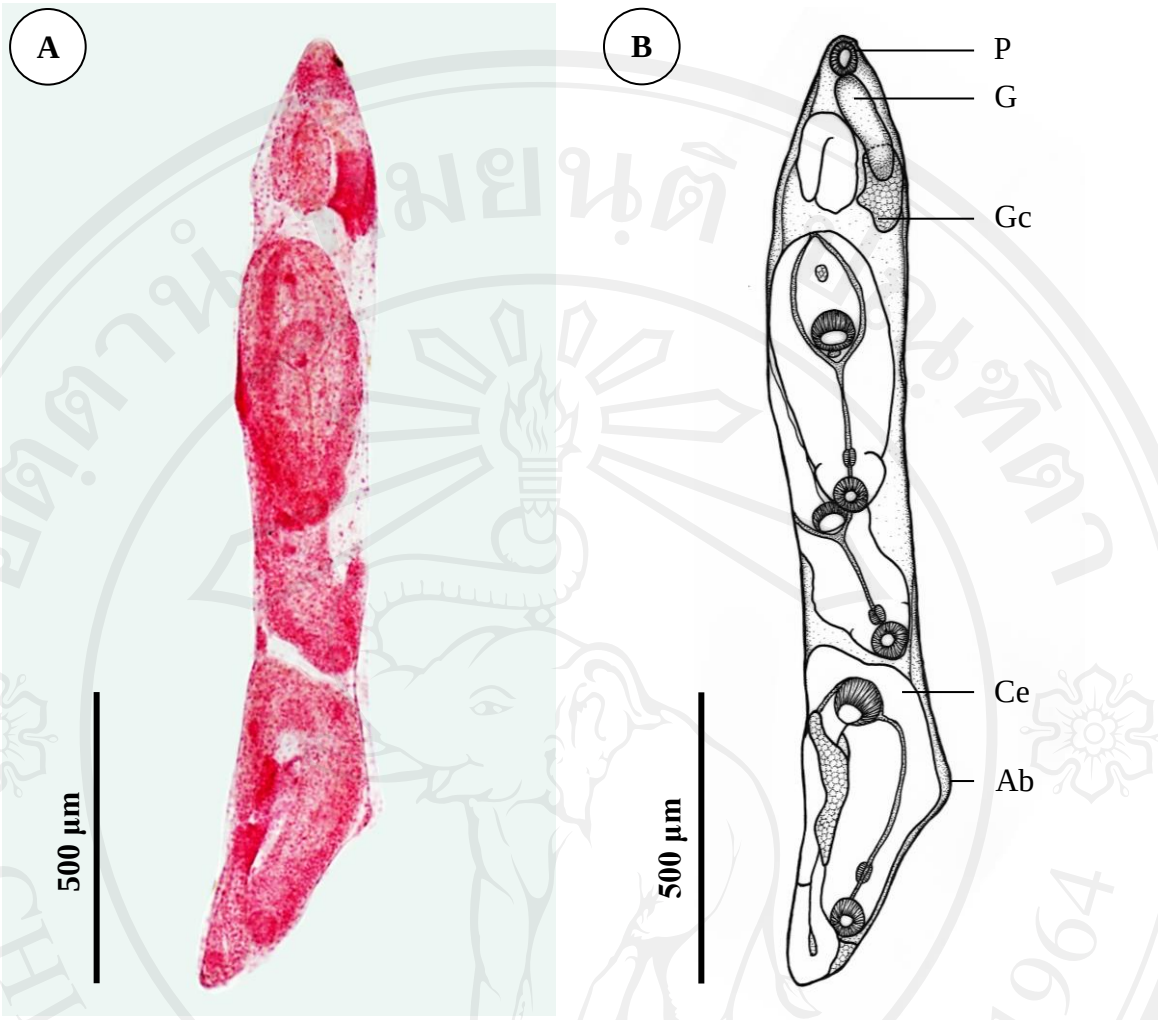

Figure 4.37 Illustration demonstrates daughter redia of days 80 PI, *Echinostoma revolutum*; **(A)** Photograph of permanent slide **(B)** Drawing. Abbreviations: Ab, Ambulatory bud; Ce, Cercaria; G, Gut; Gc, Germ ball cell; P, Pharynx.

4) Cercaria (Figure 4.38-Figure 4.39)

Description: Cercariae may first escape from snail 60 days after exposure, but usually at 62-65 days. Cercariae swimming easily through water while curving body ventrally. After swimming for 4-6 hours, they sink to bottom and die several hours later.

Measurements based on specimens fixed in 5% formalin (n=20): body 265-458 μm long by 128-281 μm wide. Collar distinct, 120-150 μm wide, with 37 spines, arranged as in adult. The collar is usually quite prominent but the collar spines are so small and transparent. Body covered with minute spines becoming sparse at posterior end. Oral sucker subterminal, measured 32-56 μm long by 40-55 μm wide. Prepharynx short, measured 7-25 μm long and pharynx 26-40 μm long by 14-25 μm wide. Oesophagus was 50-141 μm long. Caecal bifurcation at anterior to acetabulum to form two curved caeca extending almost to posterior part of body. Acetabulum protuberant, posterior to mid-body, measured 60-100 μm long by 58-100 μm wide. Penetration gland cells occur along oesophagus with 4 inconspicuous gland ducts opening on dorsal lip of oral sucker. Numerous granular cystogenous cells extend from level of pharynx to posterior end of body throughout entire width of body. Cell masses present and forms 2 genital primordial, 38-46 μm in diameter, one at anterior margin of acetabulum, other between acetabulum and base of tail. Excretory system twisted, conspicuous, extends from posterior margin of oral sucker to posterior end of body. Excretory duct consists on each side of one thin descending duct forming a loop at pharynx level. They make a triangular loop (characteristic of echinostome cercariae) and one ascending dilated duct with large refractile granules in anterior half of body. Latter duct arrives into anterior part of bipartite excretory vesicle. Flame-cells inconspicuous and excretory vesicle bipartite located at posterior end of body. Caudal excretory duct divided into 2 short ducts opening laterally at one fourth distances along tail. Tail 325-499 μm long with finger like narrowing at tip. Seven fin folds present; 2 dorsal, 3 ventral and 2 smallest ventrolateral. The entire fin fold it's difficult to see and no longer visible after fixation.

Site of infection: haemolymph space surrounding viscera and mid-gut of snail

Experimental hosts: F. doliaris and *F. martensi martensi*

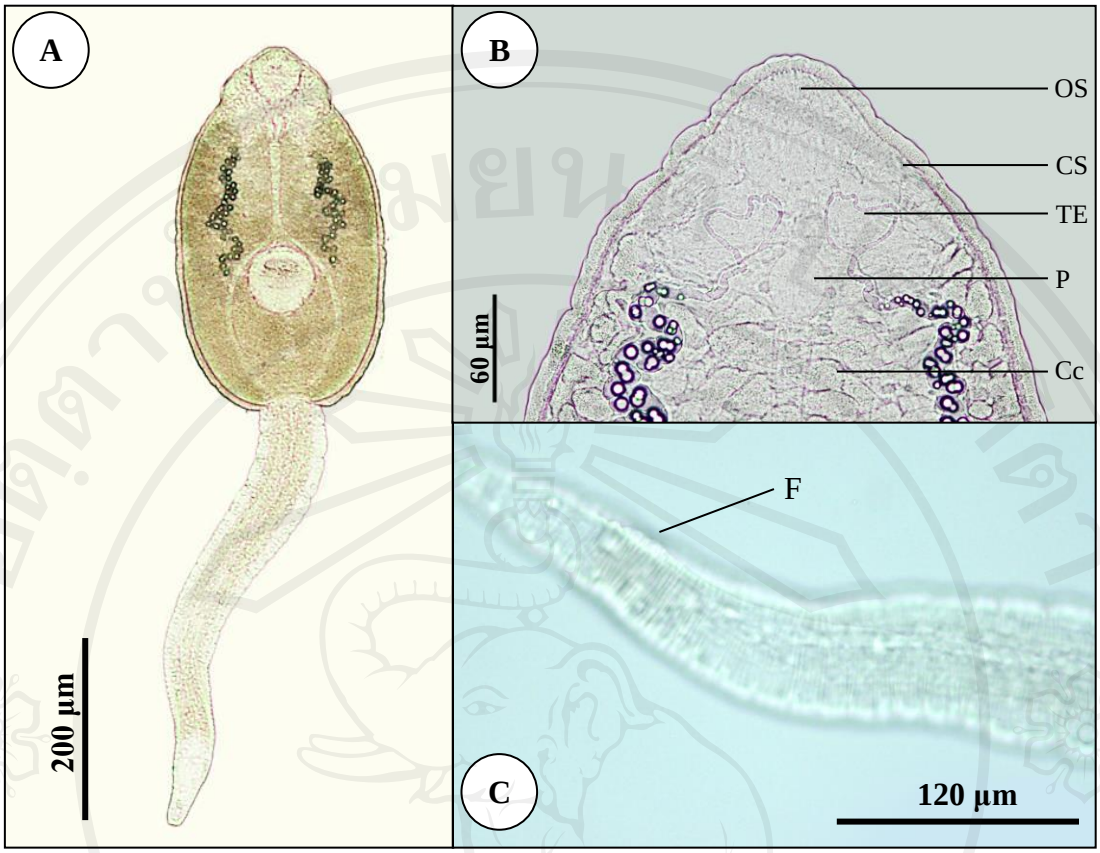

Figure 4.38 Illustration demonstrates mature cercaria of days 60 PI, *Echinostoma revolutum*: **(A)** Photograph of the whole body. **(B)** Photograph of the anterior part of body showing general morphology of echinostome cercaria. **(C)** Photograph of the tail showing fin fold of cercaria. Abbreviations: Cc, Cystogenous cell; CS, Collar spines; F, Fin fold; OS, Oral sucker; P, Pharynx; TE, Triangular loop of excretory duct.

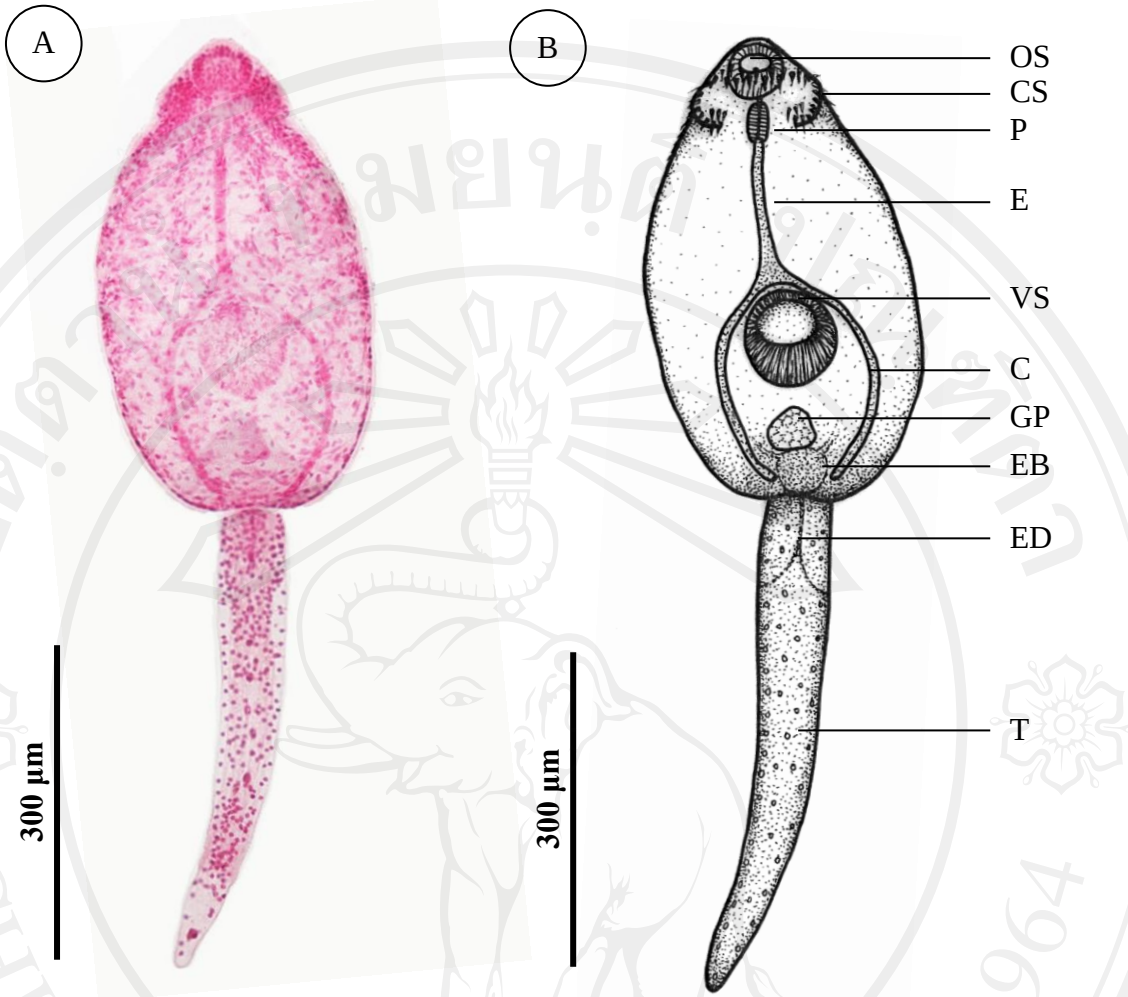

Figure 4.39 Illustration demonstrates cercaria of days 60 PI, *Echinostoma revolutum*; **(A)** Photograph of permanent slide **(B)** Drawing. Abbreviations: C, Caeca; CS, Collar spines; E, Esophagus; EB, Excretory bladder; ED, Excretory duct; GP, Genital primodia; OS, Oral sucker; P, Pharynx; VS, Ventral sucker; T, Tail.

4.2.5 The second intermediate host infections (Figure 4.40-Figure 4.41)

Freely swimming cercariae were in turn obtained after emergence or dissection from experimentally infected snail hosts after 60 PI. Experimental infection of the second intermediate host snails with cercariae were carried out by placing cercariae together with various snails: viviparid snails; *F. doliaris* and *F. martensi martensi* and lymnaea snail; *L. auricularia rubiginosa*. The experimentally infected snails were investigated for the encysted metacercariae by dissection.

The result shows that only viviparid snails; *F. doliaris* and *F. martensi martensi* became infected, but attempt to infect *L. auricularia rubiginosa* (lymnaeid snail) failed. Encysted metacercariae were found clumped together in the pericardial sac of snail host, with each cyst enveloped by thin connective tissues of the host origin. Within 2 days metacercariae become infective.

Measurements based on 30 whole mounted specimens. Metacercaria folded within transparent cyst, was spherical, 136.0-195.0 μm in diameter, with a bilayered wall. Cyst wall consisted of outer, transparent layer, about 4.4-12.5 μm thick, and inner, opaque layer, about 0.7-4.7 μm thick. Thirty seven collar spines presented in both fresh and fixed specimens, excretory granules and sucker were visible through the cyst wall and the excretory organs filled with concretions through the cyst wall.

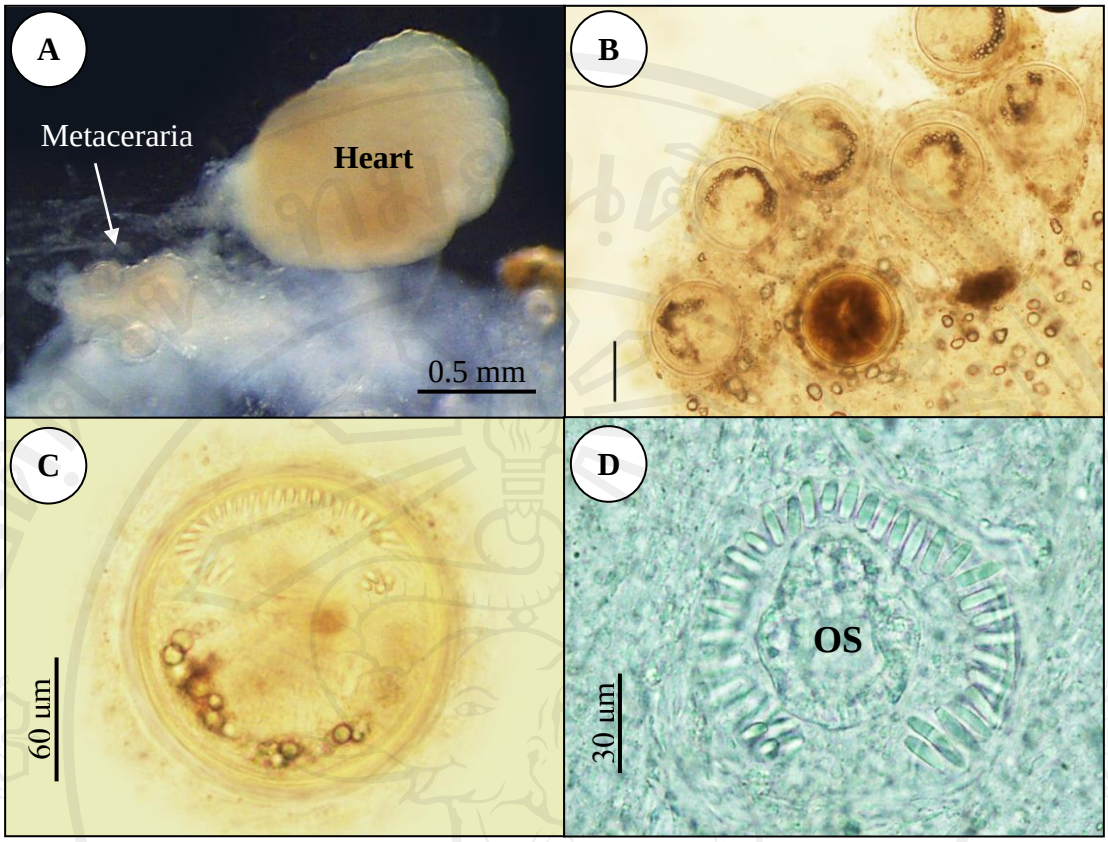

Figure 4.40 Illustration demonstrates metacercariae, *Echinostoma revolutum*: **(A)** Encysted metacercariae were clumped together in the pericardial sac of snail host. **(B)** Metacercarial cysts compressed under a cover slip. **(C)** An isolated metacercaria showing a well-developed oral sucker and head collar with collar spines. **(D)** Head crow of metacercaria (top view), compressed under a cover slip showing collar spines and oral sucker (OS).

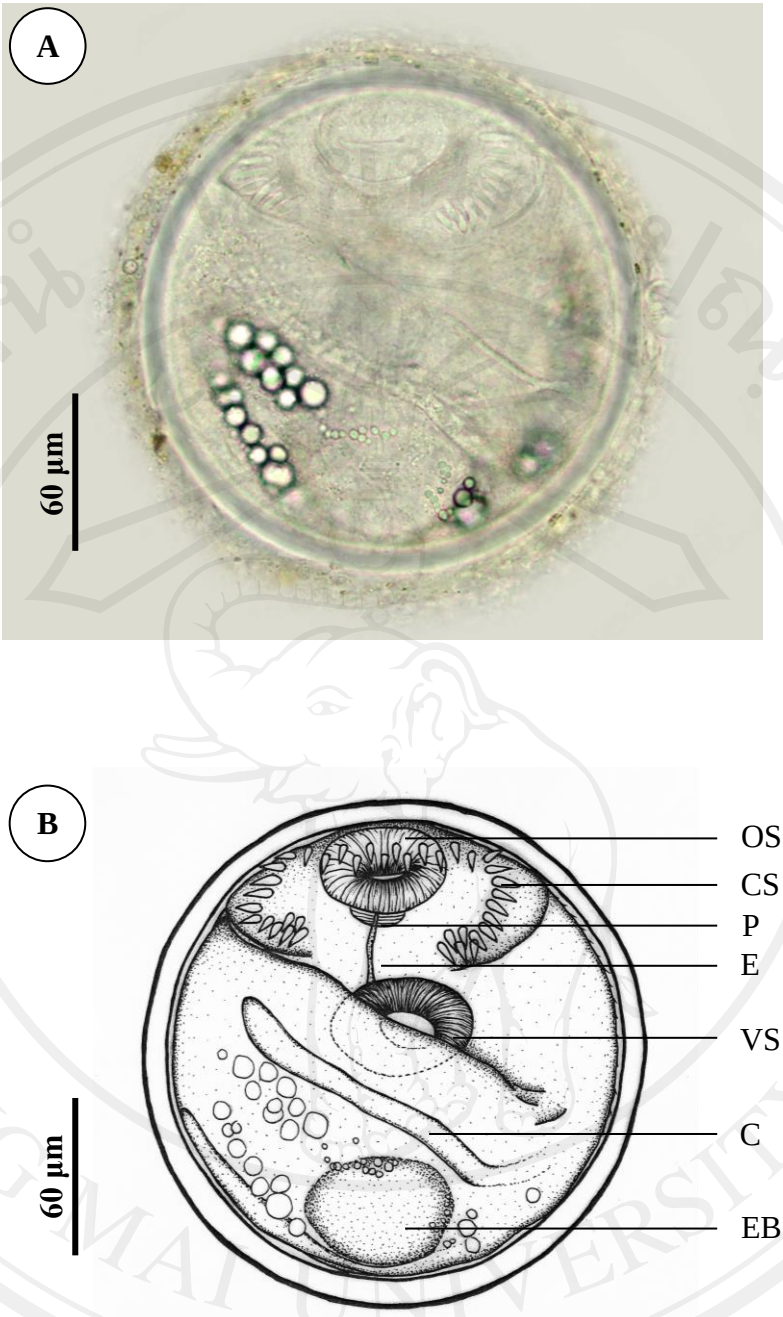

Figure 4.41 Illustration demonstrates encysted metacercaria of days 2 PI, *Echinostoma revolutum*; **(A)** Photograph of encysted metacercaria compressed under a cover slip **(B)** Drawing. Abbreviations: C, Caeca; CS, Collar spines; E, Esophagus; EB, Excretory bladder; OS, Oral sucker; P, Pharynx; VS, Ventral sucker.

4.2.6 Taxonomic summary of *Echinostoma revolutum*

Superfamily Echinostomatoidea, Looss, 1899

Family Echinostomatidae, Looss, 1899

Subfamily Echinostomatinae, Looss, 1899

Genus *Echinostoma* Rudolphi, 1809

Species *Echinostoma revolutum* (Frölich, 1802) Rudolphi, 1809

Synonyms: *Fasciola revoluta* Fröelich, 1802; *E. acuticauda* Nicoll, 1914; *E. armatum* Molin, 1850; *E. armigerum* Barker & Irvine, 1915; *E. audyi* Lie & Umathevy, 1965; *E. collawayensis* Barker & Noll, 1915; *E. columbae* Zunker, 1925; *E. coalitum* Barker & Beaver, 1915; *E. dilatatum* Miram, 1840; *E. echinocephalum* Rud., 1819; *E. erraticum* Lutz, 1924; *E. ivaniosi* Mohandas, 1973; *E. limicoli* Johnson, 1920; *E. microchis* Lutz, 1924; *E. mendex* Dietz, 1909; *E. neglectum* Lutz, 1924; *E. nephrocystis* Lutz, 1924; *E. oxycephalum* Rudolphi, 1819; *E. paraulum* Dietz, 1909; *E. revolutum* var. *japonicum* Kurisu, 1932; *E. sudanense* Odhner, 1911 and *Echinoparyphium paraulum* Diez, 1909

Morphology: See descriptions and illustrations in this chapter.

4.2.7 Life history of *Echinostoma revolutum*

The life history of *E. revolutum* has been elucidated experimentally could be established in Figure 4.42. The whole life cycle of *E. revolutum* has been completed experimentally, at least 80-83 days were required to maintain metacercaria to metacercaria cycle of this fluke.

Experimental definitive host:	domestic chick (*Gallus gallus domesticus*)
Second intermediate hosts:	*Filopaludina doliaris* and *F. martensi martensi* (Viviparidae)
First intermediate hosts:	*F. doliaris* and *F. martensi martensi* (Viviparidae)
Site of infection:	Adults, small intestine (jejunum and ilium); sporocysts, heart cavity; rediae, haemolymph space surrounding viscera and mid-gut of snail; metacercariae, pericardial sac of snail
Locality:	Ten districts of Chiang Mai province (Doi Saket, Hang Dong, Mae On, Mae Rim, Mae Taeng, Muang Chiang Mai, San Kamphaeng, San Pa Tong, Saraphi, and San Sai)

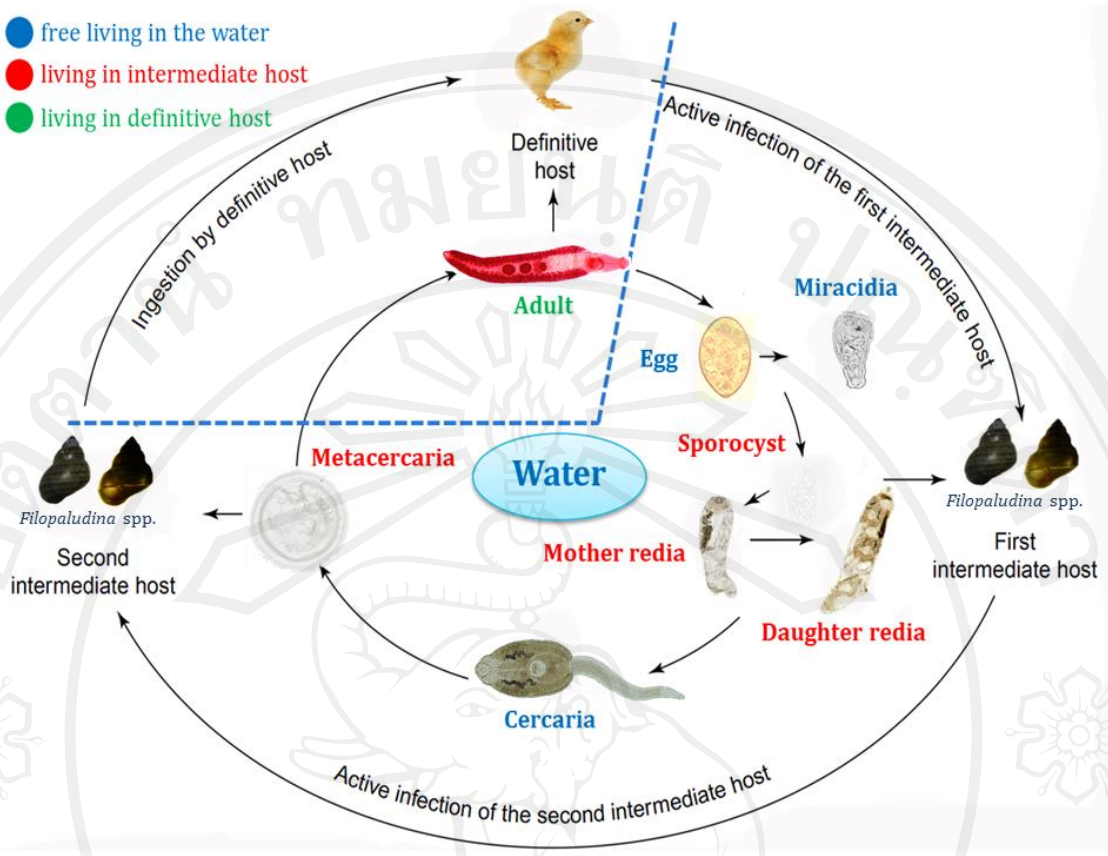

Figure 4.42 Experimental life history of *Echinostoma revolutum*. **(a)** Adult worms inhabit the small intestine of chick (*Gallus gallus domesticus*). **(b)** Eggs are avoided with the host faeces. **(c)** Miracidia hatch in water and actively infect snails (viviparid snails: *Filopaludina doliaris* and *F. martensi martensi*). **(d)** Sporocysts, **(e)** mother rediae and **(f)** daughter rediae are the intramolluscan stages. **(g)** Cercariaeare released and swims to locate the second intermediate host (viviparid snails: *F. doliaris* and *F. martensi martensi*), in which they encyst to become metacercariae. **(h)** Metacercariae are ingested by the definitive host and excyst to become adults.

4.3 Molecular Identification and Phylogenetic analysis

4.3.1 Molecular identification by loop-mediated isothermal amplification (LAMP)

1) LAMP specificity

The outer LAMP primers, F3 and B3, were used in the conventional PCR, which was verified the ITS2 target sequence of *E. revolutum*. An expected 182 bp fragment was obtained by PCR amplification and subsequent sequencing. The sequence data obtained confirmed that 182 bp of the *E. revolutum* ITS2 match to *E. reolutum*, which high alignment score (Figure 4.43-Figure 4.44, Table 4.6). The designed LAMP primers successfully amplified partial sequence of ITS2 sequence of *E. revolutum*.

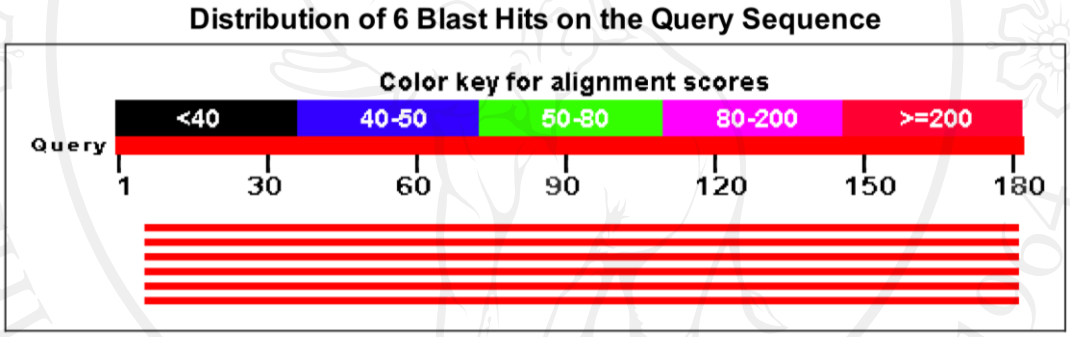

Figure 4.43 Color key alignment scores of expected 182 bp fragment of *Echinostoma revolutum* ITS2 sequence

Echinostoma revolutum

```
Score = 291 bits (157), Expect = 2e-81, Identities = 170/176 (97%),
Gaps = 1/176 (0%), Strand = Plus/ Plus
 Query  7    TGACTTGTC-TGTGAGGTGCCAGATCTATGGCGTTTCCCCAATGTATCCGGATGCATCCA  65
             ||||||||| ||||||||||||||||||||||||||||||||||||||||||| |||||||
 Sbjct  639  TGACTTGTCATGTGAGGTGCCAGATCTATGGCGTTTCCCCAATGTATCCGGACGCATCCA  698

 Query  66   TGTCCTGGTCGAATGCCATGATGGGATGTGGTGACGGAATCGTGGTTTAATATGGCTATG  125
             |||| |||  ||| ||||||||||||||||||||||||||||||||||||||||||||||
 Sbjct  699  TGTCTTGGCTGAAAGCCATGATGGGATGTGGTGACGGAATCGTGGTTTAATATGGCTATG  758

 Query  126  CCCCGTTTTCAGCATGTTTGGCGCTTCTAGTCGGCATGCATATGACTACGGGTGGA  181
             ||||||||||||||||||||||||||||||||||||||||||||||||||||||||
 Sbjct  759  CCCCGTTTTCAGCATGTTTGGCGCTTCTAGTCGGCATGCATATGACTACGGGTGGA  814
```

Figure 4.44 Alignment of expected 182 bp fragment of *E. revolutum* ITS2 sequence compared with subjects available in Genbank

Table 4.6 Demonstrate the sequence producing significant alignment of expected 182 bp fragment of *E. revolutum* ITS2 sequence compared with GenBank databases

# Accession	Max score	Total score	Query cover	E value	Max ident
AF067850.1	291	291	96%	2e-81	97%
GQ463130.1	287	287	96%	2e-80	96%
GQ463129.1	287	287	96%	2e-80	96%
GQ463128.1	287	287	96%	2e-80	96%
AY168930.1	281	281	96%	1e-78	95%
U58102.1	274	274	96%	2e-76	95%

The specificity of the LAMP assay was assessed by testing the genomic DNA samples of *E. revolutum* and other related trematodes (viz. *E. cinetorchis, E. hortense, Echinochasmus japonicas, A. tyosenense, Fa. gigantica, Fi. elongatus, P. epiclitum*, and *O. streptocoelium*). Positive LAMP products were visually observed in reaction tubes after adding fluorescent dye. Positive amplification was detected by the naked eye directly under normal light; the solution would turn to green in the presence of LAMP product, otherwise it would remain orange. Additionally, the positive LAMP product was observed under UV exposure, and the LAMP product was also confirmed by eletrophoresis.

The results showed that the LAMP assay could distinguish *E. revolutum* from other trematodes. The LAMP product was amplified only with the target DNA samples of *E. revolutum*, and no amplification was detected in other trematodes, demonstrating that this LAMP assay is specific for the detection of *E. revolutum* (Figure 4.45). These LAMP products were typical ladder-like bands on 2% agarose gel. Similar results were obtained in the reaction tubes of LAMP assay, with no amplification of the other trematodes (Figure 4.45 C). Additionally, the specificity of the LAMP assay for detection of *E. revolutum* was tested with the *E. revolutum* metacercariae. The results showed that similar pattern was detected in the DNA sample of *E. revolutum* adults,

indicating that the LAMP assay could detect the DNA sample target not only from adults but from metacercariae of *E. revolutum* (Figure 4.46).

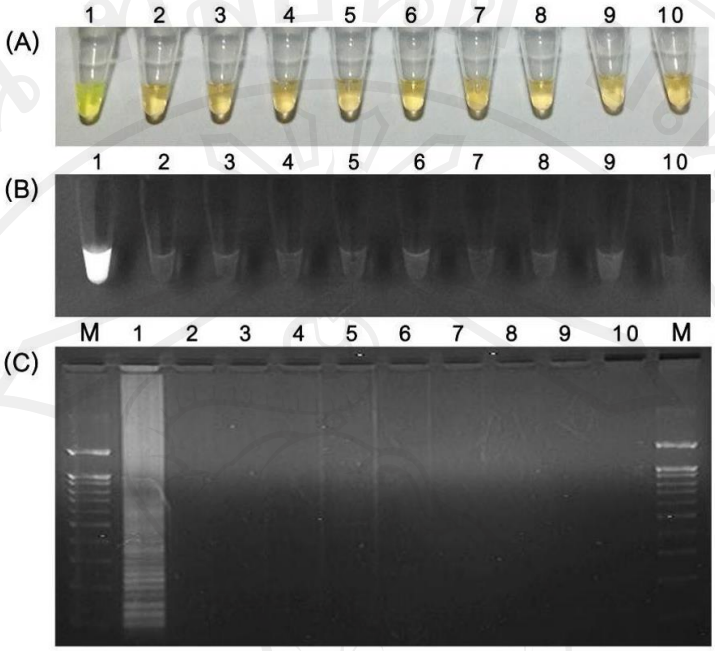

Figure 4.45 Specificity of LAMP assay for detection of *Echinostoma revolutum* after adding SYBR Green I. **(A)** under normal light. **(B)** Under UV light. **(C)** Agarose gel electrophoresis of LAMP amplified products. 1-10 represents *E. revolutum, E. cinetorchis, E. hortense, Echinochasmus japonicas, Acanthoparyphium tyosenense, Fasciola gigantica, Fischoderious elongatus, Paramphistomum epiclitum, Orthocoelium streptocoelium* and negative control (without DNA), respectively; M: marker

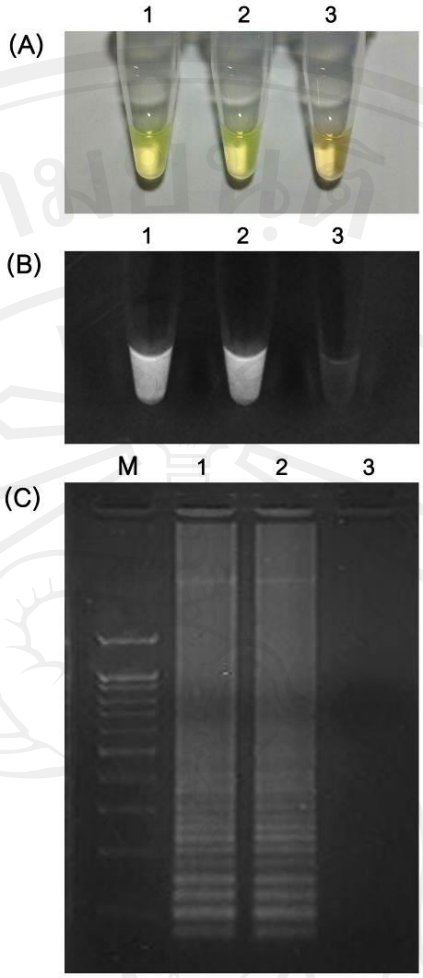

Figure 4.46 Specificity of LAMP assay for detection of *Echinostoma revolutum* was tested with the *E. revolutum* metacercaria. LAMP reaction tubes were inspected visually under normal light **(A)** under UV exposure **(B)** and confirmed LAMP amplified products by electrophoresis **(C)**. 1-3 represents *E. revolutum* adult, *E. revolutum* metacercaria and negative control (without DNA), respectively; M, marker

2) LAMP sensitivity

The sensitivity of the LAMP assay was determined by comparing the detection limits of the LAMP assay with that of the conventional PCR. Ten-fold serial dilution ranging from 10 to 1×10^{-8} ng/µl were prepared and used as a template amplified by LAMP and PCR methods. The results showed that the detection limit of both methods. The detection limit for LAMP assay was 1×10^{-6} ng/µl of DNA templates, while the minimum amount of DNA template detectable using the conventional PCR was 1×10^{-3} ng/µl (Figure 4.47). This means that under these conditions and concentrations used, the LAMP assay is more sensitive than the conventional PCR method.

3) Field sample testing with LAMP

The applicability of LAMP assay for detection of *E. revolutum* metacercariae was evaluated by using samples from naturally infected snails in an epidemic area in Chiang Mai, Thailand. Seven samples of echinostome metacercariae from naturally infected snails were verified using microscopic examinations and then subjected to genomic DNA extraction and evaluated by LAMP assay. The *E. revolutum*-specific LAMP assay was used to detect metacercariae in infected snails, as shown in the results (Figure 4.48), all samples were found positive for *E. revolutum*. These positive results in LAMP assay was in agreement with the microscopic examinations.

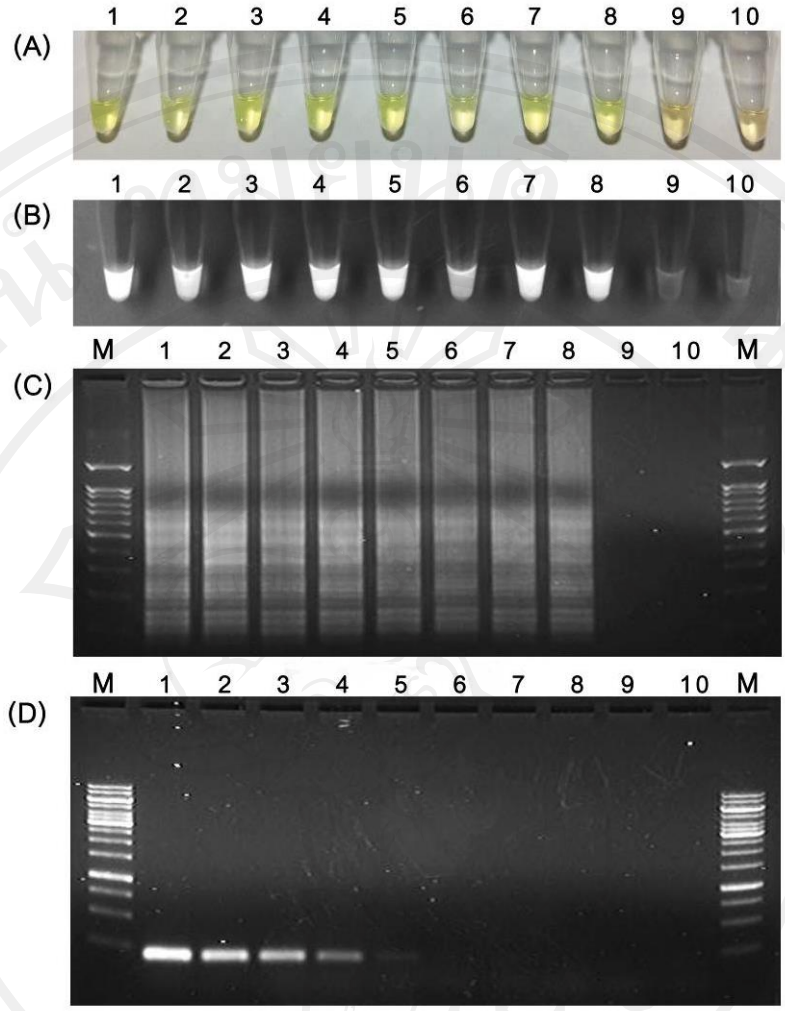

Figure 4.47 Sensitivity of LAMP assay for detection *Echinostoma revolutum* was determined by compare the detection limits of the LAMP assay **(A-C)** with those of conventional PCR **(D)**. 1-10 represents concentration of genomic DNA samples: 1, 10 ng/µl; 2, 1 ng/µl; 3, 1×10^{-1} ng/µl; 4, 1×10^{-2} ng/µl; 5, 1×10^{-3} ng/µl; 6, 1×10^{-4} ng/µl; 7, 1×10^{-5} ng/µl; 8, 1×10^{-6} ng/µl; 9, 1×10^{-7} ng/µl and 10, 1×10^{-8} ng/µl, respectively; M: marker

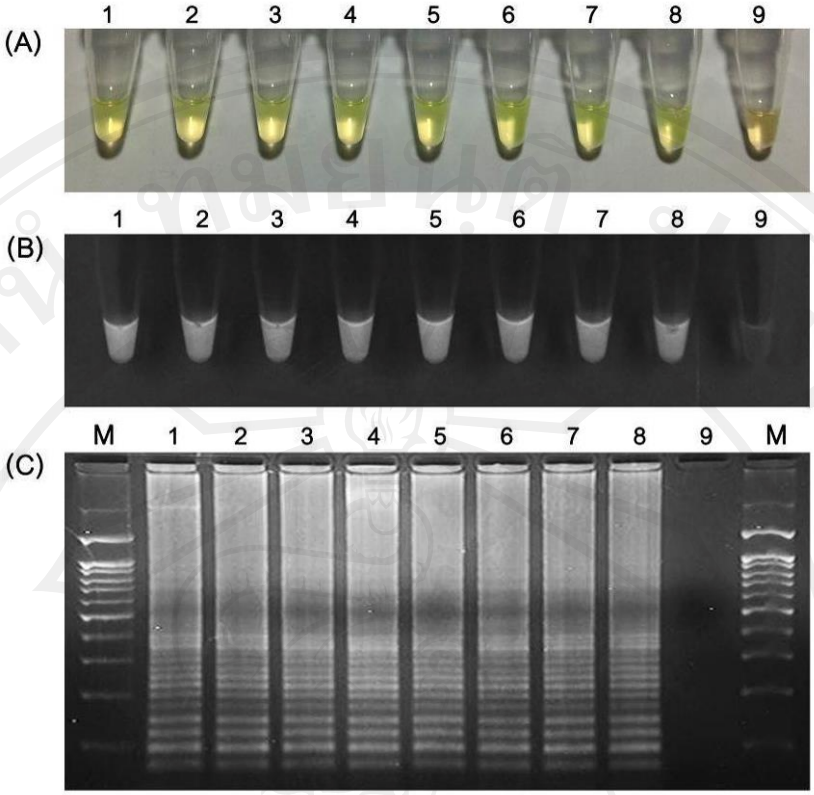

Figure 4.48 LAMP assay for detection of *Echinostoma revolutum* metaceria from naturally infected snails. LAMP amplified products were inspected visually under normal light **(A)**, under UV exposure **(B)** and confirmed LAMP amplified products by electrophoresis **(C)**. 1 represents the genomic DNA of *E. revolutum* adult (positive control); 2-8, the genomic DNA sample of metacercaria from various snails: *C. helena*, *E. eyriesi*, *B. funiculata*, *B. siamensis siamensis*, *F. doliaris*, *F. sumatrensis polygramma* and *F. martensi martensi*, respectively, and 9, negative control (without DNA); M: marker

4.3.2 Phylogenetic analysis

1) Amplification of internal transcribed spacer subunit 2 (ITS2) region and nicotinamide adenine dinucleotide dehydrogenase subunit 1 (ND1) gene

A partial region of the ITS subunit (including most of 5.8s gene and 5′ of 28s gene) and ND1 was amplified. The results showed that, the approximately 900 bp and 500 bp PCR product of ITS region and ND1, respectively, was generate in all samples (Figure 4.49). The procedures were repeated twice and the results were identical. All PCR products were subjected to sequencing directly. Based on the sequences data obtained, showed that the various length of both ITS and ND1 sequences provide in this study (Appendix D).

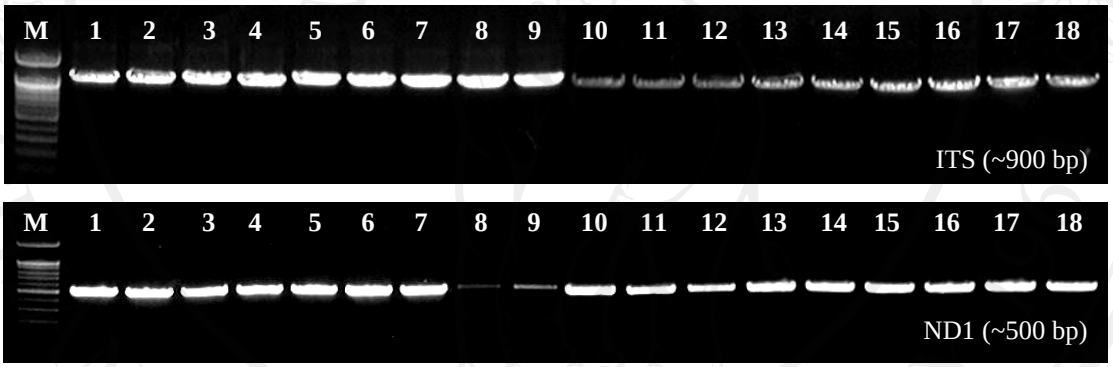

Figure 4.49 Demonstrated the ITS and ND1 PCR products of *Echinostoma revolutum*; lane M: marker (1 kb). Lane: 1: *E. revolutum* THA (Fm); 2: *E. revolutum* THA (Fd); 3: *E. revolutum* THA (Fp); 4: *E. revolutum* THA (Bf); 5: *E. revolutum* THA (Bs); 6: *E. revolutum* THA (Ch); 7: *E. revolutum* THA (Ee); 8: *E. revolutum* LAO; 9: *E. revolutum* VNM; 10: *E. revolutum* CAM (K-1); 11: *E. revolutum* CAM (K-2); 12: *E. revolutum* CAM (K-3); 13: *E. revolutum* CAM (K-4); 14: *E. revolutum* CAM (K-5); 15: *E. revolutum* CAM (K-6); 16: *E. revolutum* CAM (K-7); 17: *E. revolutum* CAM (T-1) and 18: *E. revolutum* CAM (T-2).

2) Sequences analysis

The ITS2 and ND1 sequence data of *E. revolutum* obtained, we use these sequences to further confirm the identity of these specimens by aligned and compared to ITS2 and ND1 databases available in GenBank using BLAST. Based on the BLAST results, it could be confirmed that, ITS2 and ND1 sequences found in this study were identically satisfied by revealing high alignment score. The sequences producing significant alignment of *E. revolutum* ITS2 compared with GenBank database, there were 6 accession numbers of *E. revolutum* that available in GenBank database that tended to match with ITS2 sequences of *E. revolutum* obtained in this study. While, ND1 sequence obtained, there were 54 accession numbers of *E. revolutum* tended to match with ND1 sequences obtained in this study.

The ITS2 and ND1 sequences data of *E. revolutum* derived from different geographic regions, they were trimmed to provide an equivalent sequences and then were aligned using multiple alignment method in Clustal W which is integrated in the MEGA program. Figure 4.50 show the 15 variable positions (including gaps) in the 426 bp alignments of the eighteen ITS2 sequences. These variable positions represented 3 purine transitions, 2 pyrimidine transitions, 2 transversions, 1 multiple changes and 7 gaps. The variable nucleotide sites of alignments of ND1 are shown in Figure 4.51. In total, 94/505 positions (including gaps) were variable. Of these, nucleotide presented 26 purine transitions, 11 pyrimidine transitions, 37 transversions, 15 multiple changes and 5 gaps.

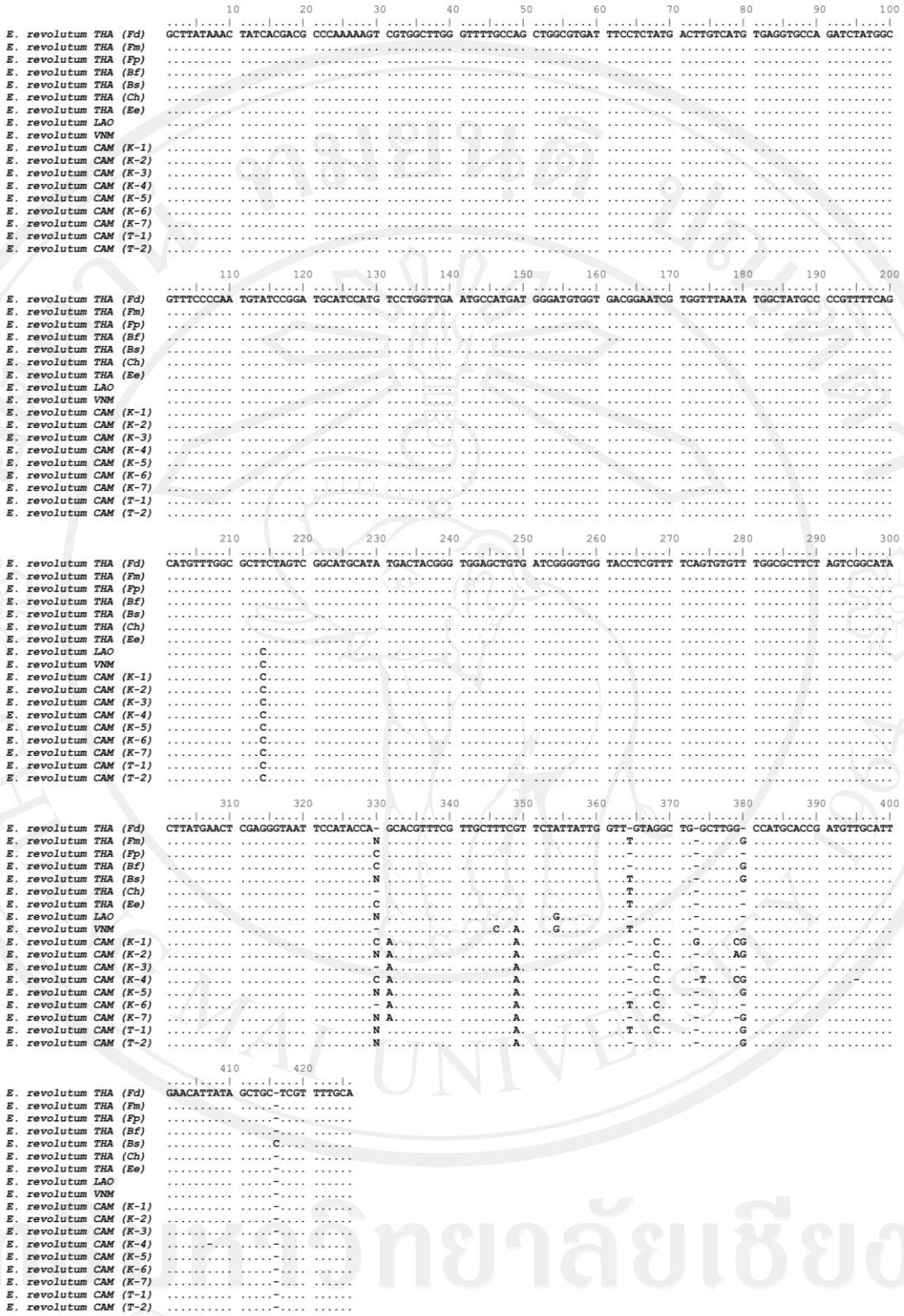

Figure 4.50 Variable nucleotide sites from aligned sequences of 18 partial ITS2 of *Echinostoma revolutum*. Bases identical to that on the top line [*E. revolutum* THA (Fd)] indicated by "." and alignment gaps indicated by "-".

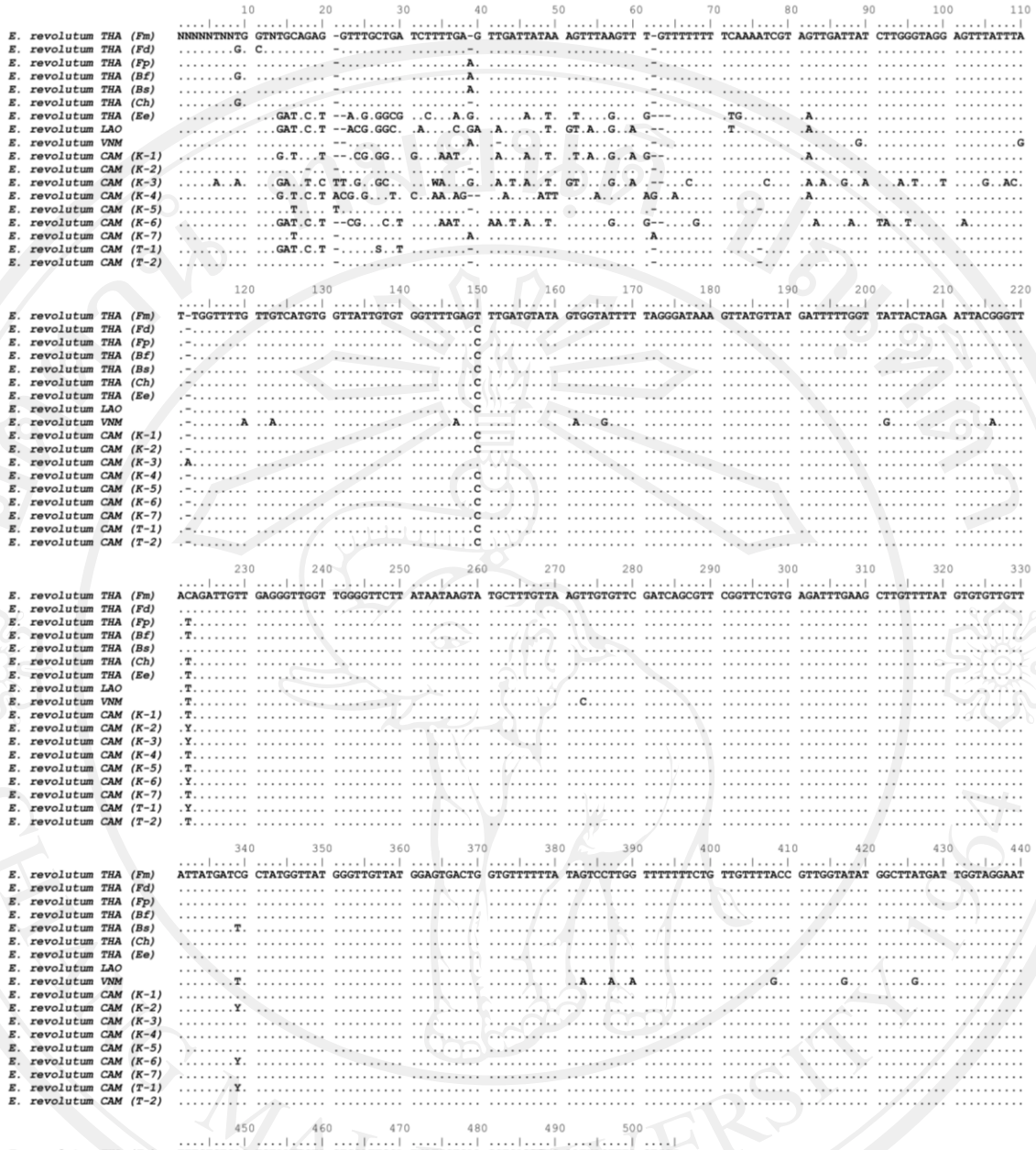

Figure 4.51 Variable nucleotide sites from aligned sequences of 18 partial ND1 of *Echinostoma revolutum*. Bases identical to that on the top line [*E. revolutum* THA (Fm)] indicated by ″.″ and alignment gaps indicated by ″-″. Y = C or T, W = A or T and S = G or C

3) Phylogenetic analysis

Phylogenetic tree was constructed based on the aligned sequence without gaps at both ends. The statistical significance of grouping was estimated using neighbor joining (NJ) method. The phylogenetic trees comparing the sequences of *E. revolutum* and available ITS2 and ND1 sequences of other *Echinostoma* species are shown in Figures 4.52-4.53. The ITS2 and ND1 trees showed that the almost topology is similar among the trees obtained.

The ITS2 tree showed strong support for monophyletic group of *E. revolutum* Southeast Asia isolates, supported with 94% bootstrap values. There was also strong support for a phylogenetically closer relationship between *E. revolutum* Southeast Asian isolates and other isolates (American and European isolates), supported with 81% bootstrap values. Additionally, the phylogenetic trees showed close resemblance among 37-collar spined group (i.e. *E. trivolvis, E. paraensei, E. caproni* and *E. liei*), whereas *E. malayanum* (43-collar spines) did not cluster a monophyletic clade and/or sister taxa of this group.

Figure 4.53 show the tree obtained by NJ method of ND1 gene. The results of the phylogenetic analysis revealed two major clusters. The first cluster contained a monophyletic group with the four isolates of *E. revolutum* were closely aligned as a monophyletic clade with other *Echinostoma* species in 37-collar spined group (i.e. *E. trivolvis, E. caproni* and *E. paraensei*). This cluster contained 35, 16, 3 and 18 sequences of American, European, Australian and Southeast Asian isolates, respectively, were aligned closely related to a monophyletic clade of other *Echinostoma* species in 37-collar spined group (i.e. *E. trivolvis, E. caproni* and *E. paraensei*). The other cluster contained the monophyletic clade of *E. malayanum* (43-collar spines), it represented as a paraphyletic taxon with 37-collar spined group.

In first cluster, there was good support for monophyletic clades for various isolates of *E. revolutum*, including American, European, Australian and Southeast Asian isolates. The samples of *E. revolutum* group were divided into four clades. The first clade included *E. revolutum* from American isolates (35 sequences), supported with 98% bootstrap values. The second clade *E. revolutum* from European isolates (15 sequences), supported with 84% bootstrap values. The third clade included *E.*

revolutum from Australia (4 sequences) plus the isolate from America (1 sequence), supported with 99% bootstrap. The final clade included *E. revolutum* from Southeast Asian isolates (18 sequences; including Thailand, Lao PDR, Vietnam and Cambodia), supported with 99% bootstrap values. In the final clade, bootstrapping of the ND1 sequences revealed significant support for the clade containing *E. revolutum* Southeast Asian isolates. All the Southeast Asian isolates, regard their second intermediate hosts and geographic origins fall into the *E. revolutum* cluster. The phylogenetic tree revealed that Southeast Asian isolates were closely related to other isolates of Australia and Europe.

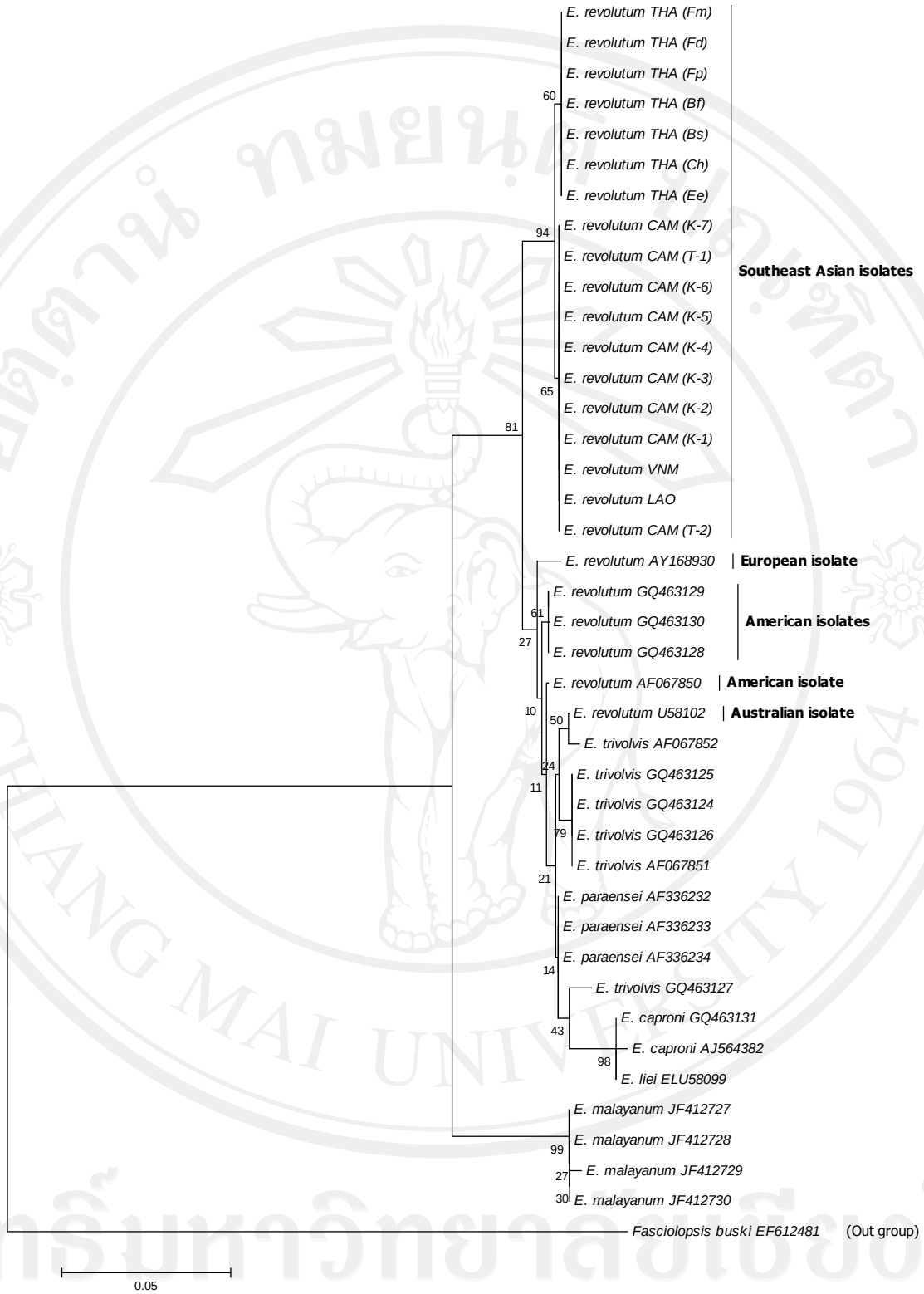

Figure 4.52 Phylogenetic tree inferred from ITS2 sequences of *Echinostoma* spp. using neighbor joining method, 1000 bootstrap replications, with *Fasciolopsis buski* as the out group. Bootstrap values are shown at internodes.

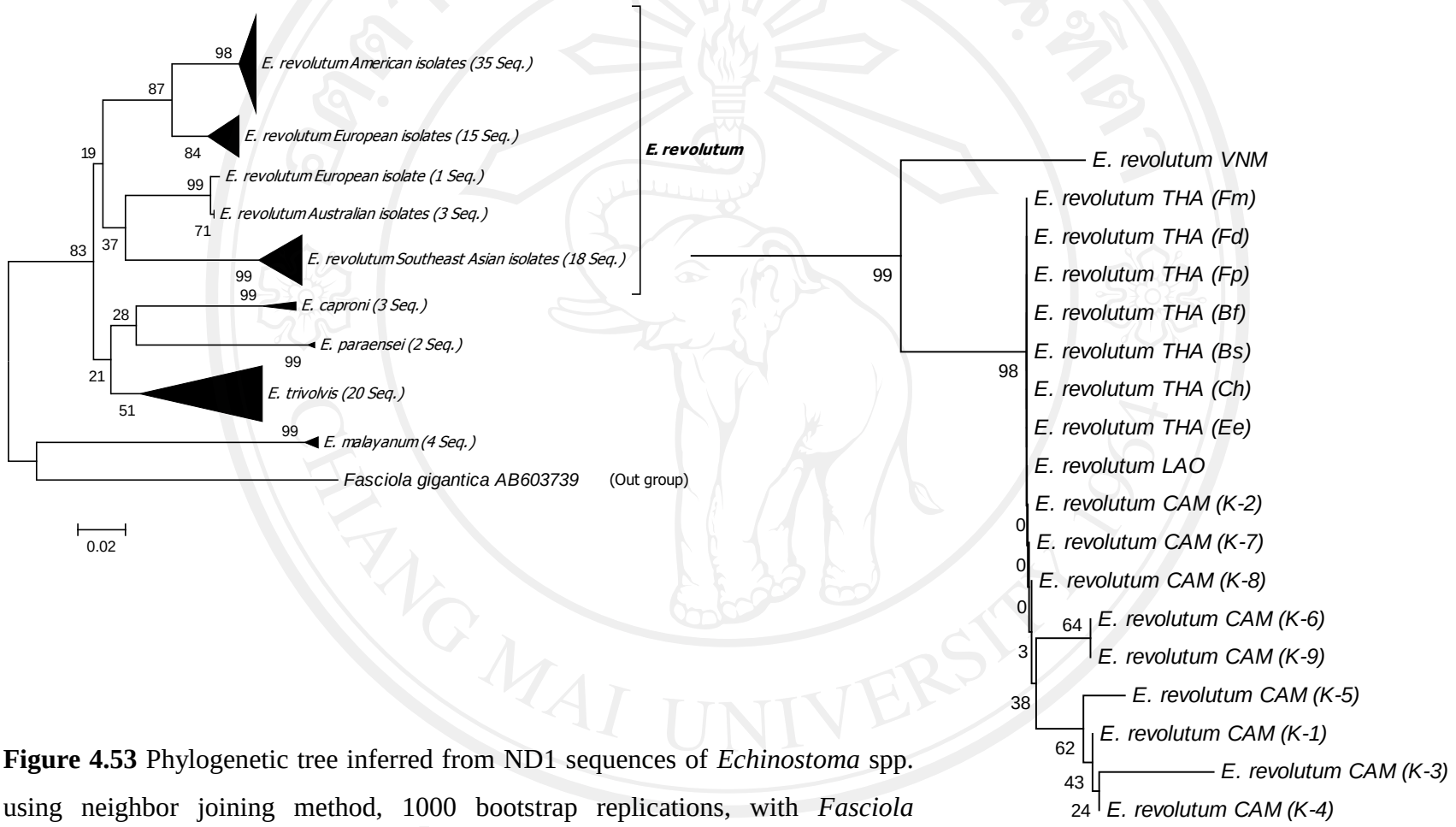

Figure 4.53 Phylogenetic tree inferred from ND1 sequences of *Echinostoma* spp. using neighbor joining method, 1000 bootstrap replications, with *Fasciola gigantica* as the out group. Bootstrap values are shown at internodes.